

Copyright Warning & Restrictions

The copyright law of the United States (Title 17, United States Code) governs the making of photocopies or other reproductions of copyrighted material.

Under certain conditions specified in the law, libraries and archives are authorized to furnish a photocopy or other reproduction. One of these specified conditions is that the photocopy or reproduction is not to be “used for any purpose other than private study, scholarship, or research.” If a user makes a request for, or later uses, a photocopy or reproduction for purposes in excess of “fair use” that user may be liable for copyright infringement,

This institution reserves the right to refuse to accept a copying order if, in its judgment, fulfillment of the order would involve violation of copyright law.

Please Note: The author retains the copyright while the New Jersey Institute of Technology reserves the right to distribute this thesis or dissertation

Printing note: If you do not wish to print this page, then select “Pages from: first page # to: last page #” on the print dialog screen

The Van Houten library has removed some of the personal information and all signatures from the approval page and biographical sketches of theses and dissertations in order to protect the identity of NJIT graduates and faculty.

ABSTRACT

MODELING OF EQUILIBRIUM POINT TRAJECTORY CONTROL IN HUMAN ARM MOVEMENTS

**by
Kai Chen**

The underlying concept of the Equilibrium Point Hypothesis (EPH) is that the CNS provides a virtual trajectory of joint motion, representing spacing and timing, with actual movement dynamics being produced by interactions of limb inertia, muscle viscosity and speed/position feedback from muscle spindles. To counter criticisms of the EPH, investigators have proposed the use of complex virtual trajectories, non-linear damping, stiffness and time varying stiffness to the EPH model. While these features allow the EPH to adequately produce human joint velocities, they conflict with the EPH's premise of simple pre-planned monotonic control of movement trajectory. As a result, this study proposed an EPH based method, which provides a simpler mechanism in motor control without conflict with the core advantages of the original approach.

This work has proposed relative damping as an addition to the EPH model to predict the single and two joint arm movements. This addition results in simulated data that not only closely match experimental angle data, but also match the experimental joint torques. In addition, it is suggested that this modified model can be used to predict the multi-joint angular trajectories with fast and normal velocities, without the need for time varying or non-linear stiffness and damping, but with simple monotonic virtual trajectories. In the following study, this relative damping model has been further enhanced with an EMG-based determination of the virtual trajectory and with physiologically realistic neuromuscular delays. The results of unobstructed voluntary

movement studies suggest that the EPH models use realistic impedance values and produce desired joint trajectories and joint torques in unperturbed voluntary arm movement.

A subsequent study of obstructed voluntary arm movement extended the relative damping concept, and incorporated the influential factors of the mechanical behavior of the neural, muscular and skeletal system in the control and coordination of arm posture and movement. A significant problem of the study is how this information should be used to modify control signals to achieve desired performance. This study used an EPH model to examine changes of controlling signals for arm movements in the context of adding perturbation/load in the form of forces/torques. The mechanical properties and reflex actions of muscles of the elbow joint were examined. Brief unexpected torque/force pulses of identical magnitude and time duration were introduced at different stages of the movement in a random order by a pre-programmed 3 degree of freedom (DOF) robotic arm (MOOG FCS HapticMaster). The results show that the subjects may maintain the same control parameters (virtual trajectory, stiffness and damping) regardless of added perturbations that cause substantial changes in EMG activity and kinematics.

**MODELING OF EQUILIBRIUM POINT TRAJECTORY CONTROL
IN HUMAN ARM MOVEMENTS**

**by
Kai Chen**

**A Dissertation
Submitted to the Faculty of
New Jersey Institute of Technology
and University of Medicine and Dentistry of New Jersey
in Partial Fulfillment of the Requirements for the Degree of
Doctor of Philosophy in Biomedical Engineering**

Joint Program in Biomedical Engineering

January 2011

Copyright © 2011 by Kai Chen

ALL RIGHTS RESERVED

APPROVAL PAGE

**MODELING OF EQUILIBRIUM POINT TRAJECTORY CONTROL
IN HUMAN ARM MOVEMENTS**

Kai Chen

Dr. Richard A. Foulds, Dissertation Advisor Date
Associate Professor of Biomedical Engineering, NJIT

Dr. Sergei Adamovich, Committee Member Date
Associate Professor of Biomedical Engineering, NJIT

Dr. Mesut Sahin, Committee Member Date
Associate Professor of Biomedical Engineering, NJIT

Dr. Kevin Pang, Committee Member Date
Professor of Neuroscience, UMDNJ

Dr. Eugene Tunik, Committee Member Date
Assistant Professor of Rehabilitation and Movement Science, UMDNJ

Dr. Yingxin Gao, Committee Member Date
Assistant Professor of Mechanical and Aerospace Engineering, Cornell University

BIOGRAPHICAL SKETCH

Author: Kai Chen
Degree: Doctor of Philosophy
Date: January 2011

Undergraduate and Graduate Education:

- Doctor of Philosophy in Biomedical Engineering,
New Jersey Institute of Technology, Newark, NJ, 2011
University of Medicine and Dentistry of New Jersey, Newark, NJ, 2011
- Master of Science in Mechanical Engineering,
Shanghai Jiao Tong University, Shanghai, P. R. China, 2004
- Master of Science in Biomechanics & Movement Science,
Wuhan Institute of Physical Education, Wuhan, Hubei, P. R. China, 2002
- Bachelor of Science in Mechanical Engineering,
Huazhong University of Science and Technology, Wuhan, Hubei, P. R. China,
1999

Major: Biomedical Engineering

Presentations and Publications:

Kai C. and Richard Foulds, "The mechanics of perturbed upper limb posture and movement control," ASME International Mechanical Engineering Congress and Exposition, Vancouver, BC, Canada, IMECE2010-37201, November 2010.

Kai Chen, Richard Foulds, Sergei Adamovich and Katherine Swift, "Experimental study and modeling of Equilibrium Point trajectory control in single and double joint arm movement," ASME International Mechanical Engineering Congress and Exposition, Lake Buena Vista, FL, IMECE2009-10251, November 2009.

Kai Chen and Richard Foulds, "Relationship between Equilibrium Point control processes and EMG pattern in elbow joint movement," WACBE World Congress on Bioengineering, The Hong Kong Polytechnic University, Hong Kong, China, July 2009.

Kai Chen, Katherine Swift and Richard Foulds, “Neural muscular delays in Equilibrium Point model of human arm trajectory,” Proceedings of IEEE 35th Annual Northeast Bioengineering Conference, Harvard – MIT Division of Health Sciences & Technology Cambridge, MA, pp. 73-74, April 2009.

Kai Chen, Richard Foulds, Sergei Adamovich, Qinyin Qiu and Katherine Swift, “Modeling of relative damping in defining the Equilibrium Point trajectory for the human arm movement control,” ASME International Mechanical Engineering Congress and Exposition, Boston, MA, IMECE2008-67879, November 2008.

To my beloved family, for supporting me and providing guidance throughout the past five years as I strive to further my education.

ACKNOWLEDGMENT

I would like to express my appreciation to Dr. Richard Foulds for his assistance in guiding me through my PhD education and teaching me the necessary skills to conduct the research independently. I would also like to sincerely thank Dr. Sergei Adamovich, Dr. Mesut Sahin, Dr. Kevin Pang, Dr. Eugene Tunik and Dr. Yingxin Gao for actively participating in my committee. Thank the Office of Graduate Studies for their assistance in my dissertation documents.

The study was supported by the National Institute on Disability and Rehabilitation Research RERC on Technology for Children with Orthopedic Disabilities (Grant # H133E050011). In addition, many of our graduate students and lab staffs in the RERC deserve recognition for their assistance throughout the past five years. I would like to specifically thank Diego Ramirez, Qinyin Qiu, Akshata Korgaonkar and Darnell Simon, who assisted in developing the MATLAB functions from C++ and voluntarily participated in the experiments.

Finally, I would like to thank my wife, Yi Deng, and my son, Rico Chen, for their support and understanding during my dissertation work, it would not have been possible without them.

TABLE OF CONTENTS

Chapter	Page
1 INTRODUCTION.....	1
1.1 Objective	1
1.2 The Fundamentals Validations of Motor Control Theory in Terms of EPH.....	3
1.2.1 A Mathematical Basis for the Equilibrium Hypothesis.....	7
1.2.2 Experimental Evidence for the EPH.....	9
1.2.3 Criticism and Problem of the EPH.....	13
1.2.4 Defense of the EPH	15
1.2.5 Equifinality and EPH	18
1.3 The Internal Dynamics Model versus EPH.....	22
1.4 The Robust and Prospective of EPH.....	25
2 DEVELOPMENT OF THE EPH	26
2.1 Concept Development of the EPH	26
2.2 Modeling of Relative Damping in the Defining of Limb Trajectory	28
2.3 Relation between Proposed EP Model and Strategy-dependent EMG Patterns .	31
2.4 The Role of Neural Feedbacks in Arm Movement Trajectory Control	34
2.5 The Roles of Intrinsic Muscle Viscoelasticity, Length and Velocity Feedback .	35
2.6 Timing Issues of Neural Control Signals	37
2.7 Control Variables in the EP Trajectory Planning	39
3 METHODOLOGY AND SYSTEM IMPLEMENTATION	42
3.1 Development of the System	42

TABLE OF CONTENTS
(Continued)

Chapter	Page
3.1.1 Overview of Experimental System	42
3.1.2 Theoretical Framework and Hypothesis	43
3.1.2.1 Model with Relative Damping	44
3.1.2.2 Overshoot of Relative Damping Model	45
3.1.2.3 Kinematics Equations of Double-joint Arm Movement	48
3.2 Hardware Implementation of the System	48
3.2.1 EMG System	48
3.2.2 trakSTAR® Position Measurement System	49
3.2.3 FCS HapticMASTER Measurement	51
3.2.4 Synchronizations of EMG, trakSTAR and Force Measurements	54
3.3 Experimental Design and Setup	55
3.3.1 Unobstructed Arm Multiple Joints Movement with trakSTAR	56
3.3.2 Elbow Flexions with trakSTAR® Only	57
3.3.3 Elbow Flexions with both trakSTAR® and HapticMaster	60
3.3.4 Voluntary Elbow Flexions with Unexpected Perturbations	62
3.3.5 Perturbed Movement	63
3.3.6 Arrested Arm Movement	64
3.4 System Calibration	65
3.5 Trouble Shooting in Data Collection Systems	66
3.6 Experimental System and Simulation Models	69

TABLE OF CONTENTS
(Continued)

Chapter	Page
4 RESULTS AND DISCUSSION	72
4.1 Preliminary Study Results in Unobstructed Arm Movement	72
4.1.1 Relative Damping Model in Human Arm Movement Simulation	72
4.1.2 Single Joint Model with Neuromuscular Delays and EMG Determined Virtual Trajectory (VT)	80
4.1.3 Summary of Unobstructed Arm Joints Movements	87
4.2 Haptic Effect in Unobstructed Elbow Movements	87
4.2.1 Unobstructed Elbow Flexions with both trakSTAR® and HM	87
4.2.2 The Influence of HM in Terms of Speeds	88
4.2.3 The Influence of HM in Terms of EMG and Force	88
4.3 EPH Control in Voluntary Elbow Flexions with Unexpected Perturbations	92
4.3.1 Statistics and Equifinality Test of Obstructed Elbow Movement	92
4.3.2 Results of Perturbed Movement	95
4.3.3 Arrested Elbow Movement	100
4.4 Optimization of Stiffness and Damping	104
4.5 Sensitivity Analysis of Obstructed Elbow Movements	105
4.5.1 Sensitivity Analysis with HM Only	105
4.5.2 Sensitivity Analysis in Arrested Movement	106
4.5.3 Sensitivity Analysis in Perturbed Movement	107

TABLE OF CONTENTS
(Continued)

Chapter	Page
4.5.3.1 Sensitivity Test of Elbow Movement with a Larger Perturbation Force	107
4.5.3.2 Sensitivity Test of Perturbed Elbow Movement	109
4.6 Mechanical Properties of Elbow during Obstructed Movements	111
4.6.1 The Duration of Shifts in the Equilibrium State	111
4.6.2 Relations of EMG and Cocontraction in Elbow Movement	113
4.6.3 Simulation Results	114
4.6.4 The Influence of Perturbation to Arm Movement	114
4.7 Mechanical Properties of Arm during Unobstructed Involuntary Movement ...	115
5 CONCLUSION AND DISCUSSION	118
5.1 Brief Summary and Discussion	118
5.2 Limitations of the Study	122
5.3 Conclusions	123
5.4 Contributions	124
5.5 Future Research	125
REFERENCES	126

LIST OF TABLES

Table	Page
3.1 Specification of the HapticMASTER	52
3.2 The Setting of Synchronization Pulse	69
4.1 Equifinality Test of Elbow Movements	93
4.2 A Least Squares Model Used to Optimize the Control Parameters Damping and Stiffness in the MATLAB Simulink	104

LIST OF FIGURES

Figure	Page
1.1 The Typical Experimental Setup	5
1.2 Graphical Explanation of EPH	8
1.3 Theoretical Predictions of the Movement Kinematics under IDM and EPH Control	23
3.1 The Schema of Model System	43
3.2 trakSTAR Device Introduction from Ascension Technology	50
3.3 HapticMASTER Workspace	51
3.4 The General Control Scheme of the HapticMASTER Comprises an Outer Control Loop, and an in Inner Servo Loop	52
3.5 The Setup of Arm Flexion	58
3.6 The HM Setup and Working Space	60
3.7 The Calibration of HM Forces, trakSTAR Positions and System Synchronization	65
3.8 The Recording of Environmental Noise	66
3.9 Raw EMG Signal	67
3.10 FFT Analysis of Raw Data	67
3.11 The Filtered EMG Signal	68
3.12 Illustration of Two Types Three Sizes Case/Supports	70
3.13 Robertson's Two Links Equations Represented with Simulink Model	70
3.14 Single Joint Simulink Model	71

**LIST OF FIGURES
(Continued)**

Figure	Page
3.15 The Schema of Multi-Joint Control Model System	71
4.1 Single Joint Movement Simulation Results	73
4.2 The Plotted Elbow Angle Trajectories in Fast Speed	74
4.3 The Plotted Elbow Moments in Fast Speed	75
4.4 Two Joints of Angles and Torques Comparing with Exp. Data in Normal Speed.	78
4.5 Two Joints Angles and Torques Comparing with Exp. Data in Fast Speed Arm Movement	78
4.6 The Schematic Illustration of Velocity Feedbacks System	81
4.7 Data for a Typical Elbow Extension Shows Timing of Flexor (biceps) EMG Onset and Triceps (triceps) EMG Termination. t1 and t2 Were Determined Graphically	83
4.8 Results of Model with Experimentally Determined Virtual Trajectory, Optimized B and K, with Elbow Data	84
4.9 The Joint Moments of Experimental and Model Data	85
4.10 Data for Arm Joints Extensions and Flexions	86
4.11 Data Comparing between the Experimental and Simulated Angular Trajectories.	86
4.12 Unobstructed Elbow Movement with trakSTAR only.....	89
4.13 Unobstructed Elbow Movement with both trakSTAR and HM Plot	89
4.14 HM Elbow Experimental Displacement vs Simulink Model Output	91
4.15 HM Elbow Experimental Torque vs Simulink Modeled Output	92
4.16 The Measured Trajectories of Elbow Movements in Equifinality Test	94
4.17 Perturbed Movement of Elbow	96

**LIST OF FIGURES
(Continued)**

Figure	Page
4.18 Perturbed Elbow Displacement in the Simulink Model	98
4.19 The Inverse Calculation of Elbow Components Torques and Total Torque	99
4.20 The Calculated Elbow Net Torque by Inverse Dynamics vs Net Torque by the Simulink Model vs HM Perturbation Torque	99
4.21 Arrested Movement of Elbow	100
4.22 Arrested Elbow Displacement in the Simulink Model	101
4.23 The Elbow Torques Plots.....	102
4.24 The Jerks in Arrested Elbow Movement	103
4.25 Sensitivity Test of Elbow Movements with HM Only	106
4.26 Sensitivity Test of Arrested Elbow Movement with $\pm 10\%$ Variance	107
4.27 Sensitivity Test of Elbow Movement with a Larger Perturbation	108
4.28 Sensitivity Result of Perturbed Elbow Movement in the Model	109
4.29 Sensitivity Test of Perturbed Elbow Movement in $\pm 10\%$ Variance	110
4.30 Unobstructed Involuntary Arm Movement	117

CHAPTER 1

INTRODUCTION

1.1 Objective

This study is an extension of previous studies devoted to the equilibrium-point hypothesis (EPH). The first part of the study is a brief account of past and present status of the hypothesis with suggestions for further development of the EHP theory.

It is well known that the EPH emerged in the unique scientific atmosphere created by a group of Russian researchers that is now known as the Russian School of Physiology. The group was founded in 1959 by a mathematician, Israel Gelfand, with the purpose of attracting specialists in mathematics, physics, engineering, chemistry and biology to join a multi-disciplinary approach to biology in general and to the neural control of movement in particular. Because the EPH resulted from the experimental analysis of the relationship between involuntary movements elicited by unloading of the arm and intentional, self-initiated arm movements (Asatryan and Feldman, 1965), the hypothesis emerged not by an instant insight but by systematic theoretical and experimental efforts triggered by the observation of human motor behavior in everyday situations.

The empirical origin of the EPH is worth emphasizing. From its conception, the hypothesis was a straightforward result of thorough and well-designed experiments. This may explain why, many years after its formulation, the EPH continues to steadily resisted attempts to reject it. Another essential result of the empirical nature of the EPH is that it is a concise formulation of the fundamentals of neural control of movements (Feldman A.G., 2009). Indeed, motor control theories that ignore these fundamentals may not be

successful. In particular, these fundamentals challenge what can be called mechanical reductionism in approaches to motor control. Specifically, it is natural to describe motor actions in terms of mechanical variables characterizing motor output (muscle forces, stiffness, damping, movement trajectories, position, velocity and acceleration of body segments) or variables directly related to them (e.g., EMG activity related to muscle force). Mechanical reductionism is based on the assumption that control processes underlying motor actions are reduced to programming of mechanical variables. In line with this assumption is the comparatively recent suggestion that control processes rely on internal inverse and forward models that program, compute and specify the EMG activity and forces required for motor actions. The continuous use of the internal model idea shows that mechanical reductionism remains popular, despite the fact that it was refuted in 1965 (Ostry and Feldman, 2003). On the other hand, it also shows that the basic notions of the EPH are not as simple as one may think. As a result, the unusual content of these notions makes it difficult to recognize that mechanical reductionism does not advance understanding of motor control. This situation necessitates a persistent clarification of the experimental and theoretical fundamentals of the EPH, which is the major purpose of the first chapter of this study. This chapter also shows that the EPH not only has survived numerous attempts to refute it, but also has extended the number of essential problems in motor control that have been solved by it, including the problem of planning and coordination in the control of multiple joints and muscles. In addition, recent developments of the EPH (earlier of this paragraph) show the reflex intermuscular interactions and the capacity of the nervous system to influence this interaction, which are fundamental to the understanding of how the nervous system guides multiple joints as

a coherent unit without redundancy problems.

The remaining sections of this chapter are intrinsically related by addressing the issue of how to advance a model which satisfies the control of fast multi-joint movement with or without perturbations, and the force generation during the movement. Among these sections, the smoothness of movement trajectory was addressed in relation to stability of movement and force generations. Stability of static posture and dynamic movement implies that any deviation from it evokes resistance of muscles and reflexes , which tends to restore the initial posture or initial movement. Stability cannot be achieved unless the neuromuscular system generates position- and velocity- dependent muscle forces that resist deviations from the posture and movement. These properties are characterized by stiffness and damping, respectively. Regarding these important issues in the EPH, the studies are to explore them step by step, started from brief accounting of fundamentals of the EPH.

1.2 The fundamentals Validations of Motor Control Theory in Term of EPH

EPH is more adequately called the threshold control theory (TCT). The basic notions of the TCT are reviewed with a major focus on solutions to the problem of multi-joints in fast arm movement. Although the TCT incorporates cognitive aspects by explaining how neurons recognize that internal (neural) and external (environmental) events match each other, these aspects, as well as how motor learning occurs are excluded in this study and subjects of further development of the TCT hypothesis. The study begins with an explanation of why EPH was chosen rather than other theories in the study of arm movement control.

Many researchers and scholars have long tried to explain the mechanism for the production of coordinated multiple segment movement mathematically and physiologically. However, an incredibly complex array of calculations must be made to model all the variables, known and unknown, involved in the production of movement. For instance, a simple single joint movement involves accounting for variables such as weight, length of segment, torque production for each muscle group involved in the movement, the muscle impedance to the movement inflicted by connective tissue, paraspinal reflexes, and any external and viscosity resistance to the movement in order to model the movement accurately. For a multi joint movement added complexity arises from the interaction torque one joint places on another. Adding more complexity to the system is the idea, developed by Bernstein et al. (Bernstein, 1967), that the body possesses kinematic redundancy, or more degrees of freedom than are needed to accomplish a movement. Yet, even with the immense complexity of the system, coordinated movements can be performed with great accuracy using minimal concentration. It has become the goal of researchers interested in this phenomenon to explain the underlying control strategies employed by the central nervous system (CNS) to create smooth coordinated movement. Meanwhile, the EPH drastically simplifies the requisite computations for multi-joint movements and mechanical interactions with complex dynamic objects in the environment. Because the neuromuscular system is spring-like, the instantaneous difference between the arm's actual position and the equilibrium position specified by the neural activity (i.e. virtual trajectory) can generate the requisite torques, avoiding the complex "inverse dynamic" problem of computing the torques at the joints.

In the 1950's researchers began conducting experiments examining the relationship between limb force, velocity and the associated myoelectrical activity of human muscle. The majority of experiments were conducted by performing tasks with the upper limb under various conditions and in populations with various levels and types of motor and proprioceptive impairment. The rationale for using the upper limb lies in the specialization of this segment for conducting accurate coordinated movement, Figure 1.1 shows typical experimental setup.

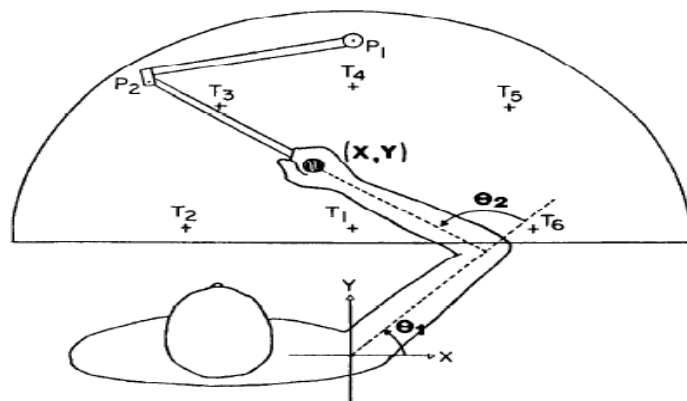


Figure 2. Experimental apparatus for measuring arm trajectories in a horizontal plane. T_1 to T_6 are the LED targets. θ_1 and θ_2 are, respectively, the subject's shoulder and elbow joint angles. Movement of the handle was measured by way of the potentiometers, P_1 and P_2 .

Figure 1.1 The Typical Experiments Setup

Source: Sainburg, R.L., et al. (2003).

The primary goal of such experiments was to identify the length/tension relationship associated with force production during passive stretch of muscle. The underlying goal was to explain the mechanism by which neural input to the muscle changes movement. In 1966, a seminal paper written by Feldman observed that when the elbow was displaced muscles produced a monotonically increasing force with

characteristics that were similar to a non-linear spring (Feldman AG., 1966). In this paper and in subsequent papers he hypothesized that the CNS uses a time series of functions that define a sequence of equilibrium states of the system based on thresholds (λ) of the tonic stretch reflexes of the participating muscles beyond which the muscle produces force. This idea matured into the Equilibrium Point Hypothesis (EPH) of motor control and is commonly referred to as the lambda model. Movement is controlled simply as a change in the activation thresholds of the agonist/antagonist muscle pairs. Therefore, motion can be generated by the CNS by assigning a series of Equilibrium Points along the desired trajectory without the need for explicit computation of movement dynamics involving all of the variables described previously. The system therefore responds to perturbations by assessing the proprioceptive information about the current state of the system relative to the Equilibrium Point (λ) set by the CNS at that time point, without the need for the CNS to modify the Equilibrium Point that form the virtual trajectory.

In the following decades more experimentation led to refinement and revision of Feldman's Equilibrium Point hypothesis by authors such as St-Onge, Adamovich, Ostry, Flash, Hogan, Bizzi, Latash and others. Rather than focus on Feldman's original description of the hypothesis, this introduction concentrates on some of the more recent experiments that support this description. As can be expected, there have also been criticisms of the EPH by authors such as Gottlieb, Dizio, and Lackner. And experiments that reject the EPH are also to be reviewed. This literature review will explore an alternative to the EPH, which has been termed the force-EMG or the internal dynamics model of motor control. In 1998 and 2005 articles were published by Feldman (Feldman,

1998), (Feldman and Latash, 2005) and his colleagues reviewing both the criticisms and the alternative models to the EPH respectively. These articles addressed the misinterpretation of the EPH. This literature review takes the form of a point/counter-point in an effort to describe the opposing views in the literature.

1.2.1 A Mathematical Basis for the Equilibrium Hypothesis

In 1966 Feldman (Feldman AG, 1966) first described the neuromuscular system acting on the human elbow joint as having similar characteristics to a non-linear spring. He described the relationship in the following equation:

$$F_{hand} = a(\exp[b(x(t) - x)\lambda(t)] - 1) \quad (1.1)$$

Where F_{hand} is the force at the hand, a and b are constants, x is the length of the muscle and $x\lambda$ (also commonly described as just λ) is the threshold length of the muscle beyond which the muscle will produce force. Using this equation, he hypothesized that change in position of the end effector is accomplished by modulating the threshold length (λ) of each muscle of the agonist-antagonist muscle pair. Many revisions of this equation have occurred in subsequent publications but the aforementioned form of the lambda hypothesis remains the central component of most revisions.

In the Feldman's theory (Feldman, 1986), Where θ is the joint angle and λ is the static threshold of the muscle, of which only λ is controlled by central commands. λ represents the point at which the IC curves deviates from the passive curve and tonic activation of the muscle begins. Other parameters, such as T , θ and the level of muscle

activation, are not directly controlled but are simply by-products of the interaction of the muscle with the specified λ and load characteristics.

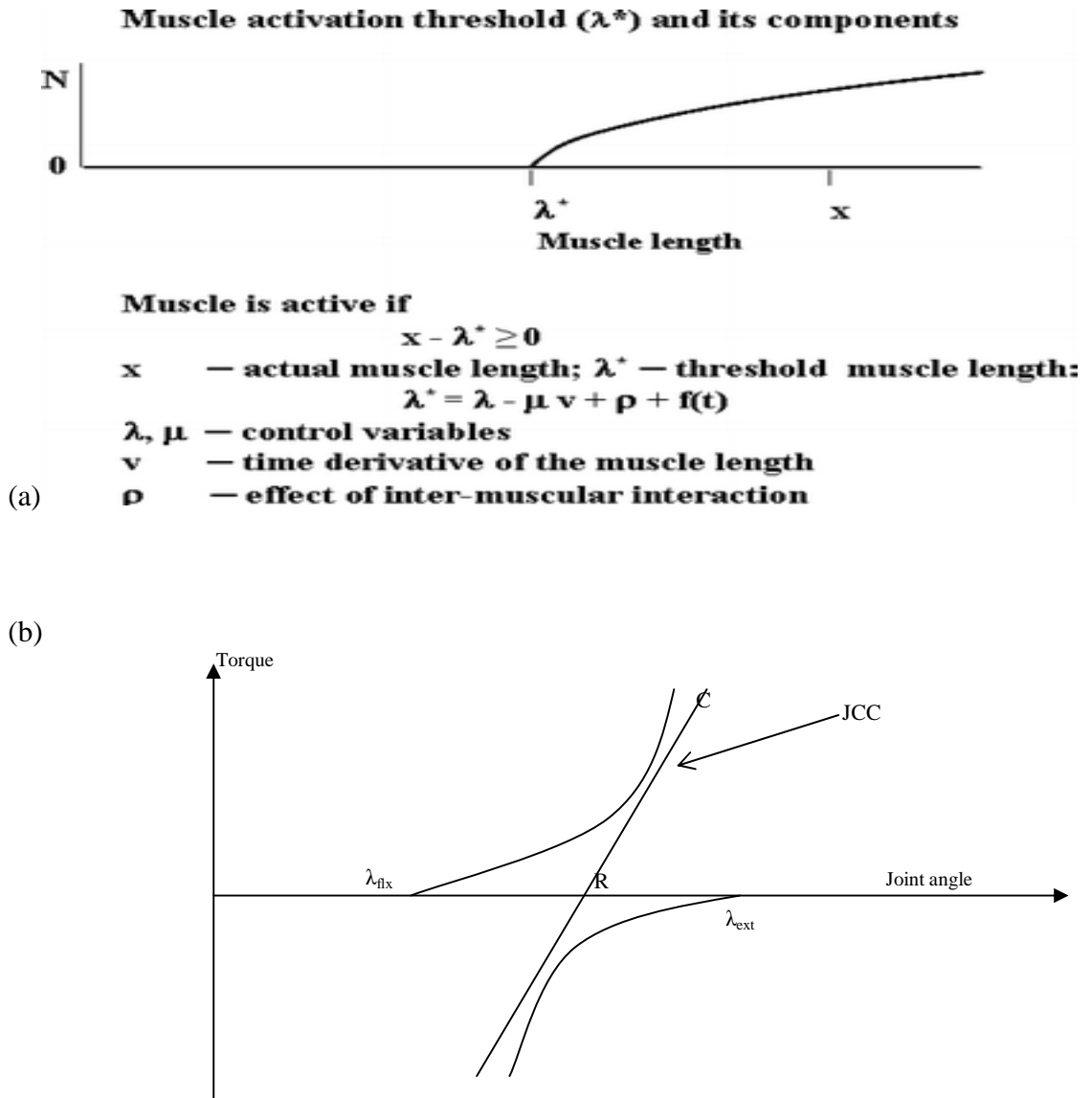


Figure 1.2 Graphical Explanation of EPH ((a). Threshold control of muscle activation in the λ model. Note that the activation threshold (λ^*) has a component (λ) that is determined by central control influences that are independent of proprioceptive feedback as well as components that are dependent on it (Cited from Asatryan and Feldman 1965; Feldman 1966). (b). The Joint Compliant Characteristic (JCC) curve is the sum of the invariant characteristic (IC) curves of the pair of antagonist and agonist muscles (flexor and extensor) controlling the joint. The intercept of this curve with the position axis represents the reciprocal command (R), which is the Equilibrium Point of the joint when no external loads are acting on it. The slope of the curve that is the stiffness of the joint, represents the co-activation command (C))

In the control of antagonist and agonist pair of muscles in a joint movement, the force-length relationship of a pair of antagonist muscles action around a joint is defined by the joint compliant characteristics (JCC) curve that is the algebraic sum of the IC curves of the two muscles. In the Fig.1, curve can be characterized by its slope (C), which represents the static stiffness of the joint, and its intercept with the position axis (R), which represents the Equilibrium Point of the joint when no external loads are acting on it. To control joint position, central commands can either define a pair of IC curves by specifying $(\lambda_{flx}, \lambda_{ext})$, or can directly define the JCC curve by specifying (R, C) . These two sets of control parameters are related by the following Equations:

$$R = \frac{1}{2} \cdot (\lambda_{ext} + \lambda_{flx}) \quad (1.2)$$

$$C = \frac{1}{2} \cdot (\lambda_{ext} - \lambda_{flx}) \quad (1.3)$$

R represents the Equilibrium Point of the joint when no external forces are acting on it, and C represents the stiffness level of the joint at the position indicated by R (Latash et al., 1991).

Descending command controls voluntary movement by specifying a time pattern of the control parameters. A time pattern of R represents the virtual trajectory, a pre-planned quasi-static movement trajectory defined by the descending commands. The time pattern of the C commands represents the profile of the static stiffness of the limb at each point during the course of the movement.

1.2.2 Experimental Evidence for the EPH

Hogan (Hogan, 1984) and Flash (Flash, 1985) presented a mathematical model to predict qualitative and quantitative features of a class of voluntary movements in the upper limb. The model was based on observations of both unperturbed and perturbed large amplitude voluntary single plane elbow movements performed at intermediate speeds by intact and deafferented monkeys. The model was confirmed based on experimental observations of human subjects performing unconstrained voluntary arm movements in the horizontal plane.

To create the model, a differential equation is formulated to relate endpoint position to neural activities, while minimizing the rate of change of acceleration of the movement. Therefore the goal of the model is to create the smoothest possible movement of the endpoint effector given the inputs. This model is kept simple and generalized by asserting that the differential equation represents the virtual trajectory independent of the physical system generating the motion. The model is unique from previous models because it requires no assumptions of linearity between muscle force and length, which though used commonly in previous models, are physiologically untrue. In this simple model only inertial, viscous and elastic coefficients are needed parameter values. The value for each of these parameters was taken from experimental measures.

Despite the simplicity of this model, trajectories produced accurately match those of Bizzi (Bizzi et al., 1982), (Bizzi et al., 1984), (Bizzi, 1987) given identical initial parameters for single joint primate movement described in Hogan (Hogan, 1984). In Flash and Hogan (Flash and Hogan, 1985), it is shown that the model is capable of accurately predicting multi joint arm movement in humans for both straight and curved path point to point movements. Hogan (Hogan, 1984) admits that many different models

could have been formulated to match the set of experimental data. The strength of the model lies in the dynamic optimization using a criterion function. Hogan (Hogan, 1984) chose to minimize jerk in his criterion function. The minimizing jerk criterion has been shown to successfully model eye movements, multi-joint movements of the upper arm, and jaw movements. Other successful models of motion have showed minimizing snap produces adequate predictions of observed movement (Flash and Hogan, 1985). A criterion function based dynamic optimization of movement trajectories supports the idea of hierarchal planning of movement. This theory suggests only the ideal trajectories of the movement of the end effector are planned at the highest neurological level. Actual torques and forces needed to create the movement are part of lower level planning. Both papers conclude by stating that use of a criterion function similar to the one presented may represent a step toward a unified description of the organization of voluntary movement.

The lambda theory states that proprioceptive feedback is necessary to determine the difference between the virtual trajectory made by the series of equilibrium positions and the actual trajectory of the limb. Many studies have examined the way in which proprioceptive feedback, specifically in relation to the stretch reflex, is integrated with central commands in the generation of electromyographic (EMG) activity and production of movement. According to the lambda model, “a fast change in limb position is produced by a rapid monotonic change of the reflex threshold (λ) of the stretch reflex.” (Adamovich, 1997). Reflex threshold is modified by CNS commands, but can also be modified by motor reflex signals from proprioceptive feedback. The lambda theory suggests EMG activity is only produced if the actual length of the muscle exceeds the

threshold length. Therefore this model accounts for the relatively weak effects of perturbations on EMG in fast movements, but allows for stretch reflex caused modifications in EMG patterns in response to strong perturbations defined as those with a speed equal to or greater than the speed of the movement. Adamovich et al. (1997) tested this model by measuring joint torque, movement kinematics and EMG activity at the arm during unassisted, assisted, and resisted rapid elbow movements with visual and without visual feedback. Assisting and resisting torques of 8-15 Nm were applied for 50 ms, at a latency of 50ms after an auditory “go” command to begin the movement. Results showed this perturbation caused significant deviations of the velocity and magnitude of the movement. Onset of the initial agonist EMG burst (biceps brachii) was found to be significantly earlier for perturbed conditions than for unperturbed conditions, and significantly earlier in the resistive condition than in the assistive condition. Also, significant antagonist (triceps brachii) EMG activity was found to precede the initial agonist burst for the assisted condition but not for the unperturbed or resisted conditions. The main conclusion of this study was that modulation of the initial EMG bursts to perturbations was observed at latency less than the minimal latency needed to alter central commands. This is therefore proof of the integration of proprioceptive afferents from the muscle having influence on the reflex threshold. These findings have two possible implications for the way proprioceptive feedback is accounted for by the lambda model. First proprioceptive afferents can modify the timing and magnitude of EMG activity without changing the central command. Second proprioceptive afferents may be used to make corrections to the end of a fast movement in relation to the external perturbation. Adamovich et al. (1997) made several assertions that this study provides

further evidence for the hierarchal command proposed in the lambda model versus a central generator model or pulse step model. In the central generator model perturbations should have no effect on the reflex threshold and EMG activity until changes can be provided from the central generator. As was stated before, the changes in EMG activity occur too quickly to be influenced by changes in central command. The pulse step model is described by an initiating pulse command and subsequent step commands bringing the system to its final position. This model would not predict fast modifications due to short perturbation times.

Another study presented in Levin and Feldman (Levin and Feldman, 1994) also tested the lambda theory suggestion that motor control of movement is based on stretch reflex threshold regulation. They tested this hypothesis by examining arm reaching in unimpaired healthy participants and those who have experienced CNS lesions resulting in impairment. They hypothesize that the increased excitatory signal associated with CNS lesions disrupt the normal regulation of the reflex threshold (λ) and often result in hypertonicity and spasticity. This disruption is believed to manifest itself in a decrease in the reflex dampening in the system. Specifically they believe that CNS lesion may be associated with “(1) a leftward shift in λ ; (2) a decrease in the range of regulation of λ ; and (3) a change in the velocity sensitivity of the threshold.” (Levin, 1994)

1.2.3 Criticism and Problem of the EPH

The λ Equilibrium Point Hypothesis is based on the hypothesis that the threshold of the tonic stretch reflex, λ , is the only centrally supplied control parameter descending to the α - and γ - motor neurons for a single intact muscle (Feldman, 1986). The tonic stretch reflex is a hypothetical mechanism describing the combined action of all the peripheral

receptors (including those from antagonist muscles) due to a slow muscle stretch. The threshold λ , marks the point at which autogenic recruitment of α - motor neurons begins due to this tonic stretch reflex. Although the threshold of the tonic stretch reflex is centrally supplied, the resultant activation level of α -motor neurons due to a slow muscle stretch is determined by the interaction between the mechanical properties of the muscle and the external conditions (Feldman, 1986).

Starting in the 1990's λ model of the EPH was the object of considerable criticism from several well respected groups. Gottlieb (Gottlieb, 1998) systematically and methodically attempted to reject the EPH offering three reasons why the EPH as described by Feldman fails to satisfy the requirements of a motor control theory to offer a complete definition of control variables, and rules by which those variables specify changes in movement features. He argues that the lambda model of the EPH requires agonist/antagonist muscle pairs have identical static and dynamic characteristics. In this way the model is physiologically unreasonable. Secondly, he states that in order to maintain system stability the necessary values of joint stiffness and viscosity are much higher than what has been determined experimentally. Lastly, he states that the EPH suggests movement of the reflex threshold which is accounted for by changes in reciprocal muscle activation (R), and makes no attempt to explain the effect changes in co-activation or system dampening that may have on the "Equilibrium Point". He concludes that it is time to abandon this theory in favor a new paradigms.

Dizio and Lackner (Dizio and Lackner, 2001) presented research that seemingly contradicted the Equilibrium Point theories of motor control. An arm reaching paradigm was used to collect details of the motor control system with the unique condition that the

participants were subjected to Coriolis forces produced by making the arm movements on a rotating platform. Coriolis forces produced by rotation provided a way to perturb the system without tactile stimuli. Feldman (Feldman, 1998) argued that large trajectory deviations caused by Coriolis forces were the result of visual and vestibular confusion. Dizio and Lackner (Dizio and Lackner, 2001) hypothesize that visual or vestibular confusions were not the cause of deviations directly contradicting the EPH. To prove this, subjects with vestibular deficits and healthy control subjects were chosen for participation. Reaching movements were performed on a rotating platform in a completely dark room to remove visual feedback. For both groups reaches made prior to rotation were directed in a straight path towards the target, reaches made while rotating were significantly displaced in the direction for the Coriolis forces, and reaches made just following rotation were displaced in the opposite direction of the Coriolis forces creating a mirror image of the trajectories made while rotating. For each condition both groups were able to correct deviations after 40 reaches. The study concluded that deviations that cannot be explained by the lambda theory of the EPH are not due to visual or vestibular feedback. The authors offer no explanation or alternative reason for the deviations.

1.2.4 Defense of the Equilibrium Point Hypothesis

In response to Gottlieb's criticism (Gottlieb, 1998), Latash and Jaric (Jaric and Latash, 2000) defended the EPH based on several methodological, statistical, and logical considerations.

- *Methodology: The predictions were predicated on an assumption on used unchanged motor command (**no corrections**) when the load changed unexpectedly*
- *Statistics: the interpreter of the data lead to type I error*
- *Logic: the basic principles of Gottlieb's model seem inconsistent*

To their conclusions, at least one version of the equilibrium-point hypothesis is able to handle modest changes in peak velocity with expected load. The data presented by Gottlieb can be handled by this hypothesis at least as well as by Gottlieb's own hypothesis, possibly better.

Feldman et al. (1998) also wrote a review article addressing some of the recent attempts to disprove the EPH. He began by distinguishing between state variables and parameters involved in the lambda model. He defines state variables as the variables of position and their time derivatives. All other variables that remain constant or change independently of the state variables are termed parameters. He states that the basis of the lambda model is that the control variables or central commands in the lambda model modulate the system parameters only and do not directly control the state variables. Only a change in system parameters, not a change in state variables will influence the Equilibrium Point of a system. This concept is important to dispute those experiments which concentrate on the characterization of state variable such as motor output, torque, stiffness, and EMG in their efforts to dispute the lambda theory. It also explains that the Equilibrium Point of the system is unchanged by external loads or external velocities (state variables) and therefore the lambda theory can be applied to both slow and fast movements.

The lambda model suggests that the control signals that underlie the point-to-point arm movement are monotonic in form. Monotonic signals lack points of inflection and are at all time steadily increasing or decreasing. Latash and Gottlieb (1991) observed a non-monotonic, "N" shaped pattern in torque/angle characteristics in fast point to point elbow movements. Feldman cites a Latash's (1993) study that showed changes in torque

or angle, both state variables, may be non-monotonic while changes in the Equilibrium Point remain monotonic.

Feldman next addresses a series of experiments that challenge the idea of Equifinality in the lambda theory. Equifinality assumes a movement would end at the same Equilibrium Point whether unperturbed or in the presence of a velocity dependent perturbation provided central commands remain unchanged. Lacker and Dizio (1994) observed positional errors in reaching movements under the influence of Coriolis forces in a dark rotating room, potentially refuting this idea. Feldman argues that Lacker and Dizio only considered the mechanical effect of these forces and not the changes in the stretch reflex threshold that may be caused due to proprioception of the rotation. In addition, other findings have also been reported for perturbed movements of healthy human subjects when they were asked not to intervene voluntarily with the perturbation (Gottlieb, 1994), (Gribble and Ostry, 2000). When one moves the hand while sitting in a slowly rotating room, coriolis forces act on the arm during the movement, but not during rest (before and after the movement). The Equilibrium Point hypothesis therefore predicts that unexpected coriolis forces will affect the shape of the movement path but not the end position.

Gottlieb (1998) claimed that the existing version of the lambda model does not address “movement features such as distance, speed, and load” (Gribble, Ostry, and Sanguineti, et al., 1998). Feldman countered that the movement distance is defined by the magnitude of the shift, and force and velocity of the movement are defined by the velocity and duration of the monotonic shift in Equilibrium Point. Feldman emphasizes

the fundamental non-linearity of neuromuscular systems in contrast to the linear models of many of the previously described studies which attempted to refute the lambda model.

Criticisms of the Equilibrium Point hypothesis have recently appeared that are based on misunderstandings of some of its central notions (Feldman and Latash, 2005). Starting from such interpretations of the hypothesis, incorrect predictions are made and tested. When the incorrect predictions prove false, the hypothesis is claimed to be falsified. In particular, the hypothesis has been rejected based on the wrong assumptions that it conflicts with empirically defined joint stiffness values or that it is incompatible with violations of Equifinality under certain velocity-dependent perturbations. Typically, such attempts use notions describing the control of movements of artificial systems in place of physiologically relevant ones. While appreciating constructive criticisms of the EP hypothesis, Feldman feel that incorrect interpretations have to be clarified by reiterating what the EP hypothesis does and does not predict. They conclude that the recent claims of falsifying the EPH and the calls for its replacement by EMG-force control hypothesis are unsubstantiated. The EPH goes far beyond the EMG-force control view. In particular, the former offers a resolution for the famous posture-movement paradox while the latter fails to resolve it. He concludes by directly addressing the recent attempts to directly attack or disprove the model rather than improve it. He reiterates several suggestions for critical tests of the validity of the model that he intends to conduct in the future.

1.2.5 Equifinality and Equilibrium Point Hypothesis

The term “Equifinality” refers to the ability of a system to reach the same final position regardless of transient mechanical perturbations (Feldman and Latash, 2005). Original

papers on the EPH stated that Equifinality could be observed in some cases of transient perturbations applied during motion of the intact system, but it has never been suggested that this phenomenon must occur under all such perturbations (Feldman and Levin 1995). In fact, Feldman demonstrated a substantially non-Equifinal behavior of the human arm long before other reports of such phenomena. The observation was made in experiments in which the arm was initially unloaded and then loaded with the same weight. If the loading was made abruptly, in a step-like manner, the arm did not return to the initial position. Using a gradual loading procedure, it was possible to transform the non-Equifinal behavior into an Equifinal one. Both types of behavior were explained within the framework of the EP hypothesis (Feldman and Levin 1995). Adaptation and positional errors (nonequifinality) of arm movements in the Coriolis force field (Lackner and DiZio, 1994), (DiZio and Lackner, 1995) have also been successfully simulated using the λ model (Feldman et al., 1998).

These simulations show that violations of Equifinality in no way conflict with the EP hypothesis. This conclusion is not negated by the fact that violations of Equifinality cannot be explained in mathematical formulations of the EP hypothesis by St-Onge et al. (St-Onge, 1997) and Gribble and Ostry (Gribble, 2000). Formulations by St-Onge et al. focused on kinematic and EMG patterns of single-joint movements and motor learning in different force fields. Although these formulations methodically incorporated the notion of threshold control of muscles and reflexes, they simplified or even disregarded some properties of the neuromuscular system. These properties might be disregarded in the explanation of the chosen phenomena but could be essential when addressing the issue of Equifinality and its violations in the λ model.

The EP is a vector quantity comprising the values of the equilibrium positions of individual muscles. Therefore, one should say that λ s do influence the existing EP but do not entirely predetermine its specific location in the torque-position space. For example, although λ s do not influence the equilibrium position in isometric conditions, they do influence the EP by changing individual muscle and net joint torques at this position. In the absence of any load, or in the presence of a velocity-dependent load, net joint torque is zero at any equilibrium position. Depending on changes in λ s and other components of activation thresholds, the system may arrive at different equilibrium positions or at the same equilibrium position while establishing different combinations of individual muscle torques, so that these steady states will be characterized by different EPs even in the cases where the equilibrium positions are the same.

The example in Figure 1.2(a) show that identifying the EP with the equilibrium position artificially narrows down the set of motor tasks to which the λ model can be applied. It is also important to emphasize that the EP is an emergent, non-programmable property of the system and that λ s only restrict sets of possible EPs, whereas a specific EP from a set eventually emerges following the interactions of neuromuscular elements between themselves and with the environment. In particular, repeating a pattern of changes in λ s in the absence of perturbations may lead to different EPs because of the variability in the non-central components of muscle activation thresholds (ρ and $f(t)$ in Fig. 1.2(a)). This variability is related to the natural variability of the steady-state properties of individual neuromuscular elements and the interactions between them. This simple analysis shows that the λ model does not guarantee Equifinality, even in the simplest case (during repetitions of movement in perfectly reproducible conditions). One

can only say that, on average, the system will reach the same final equilibrium position if the conditions and changes in λ remain the same.

The above analysis of the basic notions of the λ model implies that violations of Equifinality become even more probable in the presence of perturbations. This is obviously the case when a voluntary movement is suddenly blocked or when the limb is suddenly unloaded, bringing the limb to a new equilibrium position. In these cases, the perturbations, not the neuromuscular system, are directly responsible for the changes in the EP. Although velocity-dependent perturbations cannot directly influence the EP, the basic notions of the λ model do not prohibit an indirect influence of such perturbations on the EP, especially if they destabilize the system, as in the study by Hinder and Milner (Hinder, 2003). Theoretically, transient (particularly velocity-dependent) perturbations can influence (a) only λ s, (b) only the steady-state properties of neuromuscular elements and the interactions between them, or (c) both. The influence may result in a change of the final equilibrium position (kinematic inequifinality) or in the final combination of individual muscle torques without changes in the final position (kinetic inequifinality), or both (combined inequifinality). Indeed, by modifying (for example attenuating) velocity-dependent perturbations, one can transform non-Equifinal behavior into Equifinal behavior. Violations of kinematic Equifinality in healthy humans were observed by Feldman (1979), Lackner and Dizio (1994), Hinder and Milner (2003) and Popescu and Rymer (2000). Kinetic inequifinality was observed by Gielen and van Bolhuis (1995). The above arguments show, however, that these observations do not decrease the validity of the λ model.

1.3 The Internal Dynamics Model versus EPH

In the last 15 years a new hypothesis of motor control has gained popularity. The internal dynamics model (IDM) of motor control suggests that muscle activation patterns are the product of practice and motor learning. In this theory the neuromuscular response to a perturbation is more complex than can be completely explained using the EPH. Hinder and Milner (2003) not only designed an experiment to test the previously discussed principle of Equifinality supported by the EPH, but also introduced their internal dynamics model in terms of an EMG-Force control model. In their experiment participants were asked to produce an angular point to point wrist movement with a target angular velocity and a constant assist from a torque motor. Participants practiced the movement extensively prior to the day of testing. On the day of testing the participants were asked to perform the same task unaware that for 10% of trials the assistance level was reduced by 25 to 100 percent. Deviation from target position, angular velocity and EMG of the wrist flexor and extensor muscles were recorded. It was found that deviation from the targeted final position was proportional to the reduction in assistance level. This finding is synonymous with the IDM theory. No change in the cumulative EMG of the wrist muscles was found between the fully assisted and partially assisted trials showing no change in the set of central commands as well as no significant change in stretch reflex activity. In addition, the IDM predicts the CNS “learns” the necessary muscle activation to reach the final target for a given assistance level. Therefore with an unknown reduction in assistance level, the pre-planned motor command causes the wrist to fall short of the target as was observed in the experiment (see Figure 1.3). The authors

of the study claim that this is the first study to both disprove a central principle of the EPH and offer a plausible contradicting theory in the formulation of the IDM.

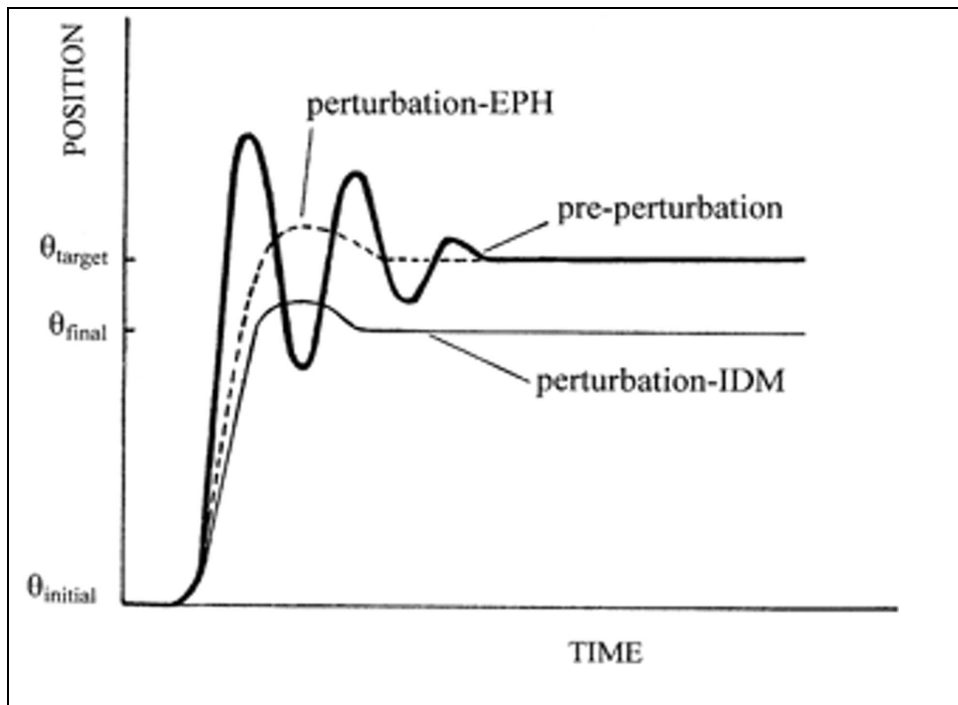


Figure 1.3 Theoretical Predictions of the Movement Kinematics under IDM and EPH Control (Movement under IDM and EPH results in identical movements after extensive learning of the control (pre-perturbation) movements (thick line) from θ_{initial} to θ_{target} , where θ represents the wrist position. On a 100 % torque-removed perturbation trial, stretch reflex activity creates extra flexor torque such that the same final position, θ_{target} , is achieved under the EPH (dashed line). In contrast, repetition of the feedforward motor command under IDM control results in an undershoot of the target (thin line) of $\theta_{\text{target}} - \theta_{\text{final}}$, directly proportional to the magnitude of the torque change.)

Source: Hinder M R , Milner T E. J Physiol 2003;549:953-963.

In a 2005 review article, Feldman and Latash (Feldman and Latash, 2005) again address recent experiments which attempt to disprove the lambda model of the EPH. Again experimental evidence against the lambda model are viewed as misconceptions about the hypothesis and flaws in the experimental design of these studies are exposed. Specifically addressed in this paper is the rise of the alternative explanation denoted by the EMG-force control model (also called the internal dynamics model) promoted by

Rymer and Popescu (2000), and Hinder and Milner (2003). This model suggests that the CNS is directly involved in the specification of EMG activity and muscle torques obtained from transformations of the desired kinematics via hypothetical inverse and forward models of the neuromuscular system interacting with the environment” (Feldman and Latash, 2005). Feldman’s article methodically addresses the criticisms of the lambda model of the EPH. And he emphasized the validation of EPH in the following aspects.

In an effort to provide simplicity to the theory, the Equilibrium Point hypothesis has been previously described as a mass spring system. The EPH is based on a threshold theory that is fundamentally non-linear. Physiologically it has also been shown that muscles behavior is fundamentally non-linear. Therefore it is not possible to decompose muscle force activation into two additive position-velocity dependent components that are the basis for mass spring models.

Proponents of the EMG-force control model argue that the stiffness of the system must be unphysiologically high to generate torque based on a difference between the actual and equilibrium positions. It is emphasized that the EPH makes such makes no unique requirements in the stiffness and dampening of the system. It is stated that sufficient levels of stiffness and dampening are needed to promote stability in any theory of motor control. The authors also attack the methodology used to determine stiffness and viscosity parameters of the authors who oppose the EPH.

Lastly Feldman and Latash (Feldman, 2003) discuss the merit of the EMG-force control model as a viable alternative to the EPH. Again, the EMG-force control model suggests an internal model of system dynamics in which the CNS directly computes the torque patterns and muscle activity needed to perform the movement. With respect to

response to perturbation the EMG-force model suggests the system quickly adjusts by integrating the new load and computing the necessary corrective torques in order to bring the system to the desired final position. Yet, oscillation at the terminal portion of a perturbed target based movement as seen in many of the experiments aimed at falsifying the EPH, provide more evidence to a deviation from an Equilibrium Point than for a well planned systematic correction by the central controller. Feldman and Latash (Feldman, 2005) attack the experiments of Hinder and Milner (Hinder, 2003) at length, from the experimental design to the lack of explanatory power. The authors again urge the scientific community to cease the attempts to refute the EPH in favor for studies which attempt to redefine and expand the EPH.

1.4 The Robust and Prospective of EPH

This dissertation uses and expands the EPH based on its merits in the motor control as listed below:

1. EPH provides a simple mechanism for limb movement control with its simplicity.
2. The spring-like properties of the neuromuscular system are applied in movement control.
3. The EP trajectory can simply be planned, which is minimize computation load of brain/system.
4. EPH can explain complex behaviors, such as expanding to multi-joint movement control along with added controlling parameters.
5. EPH incorporates human and animal movement characters physiologically. Therefore, focus of expanding EPH model is able to accommodate the complex behavior while preserving the simplicity of the EPH control strategy.

CHAPTER 2

DEVELOPMENT OF THE EPH

2.1 Concept Development of the EPH

Suppose the arm replaces each of its muscle bundles with a pair of opposing elastic rubber bands, the arm would tend to settle to the same configuration no matter from where it is released. That configuration is the Equilibrium Point of the simplest system. If changing the length-tension properties of the elastic rubber bands, for example, changes the resting lengths or stiffness, the Equilibrium Point of the system will change. Human muscles share a property with rubber bands in that the static force that they generate depends on length: the greater the length, the greater the force.

The activations received by motor neurons, whether they are from direct descending commands from the brain or from the spinal reflex circuitry, can change the force-length relation for each muscle, resulting in a change in the equilibrium position of the system. When we reach for an object, is the smooth, stable motion a consequence of a simple trajectory of Equilibrium Points? Are human muscles and the associated spinal reflex circuitry design in a way that makes control of motion particularly simple for the brain?

If the answer is yes, then it implies that many of the problems inherent in control of a multi-joint limb, for example, non-linear state-dependent dynamics, might be simplified because of a well designed muscle-reflex system. Here the study review the evidence regarding this hypothesis.

If this true, then the question is how the EPH can help to understand the movement control in terms of planning and execution? Some researchers (St-Onge and

Adamovich, 1997) suggested that λ regulation may be an essential element of motor control. Regarding the motor control they introduced the equilibrium position hypothesis to model the non-linear control of motor neurons' threshold. Thus the stimulate results of this non-linear model could be used to stimulated the movement of multi joint robot arms by employing a different λ to coordinate the movement of each joint (Chen, 2009). So the motor control can be explained by the equilibrium position regulation.

One study put forward Feldman's EP theory and expanded it into the new idea (Flash, 1987) that the EPH spring models discriminates movement planning from execution. Motor planning is to program the movement tasks by choosing a succession of discrete Equilibrium Points. Once these points are chosen, in the execution phase the muscle spring moves without further direction under CNS control (Chen, 2009).

Based on the discussion in the introduction, this study is dedicated to the investigation of how to apply and implement the EPH in given tasks for the human arm trajectory control to support evidence validating the hypothesis rather than arguing it theoretically. It is known there are few studies which have been done to demonstrate how the simple EPH mechanism can be applied to control human arm motions.

This chapter addresses several important concepts and problems in the development of Feldman's EPH theory before the application. First of all, the study proposes relative damping to define the trajectory of the human arm movement by the proposed control model. Secondly, these models are to be used to investigate the single/multi joints EP trajectory control with variable conditions such as loads, movement speeds and random perturbations induced by the robotic manipulandum (Haptic Master) along with incorporated physiological parameters. At last, recorded data from EMGs,

position/orientation sensors and robotic manipulandum are used to demonstrate the accuracy of arm movement controlled by EPH trajectories.

2.2 Modeling of Relative Damping in the Defining of Limb Trajectory

Now there are multiple versions of the Equilibrium Point models, which all have in common that the moving limb is attracted towards an equilibrium position and posture (Gribble et al., 1998), (Latish and Gottlieb, 1991), (McIntyre and Bizzi, 1993), (St-Onge, Adamovich and Feldman, 1997). The models differ considerably in how they dampen the movement. Since the damping parameters play important role in affecting the movement trajectory and velocity profile, a strong damping is required to limit the extent to which the arm overshoots the target.

As the information mentioned above, the obvious conflict between the fast movement and the heavily damped system is solved by making the parameters in the model time- or speed- dependent. This was done employing either a pulse step control (Barto et al., 1999), by letting the stiffness and damping change during the movement (St-Onge et al., 1997), by introducing non-linear muscle properties (Gribble et al., 1998), or by introducing non-monotonic shift of the Equilibrium Point (Latish and Gottlieb, 1991). Those models either have servo-control, in which position feedback regulates the speed of movement, or the use of velocity feedback in addition to position for the control of arm movement (McIntyre and Bizzi, 1993). However, all these models increased the complexity and led to the computation being unsolvable, because the brain will have to compute some sort of complex inverse dynamics (Dizio and Lackner, 1995), (Gottlieb, 1998).

In Feldman's study (Feldman, 1986), he states a limitation of a simple linear mass-spring model in describing goal directed movements is that it generates rather slow movements when the parameters are kept within a realistic range. Does this mean that the control of fast movements cannot be approximated by a linear system under the scope of EPH? And are there any models can solve the mentioned problem with simplicity? The answer may be the modified EPH model with proposed relative damping, which is elaborated by this study. In servo-control theory, it has been proposed that an optimal controller should control movement velocity in addition to position. Instead of explicitly controlling the velocity, the study proposed to modify a simple linear mass-spring model as an expansion of the EPH. The model added damping relative to the velocity of the Equilibrium Point (relative damping) beside the damping respect to the environment (absolute damping). This study's results (in the chapter on results) show such extremely simple models can generate rapid single and double joint arm movements. The resulting maximal movement velocities were almost equal to those of the Equilibrium Point, which provided a simple mechanism for the control of movement speed. Hence, the new proposed relative damping concept enables us to investigate the control pattern of arm movements by the non-linear model which incorporates neural control variables, time-, position- and velocity-dependent intrinsic muscle and reflex properties. Since the neuromuscular system creates a moveable equilibrium position for a joint without the external forces, and the joint will approach and reach its equilibrium position. However, the multi-joint movements require more complicated control variables, and any major assumptions which may limit its range of validity.

In this study, the new concept is the expansion of the EPH model. Two control variables called Reciprocal (R) and Coactivating (C) central commands are defined respectively as the sum and the difference of the λ of the antagonist muscles (Feldman, 1986). R and C are also described in terms of their mechanical properties, with R being the equilibrium position of the joint and C its stiffness. In the movement, the theory postulates the CNS specifies the temporal patterns of the central commands R and C and of another central command variable called μ which controls velocity feedback gain. Commands C and μ provide movement stability and effective energy dissipation preventing oscillations at the end of movement. These commands, in combination with peripheral feedback signals, providing angle and velocity of the joint from muscle proprioceptors, generate joint torques.

This study proposes the addition of relative damping to define the trajectory of the human arm movement. Current literature introduces Equilibrium Point models and shows that the moving arm is attracted towards an equilibrium position (Latash and Gottlieb, 1991), (St-Onge, et al., 1997). However, the models are different in how they dampen the arm movement. The goal of damping is to minimize overshoot and movement without endless oscillations around the Equilibrium Point. The setting of damping parameters can affect the shape of the movement path and the velocity curve as well. Furthermore, de Lussanet et al. proposed the concept of environmental relative damping (de Lussanet, 2002), by taking two underlying concepts of the Equilibrium Point Hypothesis: reflexes contributing significantly to the mechanical behavior of the motor system, and that reflexes function relative to the desired movement.

The damping in the existing EP models usually counteracts the joint's velocity since muscles have velocity dependent properties. However, modeling damping relative to the environment (joint) is inconsistent with this concept. An alternative is a damping term that acts on the arm's movement with respect to the actual velocity and the desired movement velocity (the velocity of the EP). de Lussanet (2002) called the first (conventional) type absolute damping (in parallel with the spring element) and the later relative damping (in series with the spring element). This relative damping gives the limb a tendency to move at the same velocity as the Equilibrium Point, and can be understood as damping with respect to the EP. Both kinds of damping are the same when the Equilibrium Point is stationary, but they differ when the Equilibrium Point moves. Hence, the study evaluated the performance of models with absolute and the proposed relative damping by modeling the movement of a single-joint and multi-joints of human arm trajectory in the chapter of results.

2.3 Relation between Proposed EP Model and Strategy-dependent EMG Patterns

From the bioengineering point of view, numerous neural, sensory and musculo-skeletal units, which can be classified into neurons, receptors, motor units, and muscle fibers, compose a complex biological system; and this system has been considered as an imperative asset to coordinate and enhance the actions, perception, and cognition. From a mechanical and engineering point of view, the motor units (MUs) can be treated as a single motor to drive the limb. As for the stability consideration, MUs requires position-, velocity-, and force-dependent feedback by the "transducers"- muscle spindles and other proprioceptors. Those units receive inputs from abundant transducers. Therefore,

questions have been raised whether control action of muscles is explicitly computed by brain with these redundant solutions? It also arises the issue as a consequence of interaction between moving equilibrium position, damping and stiffness of the arm joints.

Since limb movement is controlled by the explicitly specified forces, the approach of the study remains in the manner of specification of the Equilibrium Point trajectory and muscle activation, which elicits a restoring force toward the planned equilibrium trajectory. This study assumed that the control system used the velocity measured as the origin of subordinate variables scaling descending commands. Thus, the velocity command was translated into muscle control inputs as second order pattern generators, which yield not only reciprocal commands, but also coactivation commands, and create alternating activation of the antagonistic muscles during movement and coactivation in the post-movement phase, respectively. The velocity command was also integrated to give a position command specifying a moving Equilibrium Point with sensory transport delay, muscle activation and excitation time delay.

It is well known that proprioceptive feedback induces muscle activation when the motoneurons exceed their threshold, and the muscle reflex system produces torques depending on the position and velocity of the arm joints that the muscle span. According to the EPH, the static component of the torque-position is referred to as the invariant characteristic (IC), control systems produce movements by changing the activation thresholds and thus shifting the IC of the appropriate muscles in joint space. This control process upsets the balance between muscle and external torques at the initial limb configuration and the limb is forced to establish a new configuration in order to regain the balance. The idea is, the joint angles and the muscle torques generate an equilibrium

configuration defined by a single variable called the EP. Thus control systems reset the EP by shifting the IC. Muscle activation and movement emerge following the EP resetting because the natural physical muscle spring like property has the tendency to drive the system to reach equilibrium. Many empirical and simulation studies support the hypothesis that the control IC shifts and the resulting EP shifts underlying are gradual.

However, controversies exist about the duration and sequences of these shifts, and how the time delay, which due to these shifting, influence the system performances? Some studies suggested that the IC shifts cease with the movement; the others proposed that the IC shifts end early in comparison to the movement duration approximately at peak velocity. One of the goals of the study was to evaluate the duration of the EP trajectory underlying fast point to point arm movement. Since the study assumed that the neural signals are controlled in different levels, the study was to evaluate the duration of the IC shifts timing underlying the point to point arm movement in order to avoid the higher level neural controlling involved.

This study used the model to regulate a fast, single-joint movement, based on the equilibrium-point hypothesis. Limb movement follows constant rate shifts of independently regulated neuromuscular variables. The independently regulated variables are tentatively identified as thresholds of a length sensitive reflex for each of the participating muscles. The author used the model to predict EMG patterns associated with changes in the conditions of movement execution, specifically, changes in movement times, velocities, amplitudes, and moments of limb inertia. The approach provides a theoretical neural framework for the dual-strategy hypothesis, which considers certain movements to be results of one of two basic, speed-sensitive or speed-insensitive

strategies. This model is advanced as an alternative to pattern-imposing models based on explicit regulation of timing and amplitudes of signals that are explicitly manifested in the EMG patterns of Latash and etc (Latash , Gottlieb, 1991 b).

2.4 The Role of Neural Feedbacks in Arm Movement Trajectory Control

A single motor units (MUs) can not be responsible for the broad range of muscle force regulation because of limited capacity of force generation. The system overcomes this limitation in a natural way, by organizing gradual recruitment of MUs (Feldman, 2008). This opens the possibility of specialization of MUs according to anatomical, mechanical, reflex and biochemical properties such that the system becomes flexible in grading muscle forces in relation to the movement extent, velocity, and external resistance. Although each primary spindle afferent terminates practically on all motoneurons of the hosting muscle (Windhorst's review, 1996), the synaptic transmission and efficiency of afferent feedback is different for different MUs. This results in a broad distribution of spatial thresholds of MUs across the biomechanical range of the muscle length. To accommodate, in particular, enhanced stability demands, recruitment of MUs and resulting force-length characteristic are highly non-linear (initially exponential) such that increasing external resistance is confronted not only by increasing muscle forces but also by increasing stiffness (Asatryan and Feldman, 1965). This is achieved by appropriately increasing recruitment and overall activity of muscle spindle afferents and other proprioceptors. In addition, afferent inputs should support already active MUs and prevent unnecessary recruitment of other MUs with increasing muscle force. It is unlikely that these non-linear properties of the motoneuronal pool could be met by using a single proprioceptor.

A major topic of the review discusses the functional role of proprioceptors in action and perception by Windhorst (Windhorst, 1996). Indeed, his review is a valuable account of experimental data on proprioceptive feedback and spinal networks. However, it makes the impression that despite numerous studies on this subject, many researchers still have limited understanding of the role of proprioceptors in action and perception. And what specific roles of these feedbacks, such as force, intrinsic muscle viscoelasticity, muscle length and velocity feedback, play in the arm movement trajectory controlling. Bearing on the problem, the study needs to further investigate the relation between intrinsic muscle properties and movement condition to better understand the proprioceptors' functions.

2.5 The Roles of Intrinsic Muscle Viscoelasticity, Length and Velocity Feedback

Two important feedback pathways should be addressed for the muscle length and velocity. One describes the intrinsic muscle stiffness and viscosity, another describes the proprioceptive feedback including muscle spindles. The intrinsic muscle viscoelasticity feedback path does not have a time-delay present, and contribution is a direct function of the muscle force exerted by the force-length and force-velocity relation. By increasing the force through co-contraction, the system will become stiffer and more viscous. Rozendaal (Rozendaal, 1997) estimated that the maximal stiffness of the shoulder was always below experimental values as presented by Mussa-Ivaldi et al. (Mussa-Ivaldi, 1985), or derived from Feldman (Feldman, 1966). This means that the stiffness is dominated by proprioceptive feedback.

A distinction should be emphasized between the force, geometric and passive contribution to joint stiffness. If the muscle force increases because of the muscle stiffness or viscosity, this force increases and is then reduced by the force feedback through the Golgi tendon. Obviously, the geometrical and passive contributions do not change, since no increase of muscle force is involved. The geometrical contribution is almost always negative. Increasing muscle force increases the destabilizing geometrical contribution. Therefore, Rozendaal (Rozendaal, 1997) showed that for the shoulder the force contribution to stiffness is almost canceled out by the geometrical contribution. This means that co-contraction does not add directly to the joint stiffness.

Muscle fiber length and contraction velocity are sensed by the muscle spindle. Though the spindle is a highly non-linear processor of the length and velocity information, the author assumed that the CNS is capable of deriving the original length and velocity. The muscle spindle dynamics must be an order of magnitude slower than the extrafusal muscle fiber dynamics, otherwise the sensor information would be truly distorted. In addition, the muscle spindle dynamics can be neglected in regard to the time delay for the feedback loop. Therefore, it is acceptable to model the muscle spindle and neural pathways by a simple gain and a time delay. It shows the most important features are of the length and velocity feedback, and the optimal feedback gains can also be estimated.

Generally, the desired stiffness can not be obtained by the length and velocity feedback. Only the combination of length, velocity and force feedback results in a system that can approximate the desired impedance. However, because of the dynamics of the feedback path (time-delays, muscle activation dynamics), the stiffness and viscosity are

not instantaneous properties of the system. Hence it is concluded that force feedback increases the muscle activation dynamics, whereas the length and velocity feedback can approximate the desired stiffness and viscosity. The intrinsic muscle stiffness and viscosity due to the force-length and force-velocity relation contribute to the joint impedance. The increase of the intrinsic muscle viscosity is functional in the respect that the length and velocity feedback gains can increase further, so a larger range of impedance levels can be obtained.

The author presented a general model of arm movement trajectory control in his 2008 ASME paper (Chen, 2008) without time-delays. The principles of the model were demonstrated for elbow joint movement control with proprioceptors feedbacks, and covered arm movement has been extended to multi-joints system, which has been discussed in the chapter on results. The input of the model is the supraspinal neural input (virtual trajectory) to the close-loop actuator (a joint including an antagonist and agonist muscle). The output of the model is the joint angle of arm. This concept is described in the ASME paper (Chen, 2008) as relative damping in defining the arm EP trajectory. The overall structure of the model system has been shown in the chapter of methodology.

2.6 Timing Issues of Neural Control Signals

Because the nature of a muscle-force feedback system includes a time-delay, timing of the control signals underlying the arm movement from point to point are very important to make the human movement physiologically. However, some conflicting versions (Ghafouri and Feldman, 2001) of the timing were suggested in the framework of the EPH of motor control (Bizzi et al., 1984), (Feldman, 1986), (Latash, 1993), (Gomi and Kawato,

1996), (Gribble et al, 1998). In part of the study, the author characterizes these controversies by using several basic concepts of the EPH, starting with the concept that movement production can be described by two sets of related variables (Feldman 1986, 1995). One consists of kinematic and kinetic motor output of the arm system, such as the trajectory of the effectors, angular position and velocity of the arm segments, muscle force and torque. These outputs depend on the external environmental condition. Another set of variables consists of control variables. These are the internal variables that the nervous system and spinal cord may use to influence the output variables, although the external environmental conditions remain unchanged. These control variables imply that the nervous system can be an open-loop strategy in movement, which means the control patterns can be pre-programmed and generated independently of the motor output of the intentional actions.

In some mentioned motor tasks, Asatryan and Feldman (Asatryan and Feldman 1965) found control variables remaining invariant regarding the mechanical perturbations influencing the motor output, it replied that the reactions of the system to perturbations are determined by the spring – like properties of muscles depending on their elasticity, viscosity, neural activation and electromyographic (EMG) activity modified by proprioceptive reflexes. Since the EMG activity level is not the same for different points of the characteristic but increases according to the absolute value of the torque generated by the respective muscles (Feldman 1986) , the absolute value of the generated EMG could give the necessary information about the sequences. However, the quantitative evaluations of the neural signal delay in the arm movement have not been reported based on the literature reviews. In the current work, the author used a modified relative

damping model with velocity dependent feedbacks to model the time delay and projected the sequence of the delay in the study, the preliminary results have been published in the NEBEC 2009 (Chen, 2009).

2.7 Control Variables in the EP Trajectory Planning

Following the idea of EMG activity modified by proprioceptive reflexes, Bigland and Lippold (1954) measured the magnitude of EMG activity and showed it belongs to the set of output, rather than control variables because the observations show it depends on kinematic variables such as muscle length and velocity. The other output proposed by Asatryan and Feldman (Asatryan and Feldman, 1965) is the well grounded static relationship between muscle force and length, in angular coordination, between the muscle torque and joint angle. It is well known (Asatryan and Feldman, 1965) that proprioceptive feedback induces muscle activation when the facilitation of the appropriate motoneurons exceeds their threshold. This occurs at a specific, threshold muscle length (λ) also measurable in terms of threshold angles of the joints that the muscle spans. In the suprathreshold range, the muscle-reflex system produces position-, velocity- and force-dependent muscle activation and torques. It has been shown that the nervous system changes the activation thresholds of appropriate muscles to shift the static torque-angle characteristic in the joint space (Feldman and Orlovsky, 1972), (Capaday, 1995). Therefore, the static component of the threshold could be modified independently of output variables and might be considered a control variable in terms of concept of the EPH by Feldman.

In the present study, the term control variables or central commands imply neural processes that shift or maintain the position of the static torque-angle characteristics. To account for the interaction of muscles with the mechanical environment, the torque-angle characteristic of the external loads (perturbations as the format of external force/torque in the study) acting on the joint was also investigated. The load characteristic was specific for each motor task. In addition, the muscle-load interaction essentially depends on whether or not the system has an equilibrium position. For a joint, this is the position at which the joint segments may remain motionless while the balance of muscle and external torques is maintained. The EP of a joint is completely described by a two-dimension variable, one component of which is the equilibrium position and another net joint muscle torque at this position (Asatryan and Feldman, 1965). In static, the EP can be visualized as the point of intersection of two static characteristics in torque-angle coordinates, one for the muscles and the other for the load acting on the joint. The EP of several joints of the limb is derived from the individual EPs of these joints. It represents the two major characteristics of mechanical equilibrium of the whole limb (Ghafouri and Feldman, 2001): the set of joint angles describing the geometric configuration of the limb and the set of the muscle torques generated at this configuration when the limb is motionless. In dynamics, the nature of the EP concept can be illustrated by two examples: the reaction of the system to a mechanical perturbation and active movement production. To produce an active movement in the absence of mechanical perturbations, control systems may shift the IC and thus shift the EP. That means the nervous system may intentionally create a difference between the initial and the equilibrium combination of position and torque. In response, the system will generate muscle activity and forces

tending to minimize the difference. In particular, suppose that control systems changed the muscle recruitment thresholds and thus shifted the muscle characteristic.

However, insufficient evidence is available to determine where and how the shifting is being planned. Although Matthews, Feldman and Asatryan (1965) proposed the thresholds of muscles to shift EP in joint space, the complex computation of the brain could overburden the nervous system. Therefore, shifting, planning and executing are still unclear in both static and dynamics, but the study provided a simple model of planning strategy in terms of EP trajectory control, which satisfied both static and dynamics as an emerged new approach.

CHAPTER 3

METHODOLOGY AND SYSTEM IMPLEMENTATION

3.1 Development of the System

3.1.1 Overview of Experimental System

Feldman said: *“The tonic stretch reflex is a hypothetical mechanism describing the combined action of all the peripheral receptors (including those from antagonist distant muscles) due to a slow muscle stretch. The threshold λ , marks the point at which autogenic recruitment of α - motor neurons begins due to this tonic stretch reflex. Although the threshold of the tonic stretch reflex is centrally supplied, the resultant activation level of α -motor neurons due to a slow muscle stretch is determined by the interaction between the mechanical properties of the muscle and the external conditions.”* (Feldman, 1986).

Therefore, the overall experimental system used in this study should work under the interaction between the muscle’s physiological properties and the external conditions. The design of the experiments evaluates the enhanced model of the EPH with normal and fast speed arm movements, as well as under the condition of perturbations. The experiments include the relative damping and an EMG defined virtual trajectory incorporated into a conventional EPH model to better represent the feedback loops and the descending neural signal of the muscle. The interaction incorporated crosstalk. Appropriate neuromuscular delays have been added to the Simulink model, as have representations of the unexpected perturbations and the manipulations. The schema of the overall system is shown in Figure 3.1.

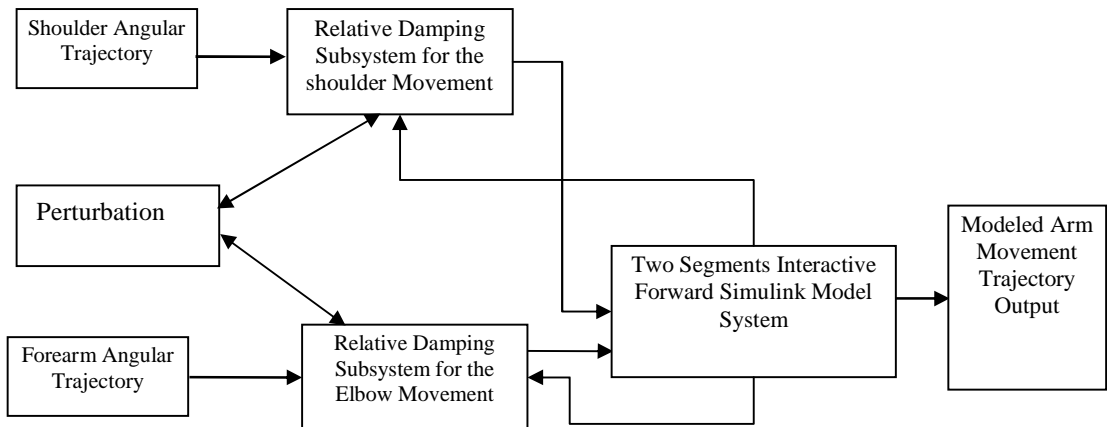


Figure 3.1 The Schema of Model System

In the block diagram of the system, inputs can be actual angular trajectories (as used by de Lussanet) of arm joints by trakSTAR® sensors attached on the elbow and shoulder. EMGs of the muscle are used to identify the onset and offset of simple monotonic virtual trajectories. That can be used as input. The HapticMaster manipulandum generated a perturbation in the format of imposed extra torque/force to the subject for 120 ms. Function blocks and performance will be discussed in the following sections in detail.

3.1.2 Theoretical Framework and Hypothesis

The study evaluated the performance of models with absolute and relative damping by modeling the fast and normal movement of a single/double joint human arm (see the Fig.1). This kind of arm flexion movement has frequently been used to test mass-spring models in previous EPH studies. Besides being used to model whole movements, linear models can also be applied to a limited range of a non-linear system (Bennett, 1992) and by a N-shape virtual trajectory (Latash and Gottlieb, 1991). In the second part, the study modeled the differences between the non-perturbed and perturbed movement. The effect

of perturbation has been investigated in different amplitudes and in different movement stages.

3.1.2.1 Model with Relative Damping

The study derives the equations for the extended EPH model with spring like property. Let's suppose $\theta_0(t)$ to be equilibrium position and $\theta_t(t)$ be the arm's actual angular position. Their time derivatives, angular velocity and acceleration, are represented with one or two dots over the variable respectfully. The differential equation with absolute viscous damping (B) and moment of inertia (I), and stiffness (K) is:

$$I\ddot{\theta} + B\dot{\theta} + K(\theta_t - \theta_0) = 0 \quad (3.1)$$

and for relative damping

$$I\ddot{\theta} + B(\dot{\theta}_t - \dot{\theta}_0) + K(\theta_t - \theta_0) = 0 \quad (3.2)$$

The configuration must enable the system in a stable equilibrium point condition, so $K > 0$, $B \geq 0$, and $I > 0$. The simplified equation can be achieved by dividing all parameters by I and defining new constants, b and k , this yields for absolute damping

$$\ddot{\theta} + b\dot{\theta} + k(\theta_t - \theta_0) = 0 \quad (3.3)$$

And for relative damping:

$$\ddot{\theta} + b(\dot{\theta}_t - \dot{\theta}_0) + k(\theta_t - \theta_0) = 0 \quad (3.4)$$

In order to find the solution for equation (3.3) and (3.4) for the movement at constant velocity $\theta(t) = \theta_0 + \dot{\theta}t$. With boundary conditions $\theta(0) = \theta_0$ and $\dot{\theta}(0) = \dot{\theta}_0$, the solution can be written for the under-damped condition ($k > b^2/4$) as

$$\theta_t = \dot{\theta}_0 t + \hat{\theta}_0 - e^{-t/\tau} \left((\hat{\theta}_0 - \theta_{t0}) \cos(\omega t) + \left(\frac{\theta_0 - \theta_{t0}}{\omega} + \frac{\hat{\theta}_0 - \theta_{t0}}{\omega \tau} \right) \sin(\omega t) \right) \quad (3.5)$$

$$\text{In this case } \tau = 2/b \text{ and } \omega = \sqrt{k - \frac{1}{4}b^2}$$

As for the over-damped case ($k < b^2/4$) is

$$\theta_t = \dot{\theta}_0 t + \hat{\theta}_0 - \frac{\tau_1}{\tau_1 - \tau_2} \left((\dot{\theta}_0 - \dot{\theta}_{t0})\tau_2 + \hat{\theta}_0 - \theta_{t0} \right) e^{-t/\tau_1} + \frac{\tau_1}{\tau_1 - \tau_2} \left((\dot{\theta}_0 - \dot{\theta}_{t0})\tau_1 + \hat{\theta}_0 - \theta_{t0} \right) e^{-t/\tau_2} \quad (3.6)$$

$$\text{In the case, } \frac{1}{\tau_1} = \frac{1}{2}b + \sqrt{\frac{1}{4}b^2 - k} \text{ and } \frac{1}{\tau_2} = \frac{1}{2}b - \sqrt{\frac{1}{4}b^2 - k}, \text{ equations (3.5) and (3.6)}$$

are valid for both absolute and relative damping. For absolute damping, $\hat{\theta}_0 = \theta_{00} - (\frac{b}{k})\dot{\theta}_0$,

whereas for relative damping $\hat{\theta}_0 = \theta_{00}$. Equation (3.5) is the equation for a gradually damping out oscillation, and Equation (3.6) contains the sum of two exponential functions that both approach zero, but at different rates.

3.1.2.2 Overshoot of Relative Damping Model

The model with relative damping for a single joint movement predicts that the target will overshoot even in the over-damped case, and for this case all equilibrium arm movements mathematically, damping and stiffness parameters are assumed to be positive. The model is linear, the trajectory does not change within a target distance. For simplicity the target distance are set at 1 radian in the preliminary study. Assuming the equilibrium movement time is t_q , while the Equilibrium Point moves, $\dot{\theta}_0 = \frac{1}{t_q}$. The initial values are $\theta_{i0} = \dot{\theta}_{i0} = \theta_{00} = 0$. From Equation (3.6), when the Equilibrium Point reaches the target at time t_q , the end point of arm has position and velocity,

$$\theta_t(t_q) = 1 - \frac{\tau_1 \tau_2}{\tau_1 - \tau_2} \frac{1}{t_q} (e^{-t_q/\tau_1} - e^{-t_q/\tau_2}) \quad (3.7)$$

$$\dot{\theta}_t(t_q) = \frac{1}{t_q} + \frac{1}{\tau_1 - \tau_2} \frac{1}{t_q} (\tau_2 e^{-t_q/\tau_1} - \tau_1 e^{-t_q/\tau_2}) \quad (3.8)$$

In the definition $0 < \tau_1 < \tau_2 < \infty$ while $b > 0$, and $0 < \theta_t(t_q) < 1$ to ensure reaching the target before the Equilibrium Point does. After the Equilibrium Point reaches the target, it remains there. The end effector (hand) will either slowly approach the target (but never reach it), or it will shoot past the target and return back. If there is always overshoot, the time t_{target} (when end effector reaches the target) must be within the range ($t_q < t_{\text{target}} < \infty$), regardless the values of b , k and t_q . After time t_q , the Equilibrium Point

$\theta_0 = 1$ and $\dot{\theta}_0 = 0$, therefore

$$\theta_t(t_{target}) = q = 1 \quad (3.9)$$

So Equation (3.6) substitute $\theta_t @ \theta_0 = \theta_t(t_q)$ and $\dot{\theta}_t @ \dot{\theta}_0 = \dot{\theta}_t(t_q)$ as given in Equation (3.7) and (3.8), the Equation (3.6) becomes

$$\exp\left\{(t_{target} - t_q)\left(\frac{1}{\tau_1} - \frac{1}{\tau_2}\right)\right\} = \frac{1 - e^{-t_q/\tau_1}}{1 - e^{-t_q/\tau_2}} \quad (3.10)$$

Then

$$t_{target} = t_q + \frac{\ln(1 - e^{-t_q/\tau_1}) - \ln(1 - e^{-t_q/\tau_2})}{1/\tau_1 - 1/\tau_2} \quad (3.11)$$

From Equation (3.11) the calculated t_{target} for positive damping ($b > 0$) ranging from $\lim_{t_q \downarrow 0}$, to $t_{target} = t_q$ for $\lim_{t_q \rightarrow \infty}$.

$$t_{target} = \frac{\ln(\tau_1/\tau_2)}{1/\tau_1 - 1/\tau_2} \quad (3.12)$$

These results suggest for $0 < \tau_1 < \tau_2 < \infty$, there is a time $t_q < t_{target} < \infty$ when $\theta_t(t_{target}) = 0$. That means there is an overshoot for all movements with positive relative

damping.

3.1.2.3 Kinematics Equations of Double-joint Arm Movement

Joint torques were calculated for shoulder and elbow using the equation listed below.

Robertson's Equation of motion for Upper Arm used in the forward model

$$(I_T + m_L L_T^2) \alpha_T + m_L L_T d_L (\alpha_L \cos(\theta_L - \theta_T) - \omega_L^2 \sin(\theta_L - \theta_T)) + (m_T d_T + m_L L_T)(a_{Hx} \cos \theta_T + (a_{Hy} + g) \sin \theta_T) = 0 \quad (3.13)$$

Robertson's Equation of motion for the Forearm Arm used in the model

$$I_L \alpha_L + m_L d_L (L_T \alpha_T \cos(\theta_L - \theta_T) + L_T \omega_T^2 \sin(\theta_L - \theta_T) + a_{Hx} \cos \theta_L + (a_{Hy} + g) \sin \theta_L) = 0 \quad (3.14)$$

Sainburg's (2003) two-segment link arm model has also been used to evaluate the arm dynamics, and equivalent performance has been achieved as Robertson's arm dynamic model.

3.2 Hardware Implementation of the System

3.2.1 EMG System

A Grass Technologies® Model 15LT Bipolar Physiodata Amplifier System was used in the study. The Model 15A54 Quad Neuroamplifiers from Grass are designed specifically for neurophysiological measurements. The 15A54 has extended high frequency response to 6 kHz. The detailed information of the system is listed.

Description: The Model 15LT completes with medical-grade specifications. The 15LT is exceptionally compact, designed to sit directly under a standard notebook style computer.

All amplifier functions are computer controlled, including individual amplifier gain, low and high filters, calibration, and other specialized functions like electrode test. A Windows 98/2000/NT program, Link15, is included for controlling all amplifier functions and saving/recalling setups. The 15LT can also be easily controlled from user software with simple ASCII command sequences (Grass Technologies, 2010).

Electrode Test Function Standard: A built-in Electrode Test function provides an accurate assessment of electrode contact quality without disconnecting the subject – even while recording. A Trace Restore function is also included for returning all amplifier outputs to zero (Grass Technologies, 2010).

3.2.2 trakSTAR® Position Measurement System

Angles of the upper and forearm of subject are measured using two trakSTAR sensors. The trakSTAR is an electromagnetic 6 DOF electromagnetic position/orientation motion tracing system. Segment angles can be measured without knowledge of the center of joint rotation with an accuracy of ~ .5 degree at 100 frames/second. Note that Flock of Birds (FOB) and trakSTAR are using the same technology, but the sensor sizes are different. They were all made by Ascension Technology Corporation. In the study, FOB were used in the preliminary study, and trakSTAR sensors were used in obstructed elbow movement with HM.

3D Guidance trakSTAR™
Class 1, Type B Applied Part



Desktop electronics unit tracks multiple sensors simultaneously

Track Objects with New Magnetic DC Technology

- **Fast, dynamic tracking** – 240 to 420 updates per second.
- **Miniaturized passive sensors** – outputs unaffected by “power-line” noise sources.
- **All attitude tracking** – no inertial drift or optical interference.
- **High metal immunity** – no distortion from non magnetic metals.



Interchangeable sensor sizes for full six degrees-of-freedom tracking



Magnetic field transmitter options for mid and short-range tracking

Ascension Technology Corporation
Tracking 2D Worlds

FAST PORTABLE AFFORDABLE

Figure 3.2 trakSTAR Device Introduction from Ascension Technology

Source: Ascension Technology Corporation Official Website.

[http:// www.ascension-tech.com/medical/pdf/TrakStarSpecSheet.pdf](http://www.ascension-tech.com/medical/pdf/TrakStarSpecSheet.pdf), accessed November 28, 2010.

An Application Programming Interface (API) in MATLAB has been used in communication with the tracker using the Ascension RS232 interface protocol. No software or driver was required to install except MATLAB. First, the transmitter and sensors have to be aligned to collect data in the desired orientation, and the data collection program needs to be set up into the multi-sensor mode when multiple sensors have been used in collection. The sample rate has been tripled in the multiple sensor data collection, which needs to be divided by three to get the correct amount of data. Custom MATLAB software was written to synchronize the collection of up to 4 channel of EMG data (agonist / antagonist muscles, shoulder and elbow) and two trakSTAR sensors. EMG

signals from the Grass Amplifier are acquired at 1000 samples/second via a National Instruments 16 channel data acquisition board, and trackSTAR data is read via a serial interface.

3.2.3 FCS HapticMASTER Measurement

The HapticMASTER (HM) is a 3 degrees of freedom, force-controlled haptic interface. It provides the user with a crisp haptic sensation and the power to closely simulate the weight and force found in a wide variety of human tasks. The programmable robot arm utilizes the admittance control (force control) paradigm, giving the device unique haptic specifications.

The workspace of the HapticMASTER is depicted in Figure 3.3. The kinematic chain from the bottom up yields: base rotation, arm up/down, arm in/out, illustrated in Figure 3.3. This makes 3 degrees of freedoms at the end effector, which spans a volumetric workspace.

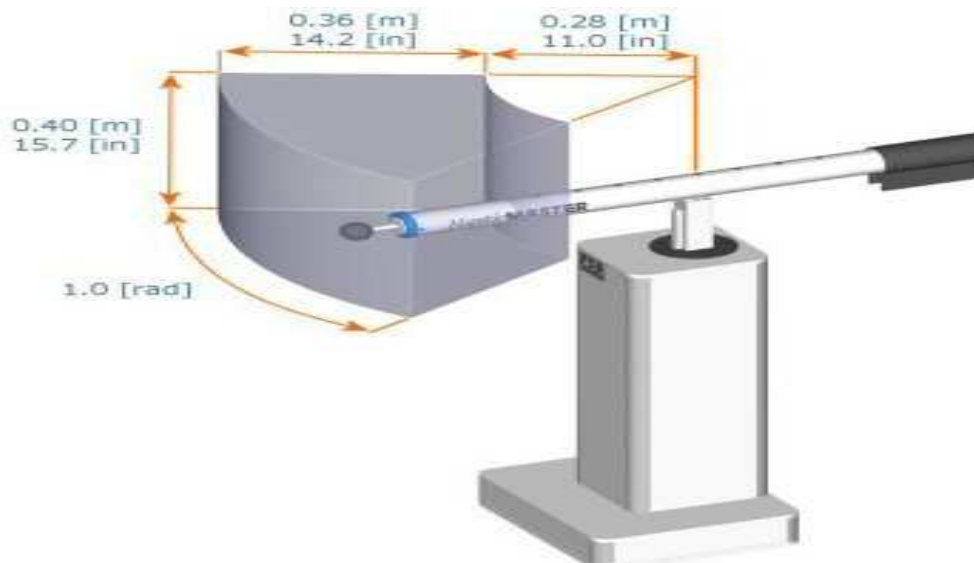


Figure 3.3 HapticMASTER Workspace (cited from H3D, 2010)

Table 3.1 Specifications of the HapticMASTER (H3D, 2010)

Position resolution	$4 \times 10^{-6} - 12 \times 10^{-6}$ [m]	1.6×10^{-4} [in]
Stiffness	$10 \times 10^3 - 50 \times 10^3$ [N/m]	285.5 [lbf/in]
Nominal/max force	100/250 [N]	22.5/56.2 [lbf]
Minimal tip inertia	2 [kg]	4.4 [lb]
Maximum velocity	1.0 [m/s]	39.4 [in/s]
Maximum deceleration	50 [m/s ²]	39.4 [in/s ²]
Force sensitivity	0.01 [N]	2.25×10^{-3} [lbf]

Source: http://www.h3dapi.org/modules/mediawiki/index.php/MOOG_FCS_HapticMASTER

The HapticMASTER measures the Cartesian forces exerted by the subject, measured close to the human hand, with a sensitive force sensor. An internal model then calculates the Cartesian Position, Velocity, and Acceleration (PVA), for which a (virtual) object touched in space would behavior as a result of this force. The PVA-vector is commanded to the robot, which then makes the movement by means of a conventional control law. The general control algorithm is illustrated in Figure 3.4. The internal model typically contains a certain mass, to avoid commanding infinite accelerations. The inner servo loop cancels the real mass and friction of the mechanical device.

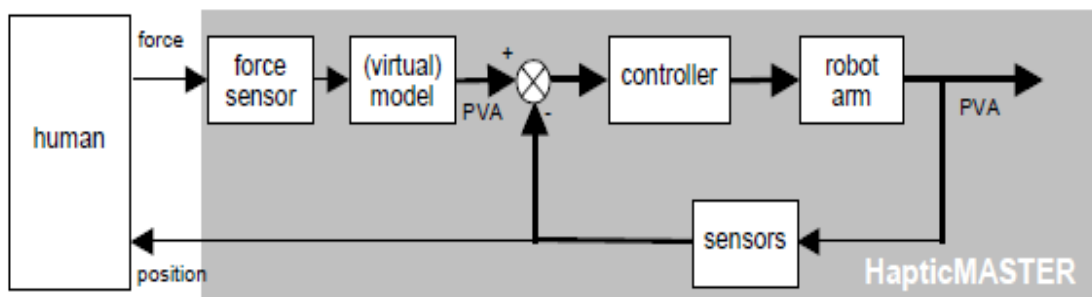


Figure 3.4 The General Control Scheme of the HapticMASTER Comprises an Outer Control Loop, and an in Inner Servo Loop. A (virtual) model converts the force sensor signal to a Position/Velocity/Acceleration setpoint vector. The inner servo loop controls the robot to the PVA setpoint values (Vander Linde, 2002)

The Cartesian velocity, position and forces of the robot's endpoint are measured. 1000 HZ are available as output via the HapticMASTER Application Programming Interface (API). The API allows one to program the robot to produce haptic effects, such as spring, damper and constant force and to create haptic objects like blocks, cylinders and spheres as well as walls, floors, ramps and complex surfaces. These effects can be used to provide a haptic interface with realistic haptic sensation that closely simulates the forces found in upper extremity tasks (Adamovich et al., 2009).

An important goal for the utilization of the Haptic Master was to take advantage of its multi-planar, 3-dimensional workspace. To accomplish this goal and to accommodate subjects with both normal subject and the subject with a variety of impairments it was necessary to design several mechanical attachments to interface the upper extremity with the Haptic Master robotic arm (Adamovich et al., 2009). The HapticMASTER can be fitted with any customized end effector, facilitating different applications. Any self-made end effector below 3 kg can be mounted at the end of the HapticMASTER robot arm. Two different sized forearm supports were fabricated for different arm shape and one universal articulating arm support was purchased to support the forearm effectively, counteracting gravity. Subjects with arm function simply grasp a stationary 1.2 inch diameter, 6 inch height cylinder connected to the Haptic Master (see Figure 3.6 and 3.12).

The HapticMASTER is programmed by means of a HapticAPI, which is a C++ programming interface that enables the subject to control the HapticMASTER. However, all other devices have been synchronized and worked under MATLAB. Therefore, the lab

research engineer, Diego Ramirez, MS, compiled these HapticMASTER C++ functions into MATLAB. To simplify the setup of the experiments, these functions are listed below:

- HM_setup (setup spring, damper, buffer and force for initialization)
- HM_cleanUp (delete all setup)
- HM_creat_block (creat a virtual block with setup center, orientation, size, stiff and damp)
- HM_creat_damping (creat damper)
- HM_creat_spring (creat spring with setup position, stiff, damp and deadband)
- HM_dataThread (send a TTL signal to another computer fro data stream with time stamp)
- HM_disable_damping (disable the damping effects)
- HM_getInfo (read the force, timestamp, position from buffer)

In the experimental application of HM, there were several critical technical problems in the data synchronization and collection and the solution for these problems are addressed as follows,

1. NJIT developed software allowed the simultaneous plotting HM / hand position relative to the targets on the LCD monitor. However, the actual experimental design did not empty visual feedback to avoid higher level processing of motor control.
2. The setting of dead band was inspired by the observed oscillation at the HM initial position. By changing the dead band setting and imposing damping, the oscillation problem has been successfully solved.
3. The added perturbation was controlled by a timer. The study found the refresh of the control in HM was less than 1 ms, so HM could be sent continuous controlling commands to refresh the controller. And it enabled us to add a 120 ms perturbation during the movement. However, the accuracy of perturbation duration is under the control of timer of Windows® Operation System.

3.2.4 Synchronizations of EMG, trakSTAR and Force Measurements

After the eight C++ functions were been compiled to MATLAB functions, the synchronized trakSTAR and EMGs data (collected in one computer) were synchronized

with dat from the HM computer. This HM synchronization with the EMG and TrackStar system was very challenging. The HM is assembled by MOOG FCS, and the company provided all drivers and API functions in format of C++, which is not directly compatible with MATLAB. HM data were collected with a 1 ms resolution time stamp. The start of HM data collection was processed by an synchronization pulse. That was read by the computer collecting trakSTAR and EMG data.

The HM computer produced a TTL pulse that was read by the second computer through a NI-USB 6216 DAQ card waiting the TTL signal for 10 seconds. A MATLAB function peekdata, which takes a "snapshot" of the most recent acquired data without removing it from the acquisition engine, was used to read the voltage value every other millisecond until signal reached its set action potential voltage.

After completion of above tasks, two collected data files from two individual computers are loaded into one data file for data processing, a data processing program sorts the data according to their time stamp, meanwhile the position data collected from HM and trakSTAR are processed to confirm the synchronization effect.

3.3 Experimental Design and Setup

Single Joint (Elbow) Movement: Ten neurologically intact young adults, participated in all trials. Subjects provided informed consent approved by the NJIT Institution Review Board. All subjects were right-handed. They all had some previous experience in similar experiments, in particular in experiments requiring them not to intervene voluntarily. Subjects were seated comfortably so that they avoided trunk movement. They were asked

to make elbow and shoulder movement or elbow movement only. All movement were made in the horizontal plane to avoid the influence of gravity.

Subjects were instructed to begin the movement from a specific initial position and move to a second position, both positions were selected to be in the middle 75% of joint range of motion to avoid known angles with major non-linearity in stiffness. Angular velocities were between 1 and 1.5 radian/second. Movements were made under 3 conditions:

1. Free arm movement with no hand constrain (trakSTAR only)
2. Movement in contact with the HM, which applied a small, but noticeable resistance.
3. Movements in contact with the HM as above, but with occasional, unexpected increases in resistance by the HM.

The unexpected resistance forces were generated by the program increasing the HM damping. Arresting forces were applied for 120 milliseconds at the start of movement, with viscosity sufficiently high to prevent movement. Perturbation forces were generated for same time ~ 120 milliseconds during the movement by increasing viscosity to a level that was noticeable by the subjects, but did not arrest movement. Subjects were insured not to consciously react to the momentary forces.

To discourage subjects from making corrections, hints and errors were not reported to subjects. Subjects were discouraged from anticipating the condition in the upcoming trials.

3.3.1 Unobstructed Arm Multiple Joints Movement with trakSTAR

In the study of multi-joint arm movement, the same subjects and similar setups have been utilized as in 3.3.1 with some changes applied to the shoulder. The subject has to adjust

the elbow angle to the initial position of 135 degrees and 45 degrees at the shoulder. After relaxing the entire arm, the subject made a reaching movement that uses both joints to the target. The target was placed at optimal range of motion approximately 25 cm away from start. Subjects hold the “Start” within the starting circle for 1 second to initiate each trial. They are instructed to move the right hand to the target using an uncorrected, normal and fast motion in response to an audio “start” command. When the hand reached the target, subjects hold the position until told to reverse the movement to the start position. That is to say 10 subjects participated in optimal angular distances with fast and medium angular speeds.

3.3.2 Elbow Flexions with trakSTAR® Only

The subjects sat comfortably in a chair with their right arm supported on a horizontal plane (a fixed leg table during the movement), adducted the right shoulder 90° and straight up to minimize the movement of the shoulder, and positioned the right hand on a horizontal plane, the upper arm of subject was supported by a height adjustable ergonomic arm support (see the configuration of designed fixed arm support in figure 3.5), the arm support mounted on the table surface firmly, the special material and surface coating were made to avoid metal interference to the trakSTAR® sensor (see the detail of design in Figure 3.3).



Figure 3.5 The Setup of Arm Flexion

The axis of rotation of the lower arm corresponded to the center of the elbow joint. The start, and end points were marked on the table surface (see the Figure 3.5). The shoulder joints were mildly immobilized using a brace when elbow movements were measured. Position and orientation of each segment was sampled using trakSTAR® (Ascension Technology) sensor. A sensor was attached and glued to the top of plastic cylinder holder (cylinder or cylinder holder all mean this plastic cylinder holder in the following study), and a laser diode attached at the cylinder bottom for movement position indication. The cylinder weighs 144 (without) /178 (with Diode) grams. One PC was used to control the experiments, and collected data from both EMG devices and 3D Guidance trakSTAR® system (Ascension Technology) to record angle, angular position at 100 Hz, and EMG at 1000 Hz. EMG' activity of short head biceps (BB) and long heads triceps (TB) were recorded. Muscle crosstalk can be reduced by careful electrode positioning, since it is difficult to distinguish crosstalk from synergistic contractions. Adult general purpose electrocardiographic electrodes (1 1/2" Foam) were adhered over

the muscle bellies and used for bipolar EMG recording. The distance between electrodes was 3 cm. Surface skin of muscle bellies were previously cleaned with alcohol to reduce skin resistance and thus maximize the signal-to-noise ratio. EMG signals were amplified ($\times 1000$) using a multi-channel electromyography card (PCI-6024E made by National Instruments®), band-pass filtered at 55-600 Hz by a 4th-order zero-lag Butterworth filter. The EMGs of trials were rectified, filtered, and averaged.

Elbow angle was measured by a trakSTAR® sensor mounted on the top of cylinder. Angular velocity was calculated by central differentiation of the position signal, so was the angular acceleration. Tangential velocity was measured by a mounted trakSTAR® sensor also. Anthropometric parameters for the subject were computed according to Winter.

Prior to each series, each subject was given 5 practice trials, during which they were encouraged to perform unidirectional elbow flexion movement as fast and accurately as possible over 1~1.5 radians from a fixed initial to a fixed final position (90° and 60° for elbow flexion in all trials). Two target lines were located at left side of body, distance between them was 1 radian, these lines were marked on the table surface as baseline (Start Position), Mid-Line (Target 1) and Final-Line (Target 2) respectively. Subjects were instructed to occupy an initial position “Start”, to wait for a beep, to move to a Target 1 staying for 1-2 second, then move back to the Start Position, and repeat movement to Target 2 until the trial ended. They were asked not to correct their movements in cases of motor-generated perturbation. Each series consisted of 6-10 repeated trials; intervals between the trials were 1 minute; intervals between the series were about 10 minutes.

3.3.3 Elbow Flexions with both trakSTAR® and HapticMASTER

The subjects sat comfortably in a chair with their right arm supported on a horizontal plane, with the right shoulder 90° adducted and straight up to minimize the movement of shoulder, and with the right hand positioned on a horizontal plane. The upper arm of subject was supported by same arm support, and arm support was mounted on the table surface firmly. The shoulder joints were mildly immobilized using a brace during elbow movements. Same Start Position, Mid-Line, Final-Line were marked on the table and a laser diode was mounted on the bottom of cylinder to indicate the movement (see the Figure 3.6). The 6 cm amplitude of vertical movement allowance was set in all trials by added wall block to lock vertical movement.

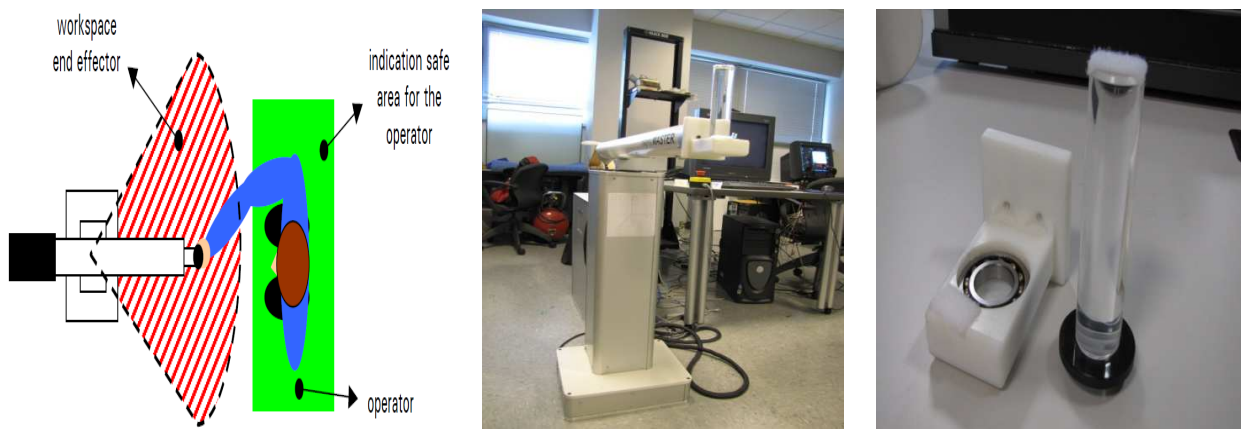


Figure 3.6 The HM Setup and Working Space

The axis of rotation of the lower arm corresponded to the center of the elbow joint. Same Start Position, Target 1 and Target 2 position were used in 3.3.1. Position and orientation of each segment was sampled using trakSTAR® sensors. A sensor was attached and glued to the top of the plastic cylinder, and a laser diode attached at the cylinder bottom for movement position indication. The cylinder was mounted on the pedestal of HapticMASTER (HM), with pedestal plus cylinder handle weight being 392.5

gram. Two PCs were used to control the experiments. One controlled and recorded force and position data from HM at 1000 Hz. Another synchronized and collected data from both EMG devices and 3D Guidance trakSTAR® system to record angle, angular position at 100 Hz, and EMGs at 1000 Hz. EMGs' activity of biceps short head (BB) and long heads of triceps (TB) were recorded. Same EMG electrodes, devices and setups were used in 3.3.1. Elbow angle was measured by a trakSTAR® sensor mounted on top of the cylinder holder. Subjects positioned right hand on a horizontal, very low-friction cylinder holder connected to robot manipulandum through a ball bearing, setting the HM Inertial to 2.0 kg. The cylinder holder, mounted to the robot manipulandum, self rotates to match the hand position during the movement. The axis of rotation of the lower arm corresponded to the center of the elbow joint, and no rotation of wrist was allowed during the experiment

Prior to each series, each subject was given 3 practice trials with HM, during which they were encouraged to perform unidirectional elbow flexion movement as fast and accurately as possible for 1 radians from a fixed initial to a fixed final position (135° and 60° for elbow flexion in all trials). Subjects were instructed to occupy an initial position "Start", to wait for a beep, to move to a Target 1 staying for 1-2 second, then moved back to the Start Position, and repeat movement to Target 2 until the trial ended. However, the actual experiments only required the subject to stay at the target till end.

Subjects were allowed to use their eyes during experiments and, in response to an auditory "beep" signal from speaker, make a fast arm movement by sliding the handle in the specified horizontal plane. They were asked not to correct their movements in cases of motor-generated perturbation. Each series consisted of 10 trials; intervals between the

trials were 1 minute; intervals between the series were about 10 minutes. Angular velocity was calculated by central differentiation of the position signal, as similarly so for the angular acceleration. Tangential velocity was measured by a mounted trakSTAR® sensor and HM to confirm the signals synchronization. Subjects' anthropometric parameters used in computation were cited from Winter (2005).

3.3.4 Voluntary Elbow Flexions with Unexpected Perturbations

Ten neurologically intact young adults, performed isotonic (50% of isometric maximal voluntary contraction (MVC) through 1 radians range of motion) elbow flexions at the fastest velocity they could achieve in all perturbed movement trials. Note that several subjects did both 1 radian and 1.5 radians range of motions of elbow in the preliminary study for statistical analysis, but 1 radian was used in actual data collection. The relevance of studies in intact humans with the “do not intervene” instruction, and factors which must be considered in predicting movement dynamics from measurements were made in the conditions. Same setups of trakSTAR®, EMG and HM were used in 3.3.1. Subjects received the Elbow flexions with unexpected perturbations in three different elbow flexion movements to assess the robustness of arm trajectory to different perturbations.

- Perturbed movement
- Arrested movement
- Pulling Movement

Torque motors of the HM provided time-varying external torque, and external torque changed once perturbation condition setups were satisfied. In trials with non-perturbation, damping force was 4.5 N to maintain the stability of the HM (minimal

stability remaining damping force); the study referred to these trials as “unperturbed”. The damping force increased to 50 N in the beginning of the arm movement, referred as “arresting movement”, 20 N perturbation added in the middle of movement were described as “perturbed movement”. All perturbations lasted for 120 milliseconds. The damping force decreased to 4.5 N after perturbation. The computer algorithms for experiment control and data collection were written in MATLAB, with 10 seconds of kinematic data recorded during each movement repeated 6 to 10 times. Because the subjects reported they were tired after running 10 times for a trial, especially a weaker EMG activity observed in second continuous flexion of elbow, experimenters decide reducing the trial to 6 to 8 times was more appropriate for each movement, with a short break between the trials.

In addition, integrals of both agonist and antagonist EMG bursts suggested that the subjects introduced a coactivation component in an attempt to stabilize the movements against the lower inertia, especially in less stable conditions. The subjects were required to performed additional trials as supplement in such condition.

3.3.5 Perturbed Movement

Subjects sit in a comfortable chair with their back supported. Subjects grasp the vertical, free rotation cylinder holder of the robot manipulandum, so the wrist and forearm are supported and rested in the neutral position. The weight of the upper arm and forearm were compensated by the arm support and pedestal base of holder of HM respectively. Most of the setups of movement were the same as 3.3.2 except added random perturbation and range of motion (ROM) is 1 radian fixed.

A radian of ROM was assigned for medium range of motion. A random perturbation was added as a format of damping force during elbow flexions, increasing the damping force to 20 N. A perturbation was automatically activated when HM tangential velocity went beyond 0.05 m/s. The minimal stability remaining damping force of 4.5 N was set. The perturbation lasted for 120 ms, then removed perturbation and kept minimal stability damping force until the end. Subjects repeated elbow flexion for 5 times, 10 second/time. Baseline, target 1 and target 2 were marked as start point, medium ROM and large ROM respectively on the table surface (showing in Figure 3.5). Subjects naturally paused at target for a couple of seconds at start point and targets.

Because the study found the extreme range of elbow motion was about 2 radians, the largest optimal range of elbow motion was set to 1.5 radians, and the peak velocity of the arm increased with the ROM increasing. The precision of stop control could cause high level control involved. Therefore, all subjects were required to make movement around 1 radian for their best comfort, however, no correction should be made even if the subject moves less or more than 1 radian.

3.3.6 Arrested Arm Movement

The ROM of arm was 1 radian in arrested movement. A random perturbation was added as a format of damping force during elbow flexions, increasing the damping force to 50 N. A perturbation was automatically activated when HM force reached 2 N, which was the force value just before the onset of movement. The minimal stability remaining damping force 4.5 N was set. The perturbation lasted for 120ms, then removed perturbation and kept minimal stability damping force until the end. Subjects repeated elbow flexion for 6

to 8 times, 10 second/time. Subjects were required to pause naturally at target for a couple of seconds at start point and each target.

3.4 System Calibration

In order to obtain reliable data, the calibration of the system is necessary and important in this study. The study ran the system calibrations before the data collection, with procedures including calibrations of EMG, trakSTAR, HM and device synchronization hardware and programs. The typical calibration results are shown in the Figure 3.7.

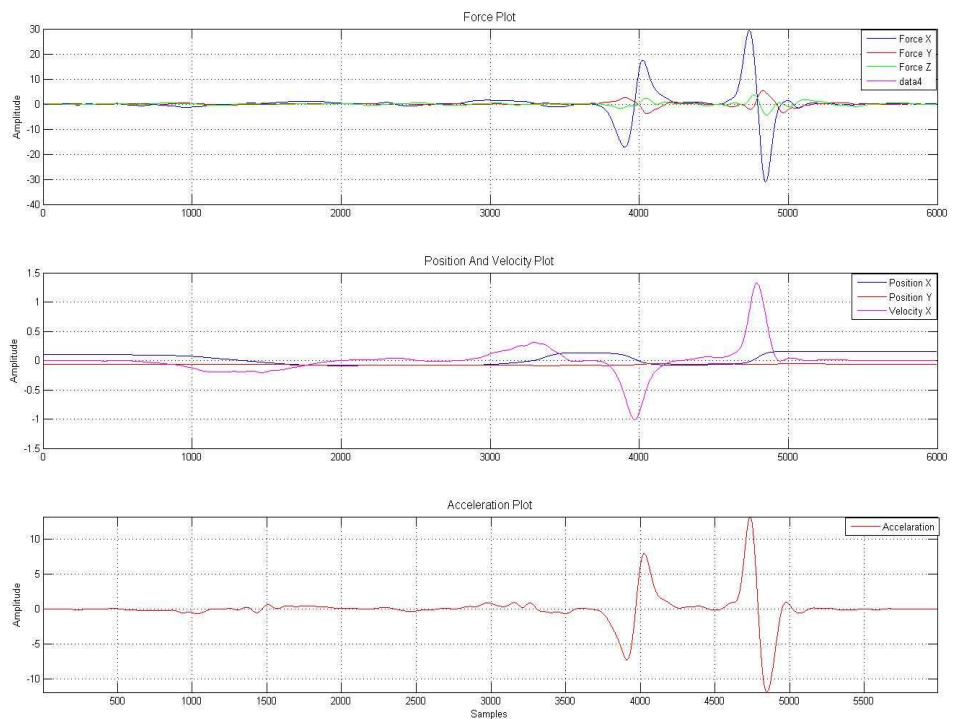


Figure 3.7 The Calibration of HM Forces, trakSTAR Positions and System Synchronization

3.5 Trouble Shooting in Data Collection Systems

In Figure 3.8, the noise of EMG was found to be much higher than the expected. It seems that the strength of signal was weaker than the noise, so the signal had been covered by the noise. The source of noise has been concluded to be from the transmitter of trackStar. After investigation, moving the trackStar transmitter to its 1 meter expired range can lead to inaccurate data, although it significantly reduced the EMG noise.

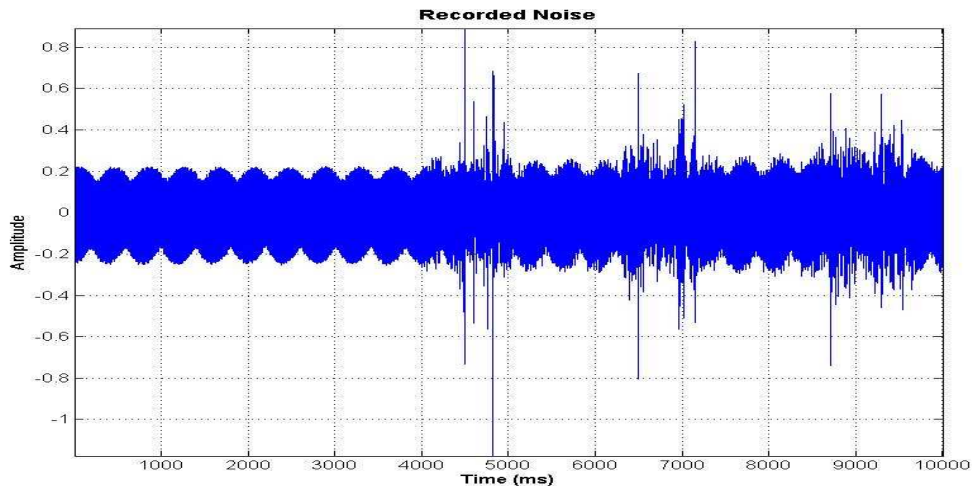


Figure 3.8 The Recorded of Environmental Noise

Then carefully studying the noise in term of frequency and known properties of, a Discrete Fourier transform has been performed to analyze noise in both domains by means of separating the frequency component from noisy signal. Considering this situation, EMG data was sampled at 1000 Hz with a signal containing 100 Hz sinusoid with amplitude 0.2, 120 Hz sinusoid of amplitude 0.3 and corrupted by zero-mean random noises.

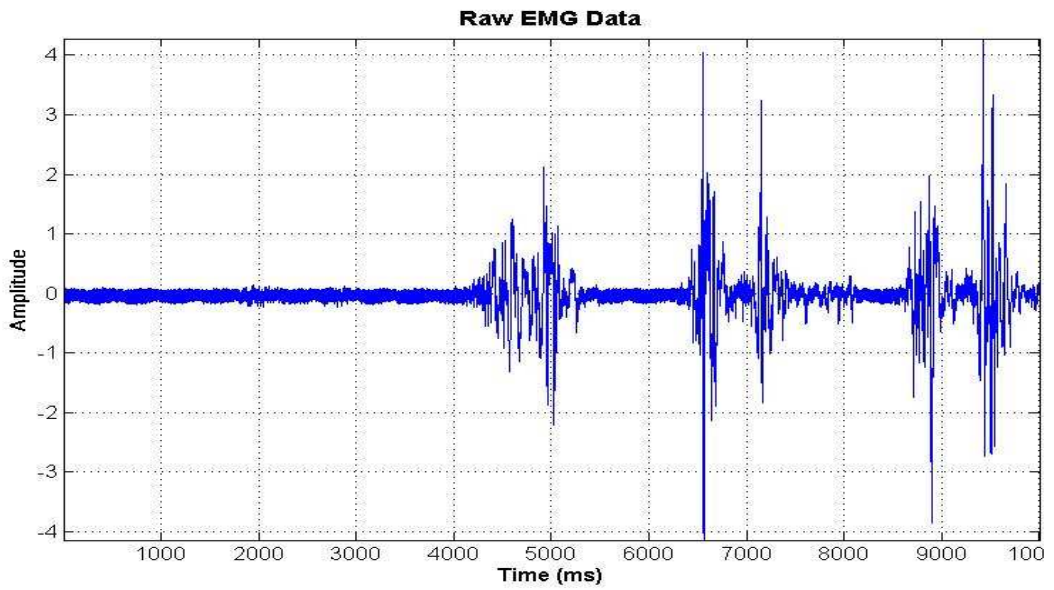


Figure 3.9 Raw EMG Signal

Spectrum analyzes the noisy signal was performed by converting time domain to the frequency domain in terms of Fast Fourier transform (FFT) in MATLAB:

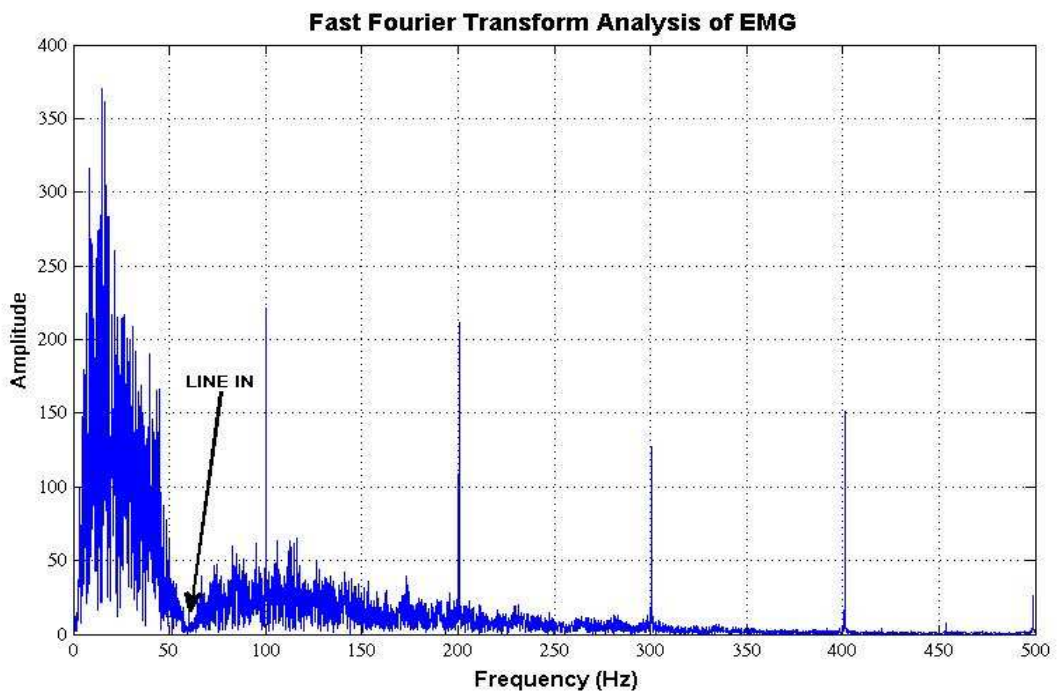


Figure 3.10 FFT Analysis of Raw Data

The FFT results shown in Figure 3.10 shows the 60 Hz notch filter of the Grass amplifier. Spikes in amplifiers occur as ~ 100 Hz and multiples of 100 Hz. This is due to the trakSTAR recording the data rate at 100 Hz. Normally, EMG studies require high frequencies, but this study only uses EMG signals to determine the onset of agonist EMG and peak of antagonist EMG, it is possible to apply a low pass filter with a cutoff below 100 Hz.

Figure 3.11 shows the filtered EMG of data collected with the trakSTAR transmitter at an optional distance. The 6th order butter filter was applied to filter the noise, and the filtered data demonstrated noise reduced significantly in Figure 3.11.

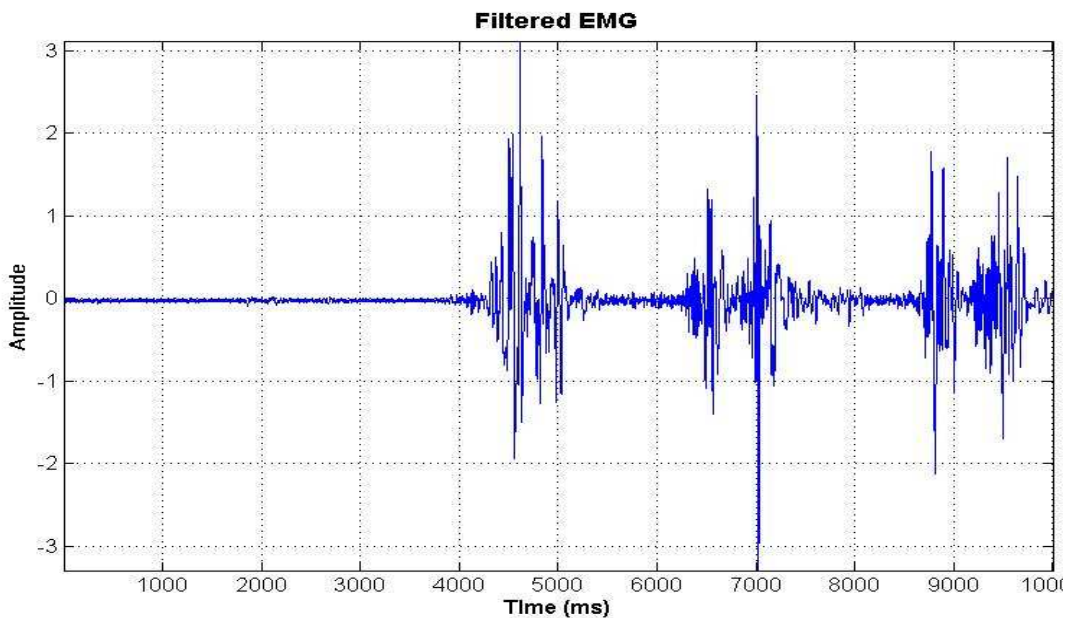


Figure 3.11 The Filtered EMG Signal

From the raw EMG signal (shown in Figure 3.9), the absolute value or rectified waveform can be derived. When this was done, the observation found a noisy appearance in the baseline in Figure 3.8. This noise was removed by high-pass filtering at 10 Hz to remove electrode motion artifact and any DC bias that was present.

Setting for synchronization pulse: A binary input has to be set in HM program in order to generate a synchronization pulse sent to the EMG and trakSTAR program in the HM control program. The input setting is 15 (Input = $8+4+2+1=15$), reset is equal to 0 for the DB25 connector.

Table 3.2 The Setting of Synchronization Pulse

	1	2	4	8	16	32	64	128
Input	1	1	1	1	0	0	0	0
Reset	0	0	0	0	0	0	0	0

3.6 Experimental System and Simulation Models

The dynamics of the joints of the arm in reaction to perturbations have been approximated by a visco-elastic model: the K-B-I model (stiffness, damping and inertia in parallel). In the preliminary investigations, it became clear that a linear second order K-B-I model did fit well to the human arm movement, despite fitting artificially constructed K and B in the systems using the same apparatus and analysis methods. The problem arose from independent motion of upper arm soft tissue within the case. This soft tissue comprises more than 70% of the upper arm mass and has also been reported as a confounding factor in the determination of the moment of inertial of limb segments (Allum and Young 1976).

In the study, the author found that as the case/support was applied tighter or uncomfortable to the arm, particularly around the upper forearm, the limb appeared to become more rigid, although there was a limit to the case tightness that a subject could tolerate, due to ischemia and discomfort.

As the remediation, all corners have been rounded and multiple shapes have been fabricated to fit the subject for their maximal comfortability, 2 types and 3 sizes cases/supports are showing in the Figure 3.12.



Figure 3.12 Illustration of Two Types and Three Sizes Case/Supports

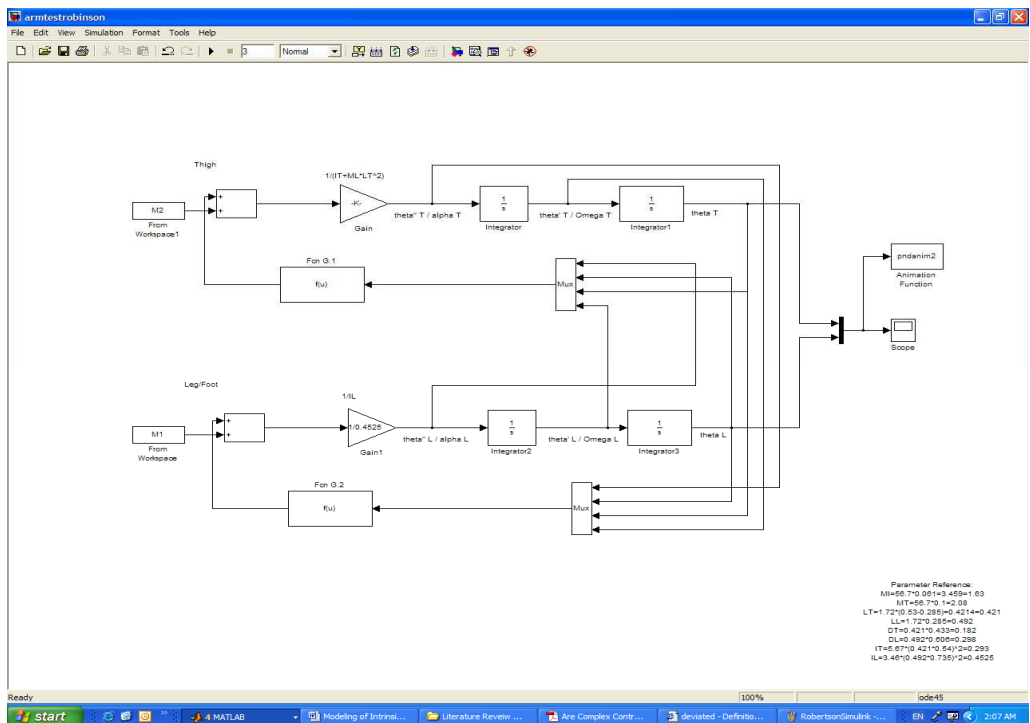


Figure 3.13 Robertson's Two Links Equations Represented with Simulink Model

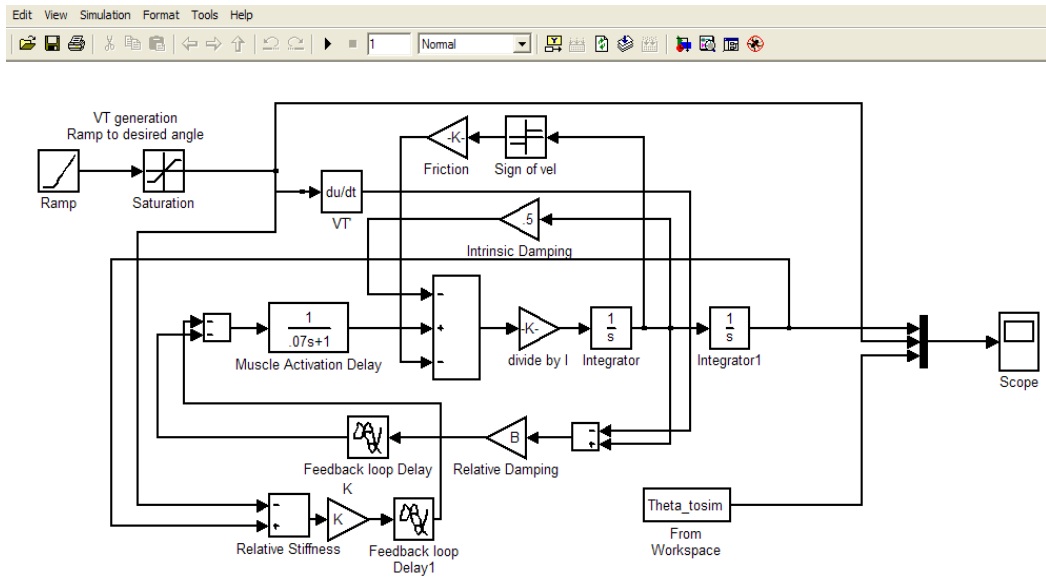


Figure 3.14 Single Joint Simulink Model

This study developed two joint (Figure 3.13) and single joint (Figure 3.14) arm movement control Simulink models with trakSTAR only. This model covered both the relative damping model in single joint (Figure 3.14) and two link segments kinematics forward model (Figure 3.13), with the schematic of the arm movements control system shown in Figure 3.15 for two links.

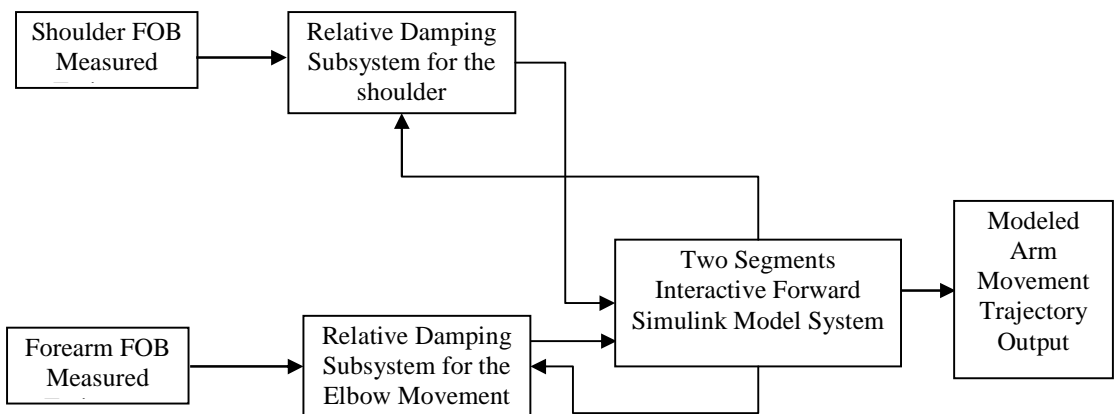


Figure 3.15 The Schema of Multi-Joint Control Model System

CHAPTER 4

RESULTS AND DISCUSSION

4.1 Preliminary Study Results in Unobstructed Arm Movement

4.1.1 Relative Damping Model in Human Arm Movement Simulation

A neurologically intact male adult, 23, sat facing a table with the right arm supported over the horizontal surface. The start, and end point had been marked on the table. The shoulder joint was immobilized using a brace. Position and orientation of segments were sampled using Flock of Birds (Ascension Technology) sensor. A sensor was attached to the upper-arm segment, and another sensor was fixed to the lower-arm segment near the wrist joints. The sensors were positioned approximately at the proximal end of the segments and parallel in the same direction. The computer algorithms for experiment control and data collection were written in MATLAB and 10 seconds of kinematic data have been saved each trial.

In the experiments, the study placed two targets that required 25 cm long movements for the reaching movement. Subject held one target within the starting circle for 1 second to initiate each trial. The subject was instructed to move the right hand to another target using an uncorrected, rapid motion in response to a visual “start” signal. When the hand reached the target, the subject returned to the initial position. The motion had been repeated until the “Motion Terminated” sign was shown on the computer. The normal speed and fast speed of two joints right arm motions were recorded.

In the following trials, the preliminary study fixed the upper arm for the elbow joint movement only. The subject was required to perform the repeated elbow movement

from full flexion to extension when he got the visual single ‘start’, and stop when “Motion Terminated” single was received. The range of forearm movement started at approximately 45 degrees to 180 degrees and three trials were recorded.

Equation (3.1), (3.2), (3.13) and (3.14) were used and incorporated the relative damping concepts in the MATLAB Simulink Models to simulate the arm movement in single and double joints reaching movement. The results suggested that the results have more merit in terms of accuracy, simplicity and compatibility over other earlier proposed damping concepts.

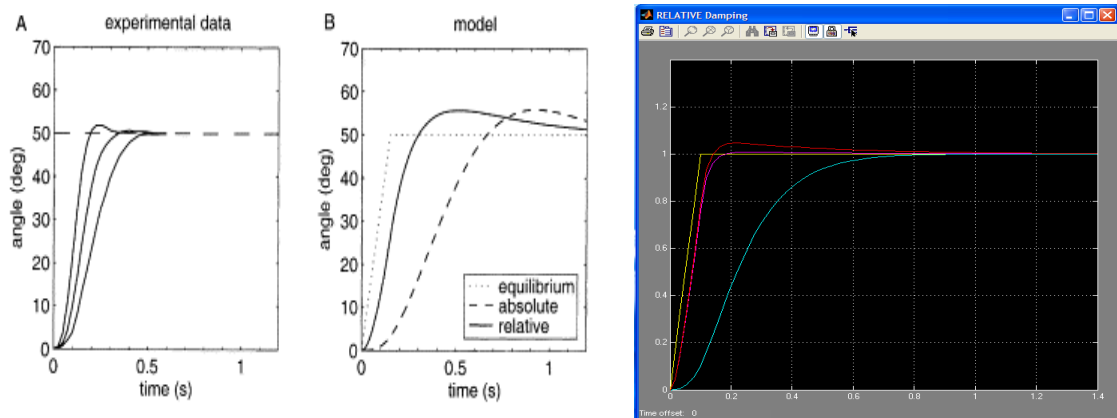


Figure 4.1 Single Joint Movement Simulation Results. A: Fast elbow flexions towards targets at 50° eccentricity with a width of 3° , 6° and 12° (data from Gottlieb, 1989). B: Examples of predicted single-joint elbow movements (source from de Lussanet, 2002). C: Author's Vs Marc's Simulation

de Lussanet et al. (2002) modeled the single joint elbow movement (see Figure 4.1), and their results appear in panel B demonstrating that relative damping makes it possible to generate faster movements with a linear mass spring model than absolute damping. The difference exists in movement time between the movements predicted with absolute and relative damping. The fastest motion generated with absolute damping was 0.5 seconds, but it was less than 0.2 seconds with relative damping. However, Mark and

et al. only studied and evaluated the EPH activation pattern for about 1 second. Few studies have been performed to quantitatively evaluate the angle or torque amplitude of EP activation pattern in longer duration for the repeated cycle arm movement.

Therefore, the Flock of Bird (FOB) sensor measured trajectories have been taken into single joint model to evaluate their amplitude. Three repeated fast movement cycles in Figure 4.2 and Figure 4.3 demonstrated the predicted angle and torque compared with relative and absolute damping of nearly 10 seconds of data. The results suggested that the angle with relative damping was almost a perfect fit to the experimental angle curve. By contrast, the angle with absolute damping did not fit the actual trajectory very well, it showed that activation amplitude with absolute damping was about 0.36 radian less than the relative damping; whereas activation delay was about 0.3 second.

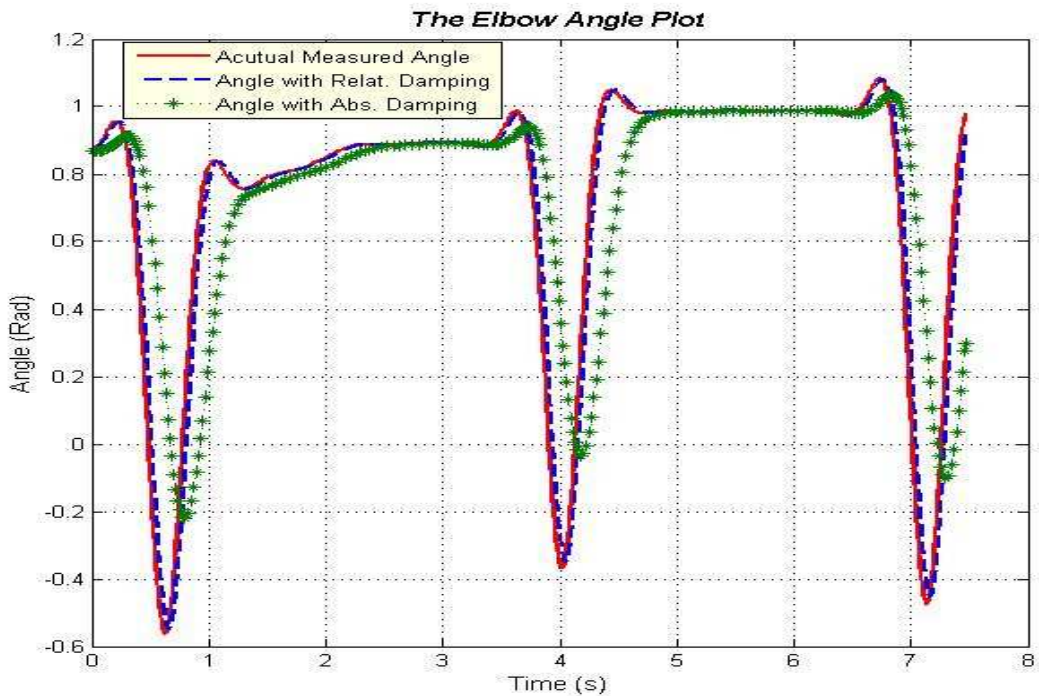


Figure 4.2 The Plotted Elbow Angle Trajectories in Fast Speed

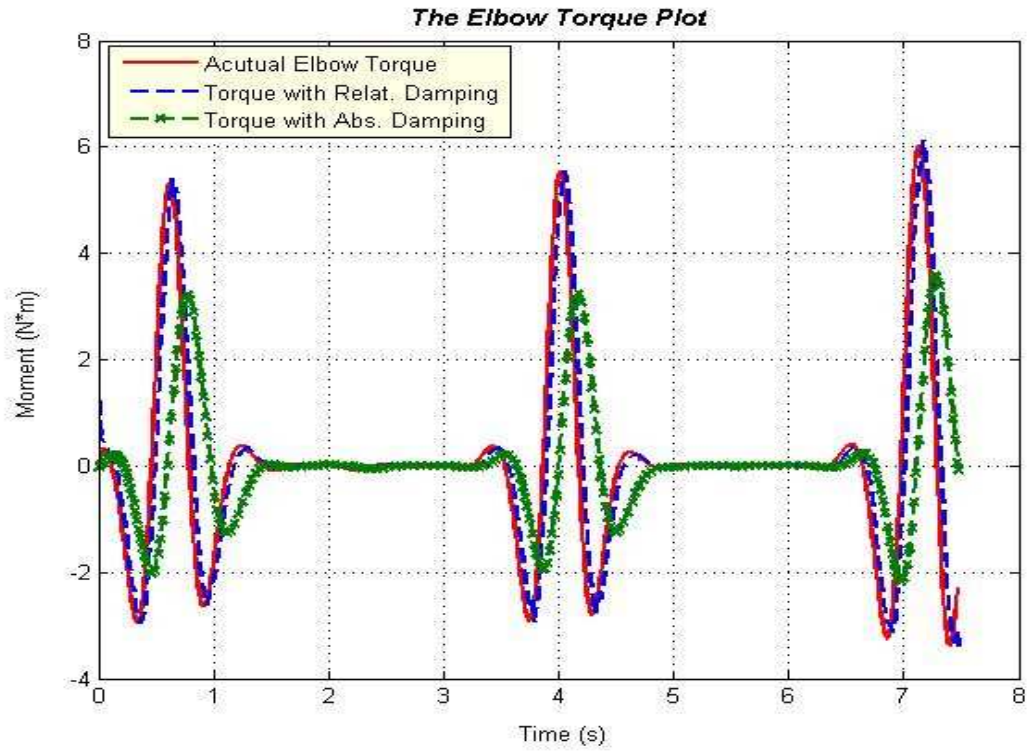


Figure 4.3 The Plotted Elbow Moments in Fast Speed

Modifications were made to the model to incorporate these added dynamics, such that the relationship between position and elbow torques was represented as simplified Equation 4.1 by:

$$\theta = T \dot{\theta} + \theta_0 \quad (4.1)$$

$$I \ddot{\theta} + B \dot{\theta} + K \theta = \tau \quad (4.2)$$

The second order model relates applied torque (τ) to joint angle (θ) through the parameters K , B and I . To address the motion of limb, a time delay (T seconds) was added as well as angle, θ_0 , which references the inertial component, where θ represents

the angle between the joint axis as opposed to the location of the elbow. With the delay, the simple dynamic model of such behavior act like a first-order filter. The transfer function of the limb impedance in the Laplace domain is shown below:

$$\frac{\theta(s)}{\tau(s)} = \frac{Ts + 1}{(BT + 1)s^2 + (B + KT)s + K} \quad (4.3)$$

As the time lag, T , approaches zero, the transfer function approaches that of a standard K , B and I system. The time delay, T , was chose to be 10 ms for all subjects. The inertial parameter, I , was fixed for each subject using the calculation procedure in Winter Textbook (2005). Stiffness and damping parameters were adjusted and optimized to fit the mean position response to the mean torque input before each perturbation condition. For a given perturbation condition, the study collected torque and position in 5 trials. Regression analysis result was showed as 0.1579, which is not able to decide whether or not there was a single-valued relationship between B and K with limited sample size.

To analyze kinematic and EMG patterns of primary movements, the traces were aligned according to the movement onset and then averaged. Traces in control and test trials for each series were averaged separately for comparison. The mean final positions in the test trials were compared with those in the control trials, in which movements were unopposed (the Equifinality test), using t-tests. The movement duration in perturbed movement was measured as the time from the movement onset (first visible deflection in the velocity trace from 95% confidence interval for baseline variations or 2-5 degree/s) to the point after which the velocity trace remained near zero. The duration of movements

opposed by minimizing stable damping were compared with the time to peak velocity of unopposed movements, using t-test.

The EMG amplitude (peak value) of agonist and antagonist activities were determined from the averaged traces for each test by integrals. When compared to a similarly evaluated EMG waveform of different subjects, it could tell which case represents the greatest amount of work done by the muscle. The duration of the first agonist and antagonist burst was defined as the time when averaged EMG activity increased and remained higher than 10% of the maximum EMG amplitude to when it decreased and remained lower than 10% of the same amplitude.

To characterize the EMG changes in response to the release of perturbation, mark lines have been used to separate the movement. The latency of the reflex decrease in the EMG activity in agonist muscles leading to the silent period was defined as the time between the beginning of the releasing and the time when the EMG trace began to decrease steadily. The latency of the silent period was determined as the time between the beginning of releasing to the time when EMG activity reached and remained at a minimal level. Multiple-regression ANOVAs with significance levels $p < 0.01$ were used to measure the difference between the different perturbation groups.

In the Figure 3.13, the calculated elbow and shoulder joint torques have been taken into the model as input. The model generated not only the same angular velocities, but also was nearly identical to joint angles as measured in the experiments. Then the relative damping model has been combined with this two link interactive forward kinematics model (see Figure 3.13) into a new model (Figure 3.15).

The results running in Figure 3.14 implies that the relative damping model could generate the ‘parameters’ called by Feldman to control the complex “Non-Linear Movement” system. The output of the complex system in Figure 3.15 gave identical output as measured in the experiment. Based on this hypothesis, this study took the FOB measured data as input into the model system; it ran in normal (slow) and fast speed of arm movement.

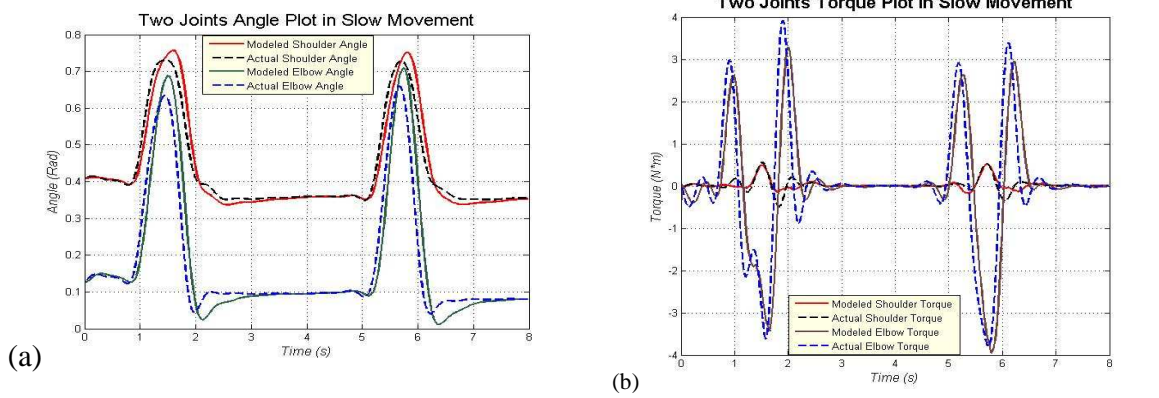


Figure 4.4 (a), (b) Two Joints of Angles and Torques Comparing with Exp. Data in Normal Speed

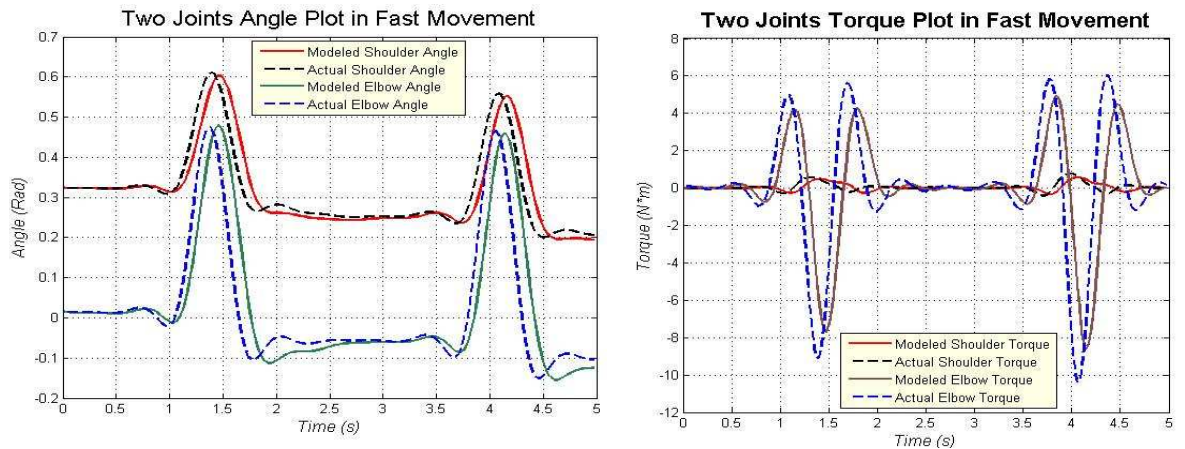


Figure 4.5 Two Joints Angles and Torques Comparing with Exp. Data in Fast Speed Arm Movement

It is well known that a simple linear mass spring model with absolute damping usually generates the slow movement with a realistic value of stiffness and damping. But with a stiffness that is higher than what is measured experimentally, Gible et al. (1998) proposed that the control signals underlying voluntary human arm movement have a “complex” non-monotonic time-varying form. Such solutions suggest that the human motor system but can be validated in slow movement only (Gomi and Kawato, 1997).

In the model, not only can similar performance be achieved by the simple mass spring system with relative damping for the single and multi joints performance, in which the author proposed a model with relative damping which generated much more accurate results rather than the traditional absolute damping model; but also this study has developed it into a two joint interactive forward kinematics model system. Preliminary results showed both torque and angle were very close to the experimentally measured curve except the study found the modeled data had approximately 0.1 second delay observed from the Figure 4.4(a). In the next part, intrinsic tissue properties and neural feedbacks integrated into the enhanced relative damping model could improve the performance and robustness of the system.

The study has not investigated both damping and stiffness in this part, but it is also very important to study neurally induced K and B modulated with the EPH. As acquisition of knowledge about how to regulate many muscles for the required movement proceeds, this knowledge corresponds to an internal model of the controlled object. As the brain acquires internal models of the controlled object, excessive damping can be avoided and mechanical properties of the musculoskeletal system could be optimally regulated according to constraints and the desired tasks. These internal models, which

discover the profound biological system through the investigation of the voluntary movement with loads and perturbation, continued in the following sections.

4.1.2 Single Joint Model with Neuromuscular Delays and EMG Determined VT

Ghafouri and Fedman (Ghafouri and Feldman, 2001) studied the timing of control signals underlying fast point-to-point arm movements. In a nutshell, they address the question of the timing of the virtual trajectory. Does the VT last as long as the actual movement, or does it end early? This question addressed one of the essential issues in the trajectory planning, the planning sequences.

Ghafouri and Feldman (Ghafouri and Feldman, 2001) did not have a simple way of explaining how the VT ends before the end of the actual trajectory. They offer a complicated discussion that is not overly convincing. This appears to rely upon an earlier study (St. Onge and Adamovich, 1997), in which they introduced the controlling variables as R , C and μ . R is the VT and it appears as a ramp between two angular states. μ is a constant damping coefficient, and C is the K . But, to make this work, they generate a non-linear K based on the idea that muscle stiffness increases with activation. To the understanding, this is counter to the EPH and their results can be explained by the relative damping model, which is physiologically feasible and incredibly simple. It does not involve contriving a non-linear K .

The musculoskeletal model is not only simple but also incorporates the timing issue as shown in the schematic (Figure 4.6). The muscle block contains the muscle dynamics, transferring the neural input signal (α -activation) to muscle force. The moment arms r transfer muscle force into muscle moment. In the inertia block muscle moment is transferred into accelerations, subsequently twice integrated to obtain the actual position.

Proprioceptive feedback can be divided into force feedback in the Golgi tendon organ, and length and velocity feedback (represented by K and time delay) in the muscle spindle. The moment arm r transfers joint angle to muscle length and joint angular velocity to muscle velocity.

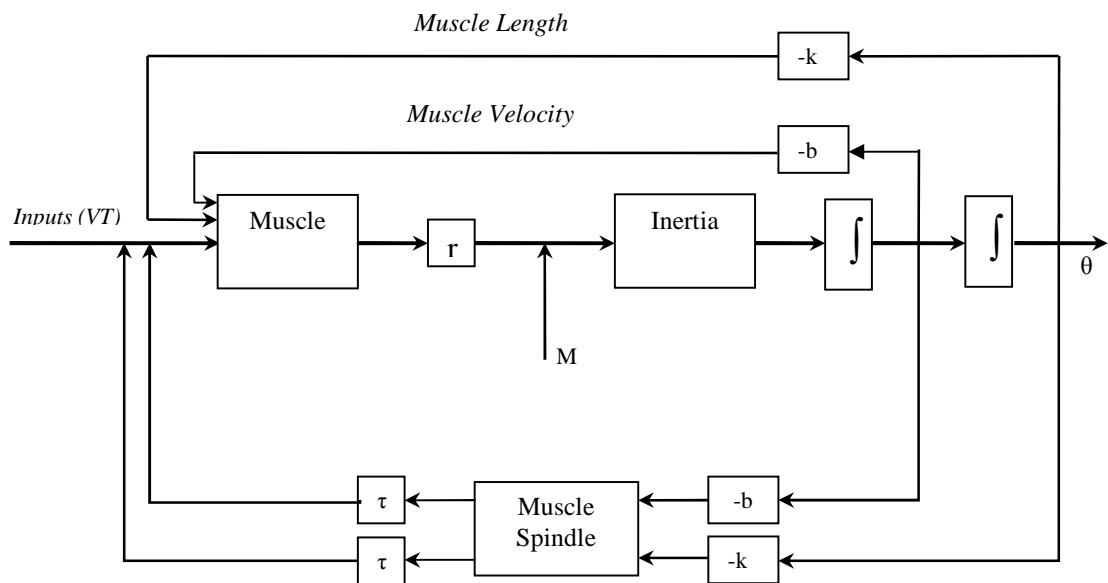


Figure 4.6 The Schematic Illustration of Velocity Feedbacks System

In this feedback loop, the study assumes it is a low-level spinal reflexes control system, generally assumed to be mono- or bi-synaptic. Muscle spindles contain nuclear bag and nuclear chain fibers, each with a sensory organ and intrafusal muscle fibers. Inputs to the muscle spindle are the γ motor-neuron activation of the nuclear chain, and length and velocity of the extrafusal muscle fiber. Outputs of the muscle spindle are the $I\alpha$ -afferent signals, containing length and contraction velocity information, and II -afferent signals containing only length information.

The problem in the control scheme presented is to find reasonable values for the feedback gains and time delay components. Although the control scheme may contain highly nonlinear elements, for sake of analysis it can be linearized in any state. In one word, the relative damping model has been modified concerning the timing delays, following configuration is the schematic demonstration of modifications.

In terms of simulation model, the above schematic has been cooperated in the Simulink model to test single ramp angle joint movement in the preliminary study. Simulations showed the role of velocity and length feedback for the behavior of the elbow. An extensive description of the values and perimeters employed in the simulation can be referenced from Rozendall (Rozendall, 1997) and Hogan (Hogan, 1984), (Hogan, 1985). Rozendall proposed sensory time delay (0.035), muscle excitation time (0.04) plus muscle activation time (0.03) are pretty closely matched to the results shown in Figure 4.7 with 0.1 second time difference between the VT and EMG.

In the study, the subject has been required to follow the instructed procedures as mentioned in unobstructed elbow movement (3.3.1), and run the simulation by the enhanced trajectory control model with timing delay. The angles, velocity, acceleration of elbow joint and raw EMG signals of triceps and biceps plotted in the Figure 4.7 compare the onset sequences between the angular and EMG activation pattern. The observed EMG pattern showed EMG amplitudes are generally less during negative (eccentric) work versus positive (concentric) work.

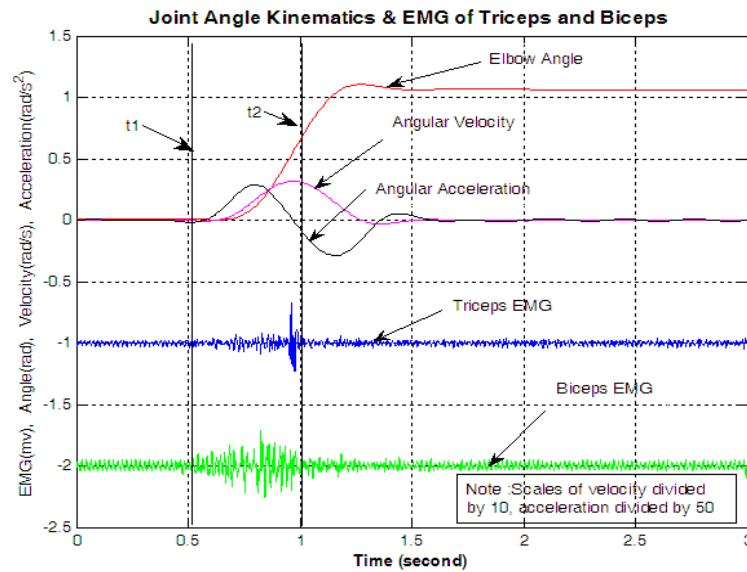


Figure 4.7 Data for a Typical Elbow Extension Shows Timing of Flexor (biceps) EMG Onset and Triceps (triceps) EMG Termination. t_1 and t_2 Were Determined Graphically

In the study of Ghafouri and Feldman (Ghafouri and Feldman, 2001), they argue that the Virtual Trajectory (VT) (movement of R) ends at about the time at which the actual trajectory reaches its maximal velocity. They argue that this trajectory is monotonic (in their case, a ramp between two angular states). They contrast this with the Latash (Latash, 1991) and Gottlieb (Gottlieb, 1989) notion of a VT that continues to the end of the actual movement and is non-monotonic. (Assume the latter to be Latash's N-shaped trajectory). However, looking at the EMG patterns in Figure 4.8, assume the beginning of the agonist (biceps) burst is the starting time of the VT at t_1 . Then find the time of the ending of the antagonist (triceps) burst (braking). Assume that this is the time at which the VT ends at t_2 . Observing the plot in Figure 4.7 and one can see a VT that parallels the actual trajectory, separated by a time lag of roughly 0.1 second.

EMG is the result of EPH ($\dot{\theta} - \dot{\theta}_{vt}$), $\dot{\theta}_{vt}$ is zero at time t_2 , and $\dot{\theta}$ is maximum at time t_2 , as shown in the Figure 4.8:

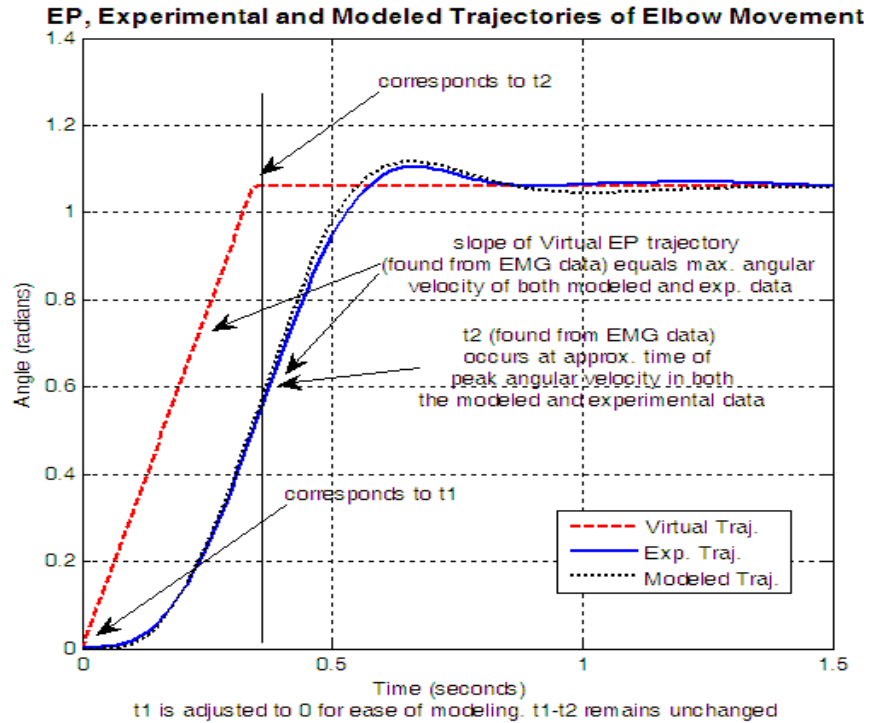


Figure 4.8 Results of Model with Experimentally Determined Virtual Trajectory, Optimized B and K, with Elbow Data

Therefore, this study chooses the peak of antagonist EMG, which is at time t_2 , as the end of the virtual trajectory, and the experimental results show that the peak velocity occurs at the peak of antagonist EMG.

The results are summarized in Figure 4.7. The virtual trajectory was defined by values of t_1 and t_2 from the EMG data, and an output angle equal to final angle by the experimental data. The output of a Simulink model driven by this trajectory was compared with the experimental data, and values of B and K were optimized (see Equation (3.2)). Figure 4.9 shows accurate fit of model output to experimental elbow

angle. Additionally, the ending time of the virtual trajectory ramp occurred at approximately the same time as the peak angular velocity predicted. In addition, the slope of the graphically extracted virtual trajectory matched the peak value of the angular velocity (3.15 rad/s). The net joint moment of the experimental data was computed using inverse dynamics and was compared to the net joint moment of the model in Figure 4.9. The model successfully produced the expected activation and braking pattern of human joint movement.

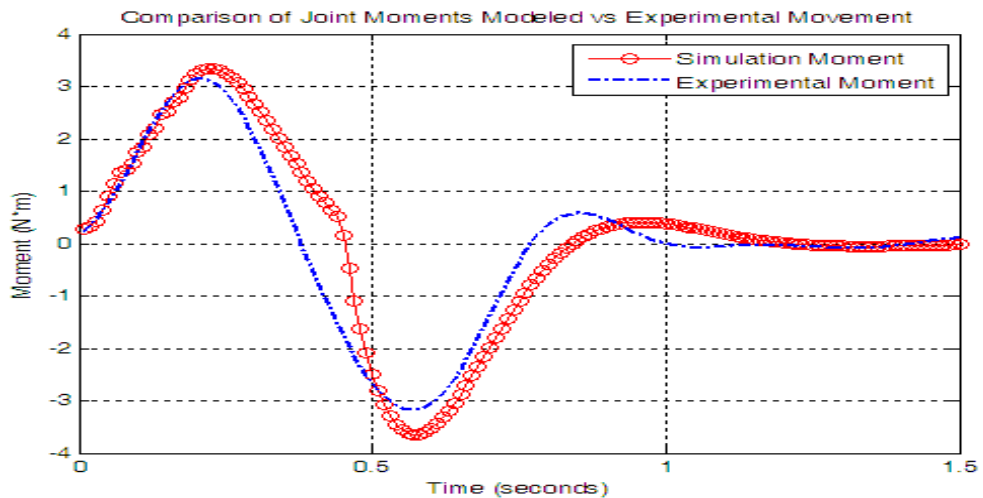


Figure 4.9 The Joint Moments of Experimental and Model Data

Then subjects were requested to perform more complex tasks, such as to reaching the target and returning 5 times in the 10 seconds' trial. The EMG of extensor and flexor of arm muscles were filtered and rectified to identify the onset sequences of activations (see the Figure 4.10).

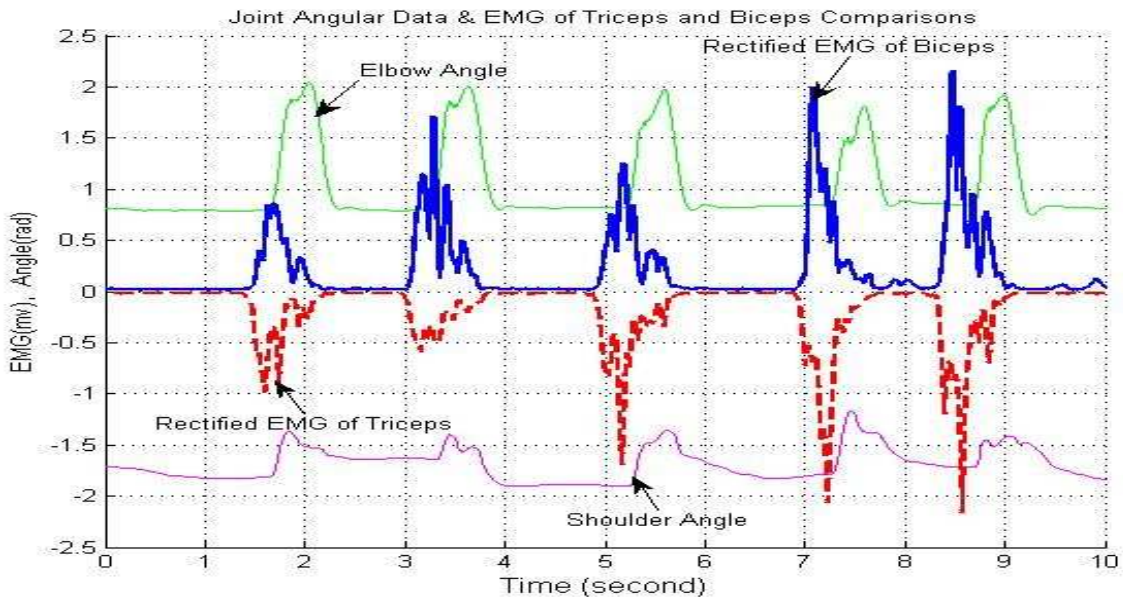


Figure 4.10 Data for Arm Joints Extensions and Flexions (Angles has been shifted for better comparing)

The modeled results showed comparisons between input virtual trajectories and simulated Equilibrium Point trajectories of elbow and shoulder (see Figure 4.11).

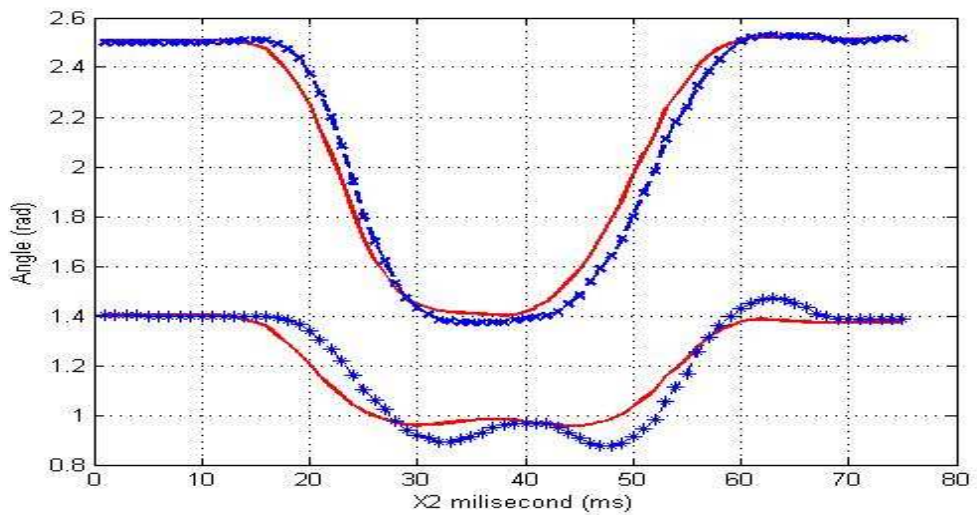


Figure 4.11 Data Comparing between the Experimental (Red Solid) and Simulated (Blue Stars) Angular Trajectories. (The upper are elbow angles, the lower are shoulder angles, multiplied X2 by 10 is the time-milliseconds)

4.1.3 Summary of Unobstructed Arm Joints Movements

All the results shown in 4.1.1 and 4.1.2 can be summarized. The control evidence implied the elbow trajectory planning could be completed without continuous control guidance, which supported the idea that the planning command could be preset in timing sequence. Secondly, the simulation result suggested that the model was robust enough to incorporate the timing in the physiological feasible range after successfully using the study's proposed neuromuscular delays into the arm trajectory control models. 4.1.1 and 4.1.2 together can be draw to the conclusions for preliminary study:

- The enhanced relative damping model allows the model to produce a trajectory that is reasonably fast and accurate.
- The model is able to incorporate the timing of a hypothetical EP trajectory that is taken from experimental EMG data and produce a realistic output that is close to the experimental data from which the EMG resulted (see the Figure 4.7) and is consistent with St. Onge et. al. 1997 (St-Onge and Adamovich, 1997)
- The model can incorporate a realistic 70 msec combined muscle stimulation and activation delay as well as 35 msec reflex loop transport delays.

Hence, the preliminary study provided a substantial and acceptable groundwork to explore a more complex movement conditions in arm motor control and movement trajectory planning.

4.2 Haptic Effect in Unobstructed Elbow Movements

4.2.1 Unobstructed Elbow Flexions with both trakSTAR® and HM

HapticMASTER (HM) required minimal mass and damping to maintain its stability, 2 kilograms' moment of inertia and 4.5 N·s/m of damping are minimal setup for stable movement. As this will be felt by subjects, it is expected that they will load to

accommodate the presence of the HM. Thus, it is unlikely that the VT and optimized B and K from this Non-HM trial will apply in this occasion. In such case, optimized B and K from no HM trials could not match model outputs to experimental HM adds an interruption, and subject can not help but accommodate and reset K, B and possible VT. New K, B and VT were found in trials using HM. With new K, B and VT model match quite well. Now B and K variances were optimized, and new VT was determined from this agonist and antagonist EMG.

4.2.2 The Influence of HM in Terms of Speeds

A Random selected subset of subjects were asked to make similar elbow flexions of the same magnitude as fast as possible with and without HM. The subject data was averaged for HM trials. Tangential velocity of the free hand movement was 4.430 m/s, and the angular velocity of the movement was 8.465 rad/s. Movement data with HM were averaged and the tangential velocity of the hand movement was 1.460 m/s, the angular velocity of the movement was 2.770 rad/s. These results show that the inclusion of the HM introduces a continuous perturbation throughout the movement, confirming the need to reoptimize the B and K.

4.2.3 The Influence of HM in Terms of EMG and Force

EMG Pattern were extracting from the above HM and non-HM fast movements. The HM applied to alter EMG duration indicating that the subjects will have their VT altered. This supports that determination of new VT for the HM tests. Figure 4.12 and 4.13 showed that the identical time used in EMG and kinematics properties plots of both conditions as descriptions.

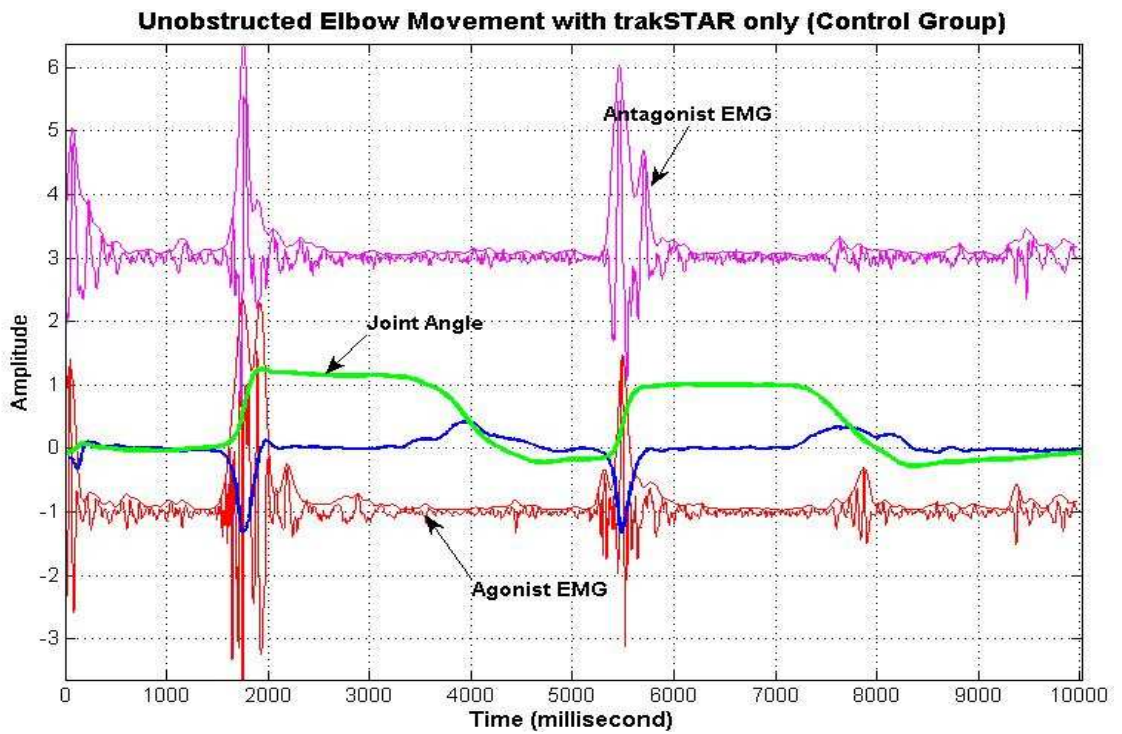


Figure 4.12 Unobstructed Elbow Movement with trakSTAR only (S1)

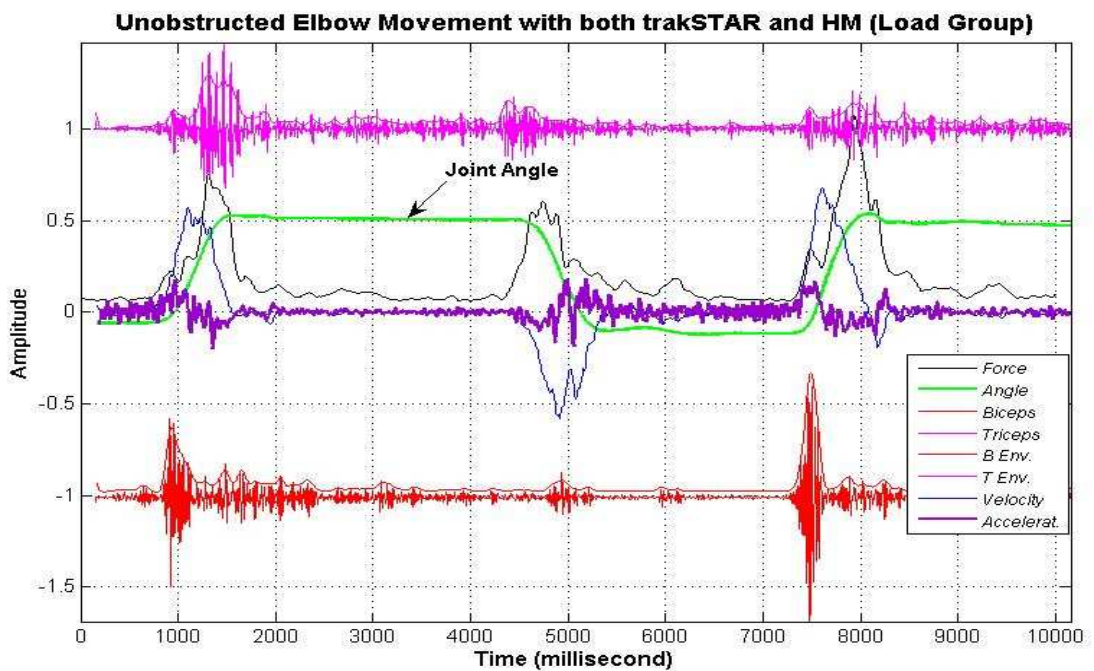


Figure 4.13 Unobstructed Elbow Movement with both trakSTAR and HM Plot

To analyze kinematic and EMG patterns of primary movements, the traces were aligned according to the movement onset and then average of subjects. Traces in control and test trials for each series were averaged separately for comparison. The mean final positions in the test trials were compared with those in the control trials, in which movements were unopposed by the HM initial load. The duration of movements opposed by the minimal load was compared with the time to peak velocity of unopposed movements. Using t-test, the time to peak velocity of tested arm movements opposed by the minimal load was significantly increased for all trials in comparison with control group ($P < 0.005$; group means: 359 ms and 229 ms, respectively).

As for the EMG patterns, the control, unopposed/free movement was associated with agonist followed by antagonist muscle activity, while the end of the movement was characterized by some additional agonist/antagonist bursts, which was similar to that which Brown and Cooke found (1986).

The introduction of the minimal load in the loaded trials elicited substantial changes both in the phasic and the tonic EMG pattern. Although the changes in the amplitude of the first agonist burst were insubstantial, the burst was substantially prolonged and displayed a high level of steady state, tonic activity maintained as long as the load. The antagonist burst was also suppressed during the dynamic and static phases of opposed arm movement.

In the Figure 4.13, the HM force was plotted in black and angular velocity in blue respectively, the plots showed the peak velocity was reached at the middle of movement and the peak force was reached nearly the end of the movement. These findings suggested that the rate EP shifts is adjusted according to the desired movement velocity.

As a result, in the slow movement, the difference in the duration of control signals and movement may hardly be distinguished, and therefore many researchers argued the EPH is good for slow movement. The activity of arm muscles and its neurons investigated was movement and force related. The motor cortex itself and signals may be distal to the end-point specifying process (Feldman et al., 1995).

In the fast movement, a 1.5 second arm flexion data have been extracted and used in the model to investigate the HM effect in the arm movement, the measured force of HM used as perturbation in format of perturbation torque in the model. The simulation model input, a virtual trajectory that found the EMG plus estimated B and K, run in the MATLAB Simulink generated a model output, which is nearly perfectly synchronized with the experimental data. The result in Figure 4.14 showed that the model produced the timing as well as the shape of the curve in the experiments. Therefore, the results of simulation suggested the HM could be used as a reliable resource of perturbation in the model.

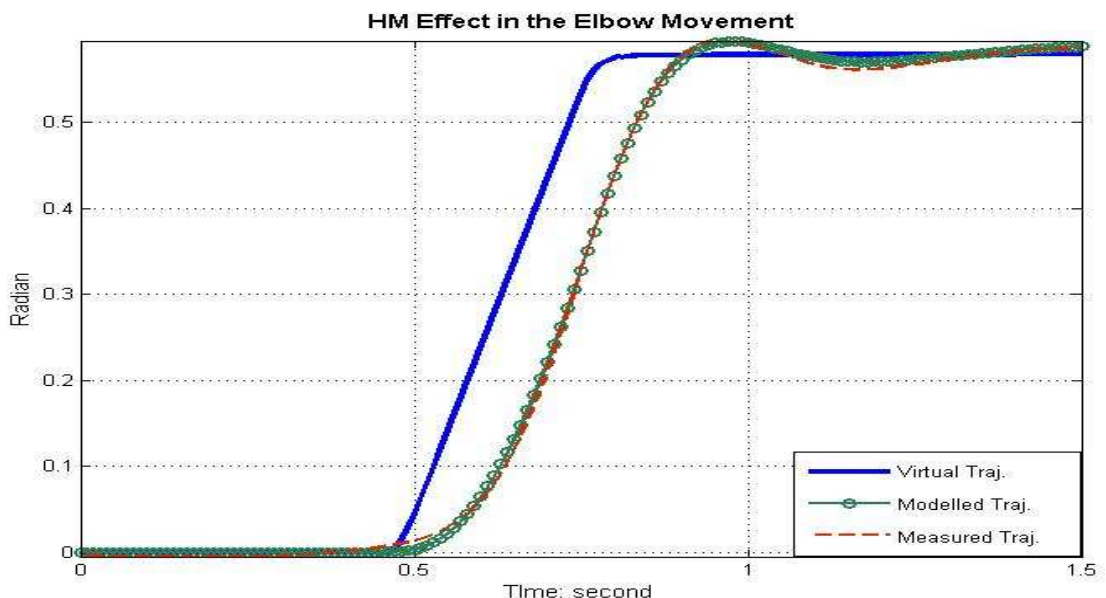


Figure 4.14 HM Elbow Experimental Displacement vs Simulink Model Output

Torques have been shown in Figure 4.15 between the simulated and inverse calculated results, the corner effect at the Zone 1 influenced the performance of model, it caused some distortion of the red curve at Zone 1. However, the model still can match up with the general trend of the elbow movement.

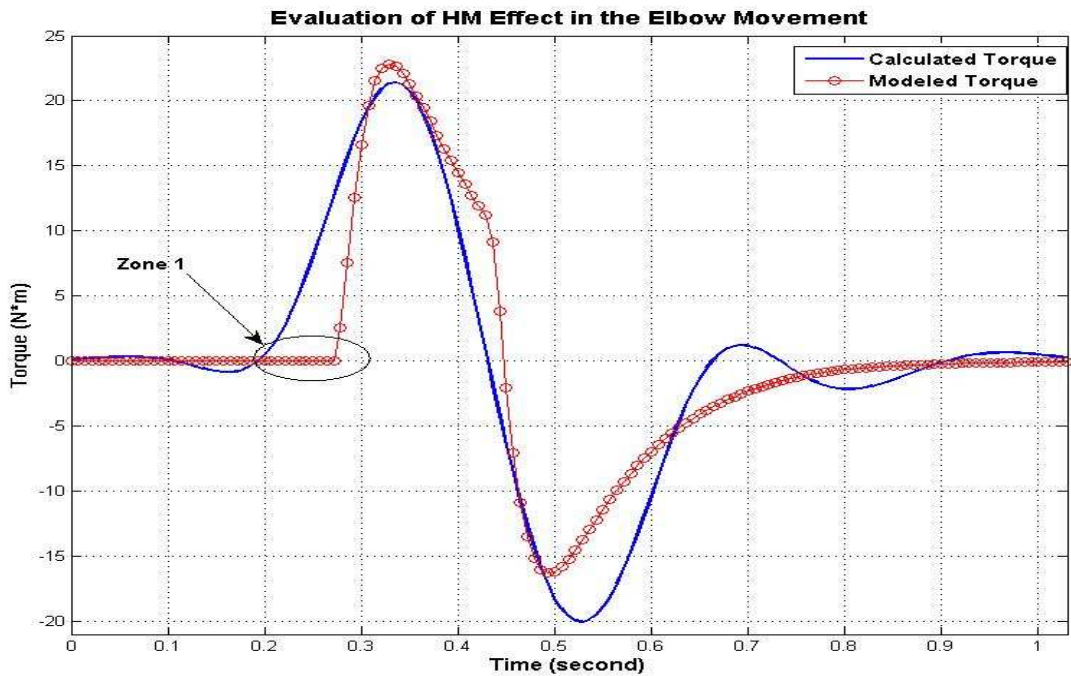


Figure 4.15 HM Elbow Experimental Torque vs Simulink Modeled Output

4.3 EPH Control in Voluntary Elbow Flexions with Unexpected Perturbations

4.3.1 Statistics and Equifinality Test of Obstructed Elbow Movement

In order to find the influence of range of motion in perturbed elbow movements, a Chi-square analysis was performed to investigate whether 1 radian ROM was different from 1.5 radian ROM in terms of force, time to the peak velocity and average velocity of movement. A Fisher's exact test technique was also used in statistics due to limited replications in the cell. The P value (0.9) was obtained from both Chi-Square and Fisher's

exact tests, which was much larger than 0.05. The statistical result suggested that the three evaluating criteria were the same for two ROM in obstructed elbow movements.

The tablet (Table 4.1) shows mean peak angle, known as mean range of motion, recorded from control (1), perturbed (2) and arrest (3) groups. After training, in control trials, the subjects made their fastest elbow flexion movements. When a high-gain perturbed force (also named loads) was applied in the perturbed (mid-movement) and arrested (early movement) trials, the movement displacement substantially decreased. Notably, the subject did not make corrections in both test trials when the arm significantly undershot the final target position. After a 120 millisecond holding period, the load was removed and the arm arrived at a final position coinciding with that in control trials ($P(0.631) > 0.05$, One-Way ANOVA). Equifinality was shown in Table 4.1 and Figure 4.16.

Table 4.1 Equifinality Test of Elbow Movements

Subjects	Elbow Displacements					
	Control		Perturbed		Arrested	
	Mean	Std	Mean	Std	Mean	Std
1	0.568	0.029	0.261	0.057	0.325	0.036
2	0.673	0.034	0.604	0.026	0.467	0.048
3	0.521	0.025	0.551	0.031	0.564	0.031
4	1.089	0.088	1.026	0.076	1.005	0.052
5	0.362	0.027	0.350	0.014	0.352	0.026
6	0.679	0.091	0.382	0.021	0.364	0.033
7	0.275	0.035	0.231	0.013	0.264	0.026
8	0.449	0.054	0.386	0.025	0.478	0.067
9	0.286	0.042	0.195	0.016	0.232	0.062
10	0.384	0.030	0.360	0.033	0.411	0.027

The statistical results in Figure 4.16 show the arm movement had a strong trend of elbow trajectory to return to final target regardless of perturbation conditions changes. Three groups were likely distributed and the results did not reject the null hypothesis, which means three groups did not have significant difference. The P value was 0.631 statistically supported the idea of Equifinality.

To understand the Equifinality test of single subject, the Figure 4.16 was shown all trials of subject S3. The figure illustrated the measured elbow angles with the HM only, perturbed and arrested conditions. The final angles converge in a small range (0.5-0.6 radian) in the Figure 4.16.

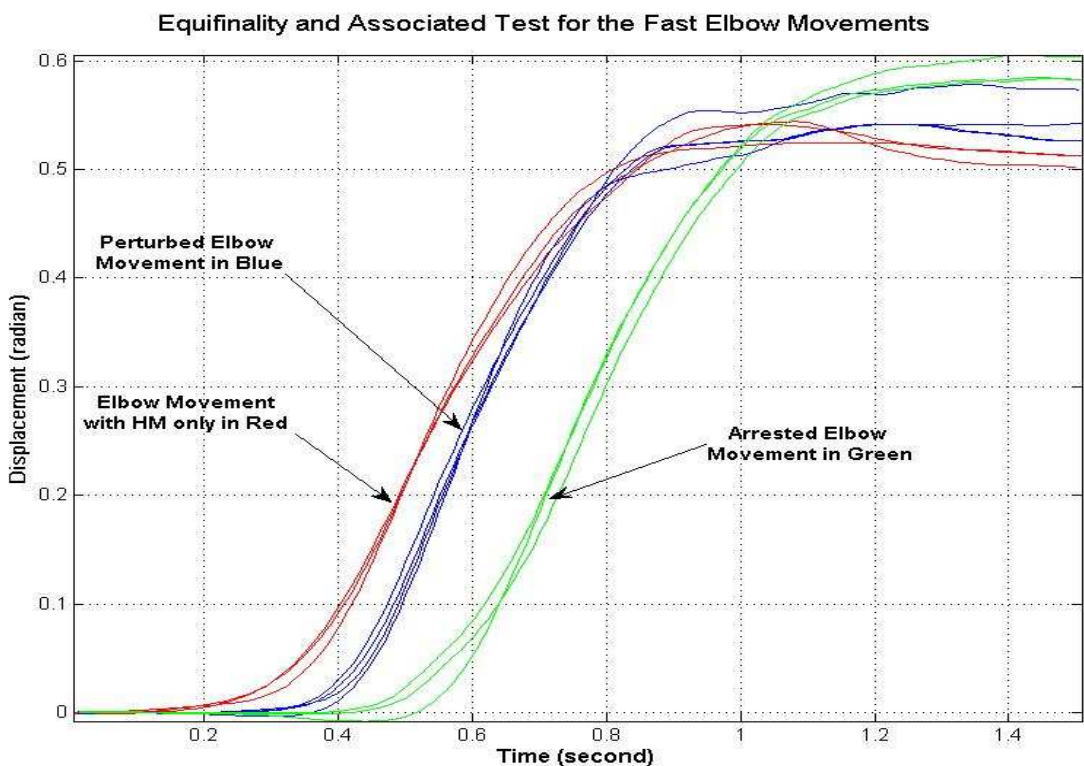


Figure 4.16 The Measured Trajectories of Elbow Movements in Equifinality Test

The introduction of the perturbation as minimizing load in all HM test trials reduced the movement duration so that the HM tests approached the time to peak velocity

of control shorter than non-HM movement tests. After comparing the velocity profile of the loaded movement and a non-loaded movement traces, the peak angular velocity was 1.984 radian/s and 7.480 radian/s, respectively by normalized traces accordingly.

In both perturbed and arrested movement of the study, the time to peak velocity of tested movements opposed by the minimizing load and perturbation was significantly increased for all subjects in comparison with control movement ($P < 0.05$). Test movements made with the minimizing load ended near the peak velocity of control movements. Compared with the time to peak velocity of control movements (non-perturbed HM test), the duration of the movements opposed by the perturbations were greater in perturbed and arrested tests (0.231 second, SD 0.035 and 0.297 second, SD 0.041). In all subjects, the difference was less than 100 ms.

4.3.2 Results of Perturbed Movement

The study is based on the idea that the central nervous system may take advantage of the apparent mechanical behavior of the neuro-musculo-skeletal system in controlling movement, and considers its ramifications in the case of multiple degree of freedom movement. The relation between force, EMGs and displacement of the end-point of a hand can be determined experimentally by displacing the end-point from an equilibrium position and measuring the resulting steady-state force opposing the displacement.

Since two preliminary studies (Chen, 2008), (Chen, 2009) have investigated movement control among unperturbed single and double arm joints, focusing on the control of perturbed movements of elbow. The following experiments demonstrated the relationship between movement production and associated kinematics and

electromyographic (EMG) patterns under the condition of perturbations. Amplitudes of data have been rescaled to enable the plot to be displayed in same picture for comparison.

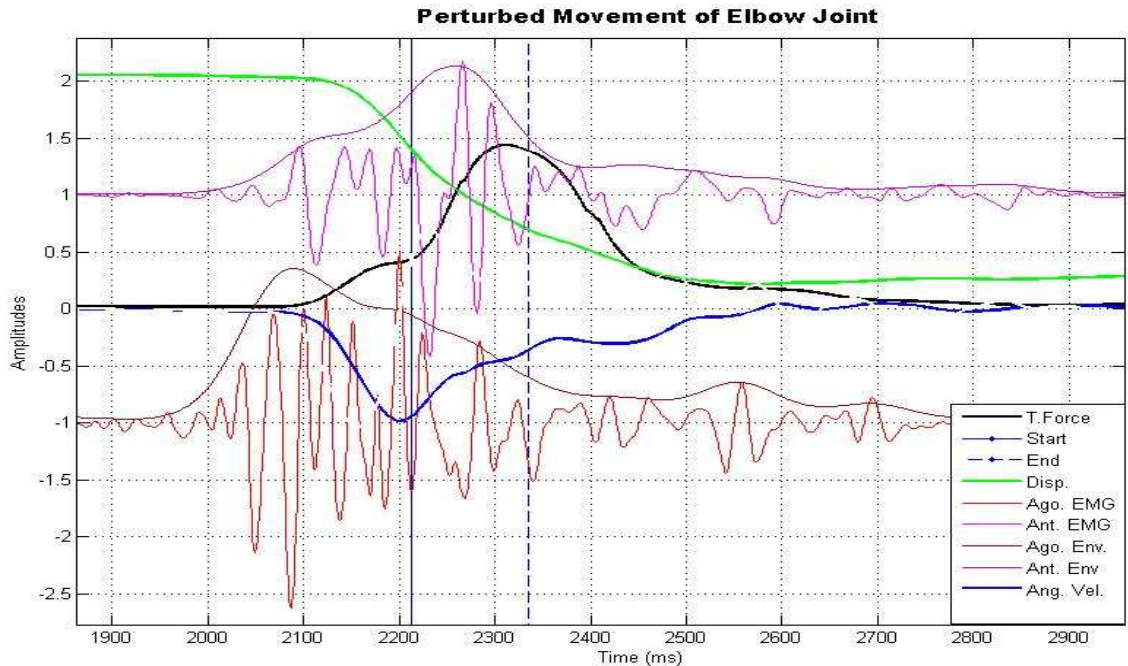


Figure 4.17 Perturbed Movement of Elbow

Figure 4.17 shows the relationship between EMG levels, forces measured of end effectors (hand), movement amplitude and maximum velocity for elbow with perturbation during the preceding movement. The plot demonstrates the times of perturbation onset with solid blue, and termination with blue dashed vertical lines in the figure. All data from HM, EMGs and trakSTAR® were synchronized by their own time stamp and plotted curves were aligned according to the movement onset and then averaged.

In the perturbed movement, the perturbed forces approaching the maximal isometric voluntary torque and minimizing the movement time were presented and then removed. Movement duration, displacement and peak velocity were significantly

diminished, whereas joint force increased in the perturbed trials. EMG traces (triceps brachii, TB; biceps brachii, BB;) were shown together for the perturbed movement (BB in red, TB in pink). The envelope above the EMG shows a low-pass (24 Hz) filtered and rectified EMG envelope of perturbed movement for the same subject. In the perturbed movements, perturbation in the test trials elicited substantial changes both in the phasic and tonic EMG pattern. The activity in the agonist muscle (BB) was prolonged and displayed a high level of steady state, tonic activity were remaining as long as arrested movement, which would be discussed next in arrested movement.

In response to release of perturbation of the elbow, agonist activity began to decrease (latency around 45 ms for the subject) and eventually moved toward zero level (silent period). The calculated data also showed subjects exerted more than 60 Nm of elbow torque, when the movement was opposed by the arrest force. During approximately the first 100 ms, the agonist EMG activity did not depend on load condition (Feldman, 1995), so this study set the perturbation lasting for 120 ms.

Changes in agonist and antagonist EMG integrals in unperturbed and perturbed trials, averaged across the subjects, showed a small decrease in the amount of activity in the antagonist muscles, and a slightly higher increase in the activity of agonist muscle. During perturbed trials, both agonist and antagonist integrals increased by considerably larger amounts (on the average, a 142% increase in the amount of activity of the agonist muscles; and a 106% increase in the amount of activity of the antagonist muscle).

The earlier study of perturbed movement of elbow (Chen, 2010) illustrated elbow displacement curves obtained for the 0.95 radian movement with perturbed task conditions (Figure 4.18).

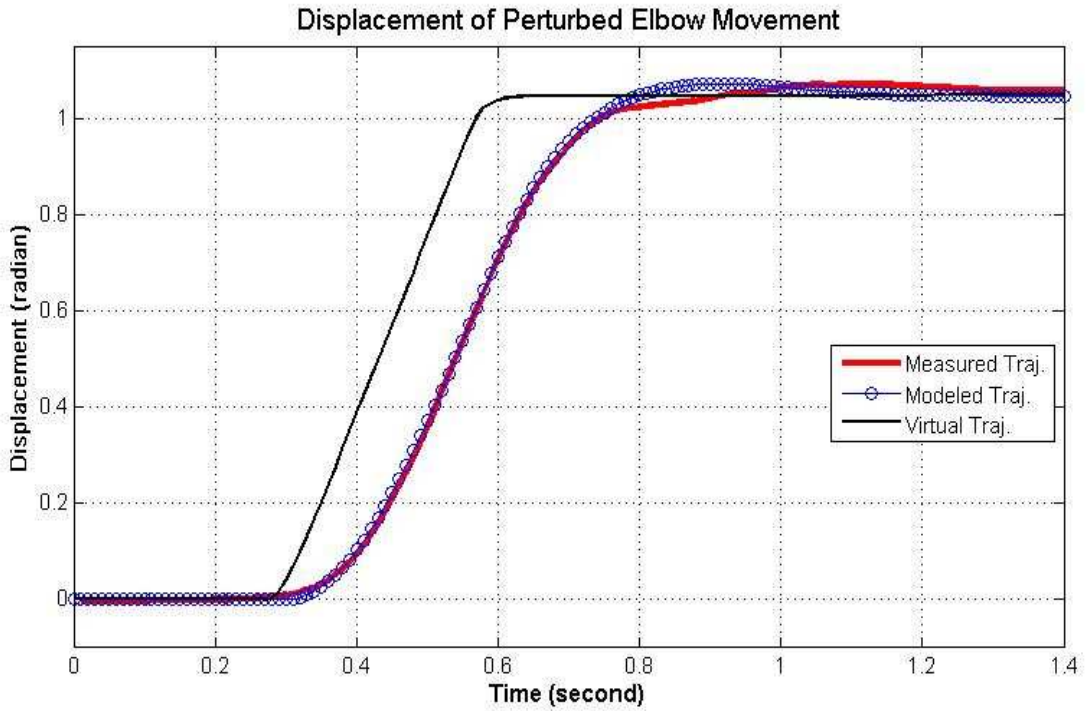


Figure 4.18 Perturbed Elbow Displacement in the Simulink Model

Figure 4.18 shows an excellent model corresponding to unexpected unexpected perturbations during movement. Comparison of this Figure to Figure 4.14 shows the same VT and same B and K as well. With actual and modeled trajectories having been modified by the unexpected perturbation, note that the actual and modeled trajectories in Figure 4.14 parallel this VT, with in Figure 4.18, the actual and modeled trajectories have a less steep slope.

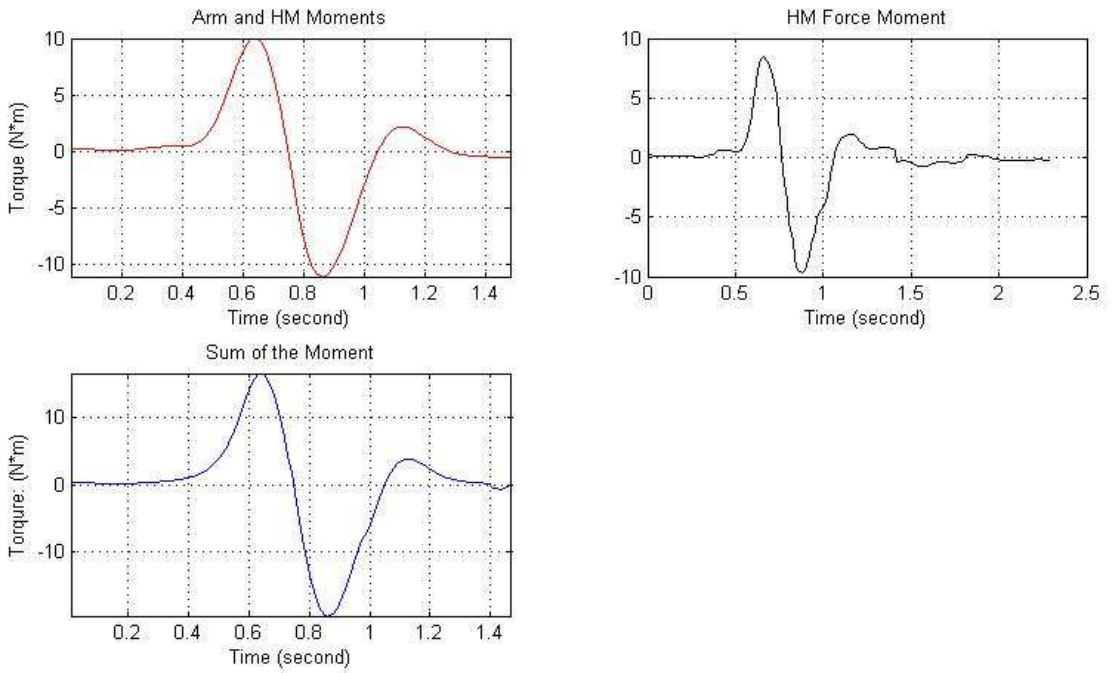


Figure 4.19 The Inverse Calculation of Elbow Components Torques and Total Torque

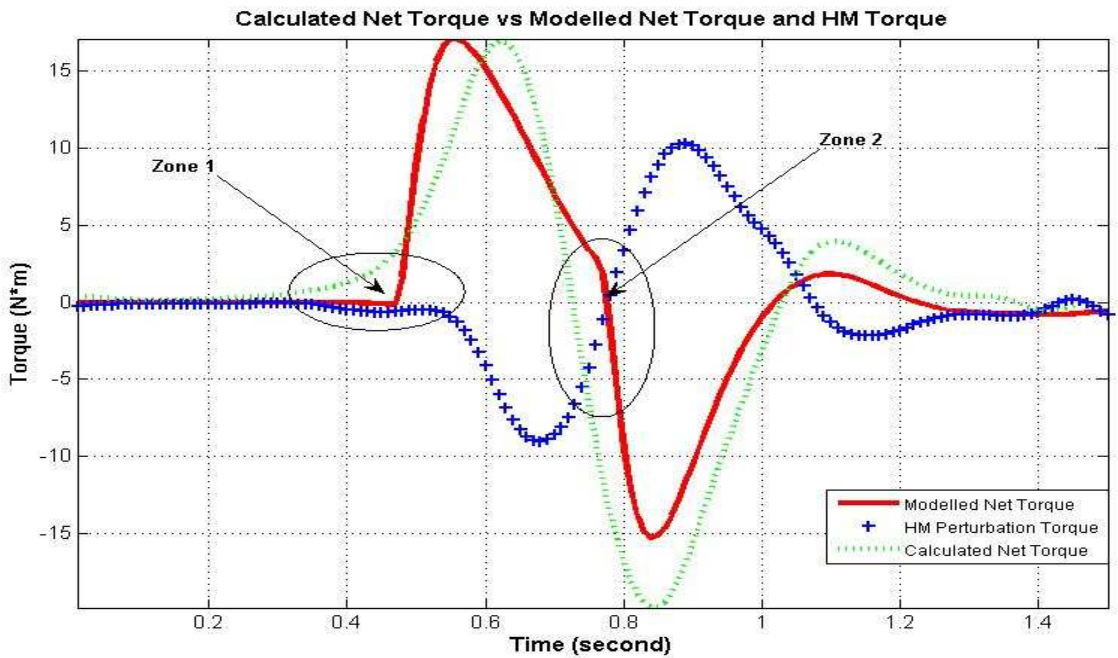


Figure 4.20 The Calculated Elbow Net Torque by Inverse Dynamics vs Net Torque by the Simulink Model vs HM Perturbation Torque

The modeled net torque is quite close to the calculated net torque in Figure 4.20, with some difference seen in Zone 1 due to the immediate start of virtual trajectory in the model. In addition, trakSTAR, EMG and HM devices have different resolution, so the missing frames, plus accumulated calculation tolerance errors, lead to Zone 2 showing some system distortions in the plotted Figure 4.20.

4.3.3 Arrested Arm Movement

Figure 4.21 shows arrested force influences on electromyographic (EMG) activity, movement duration, and displacement joint velocity. Elbow torque and kinematic traces from a non-perturbed movement can be referenced from the earlier study. Unperturbed movement was associated with agonist followed by antagonist muscle activity, while the end of the movement was characterized by additional reciprocal agonist/antagonist bursts (Brown and Cooke, 1986).

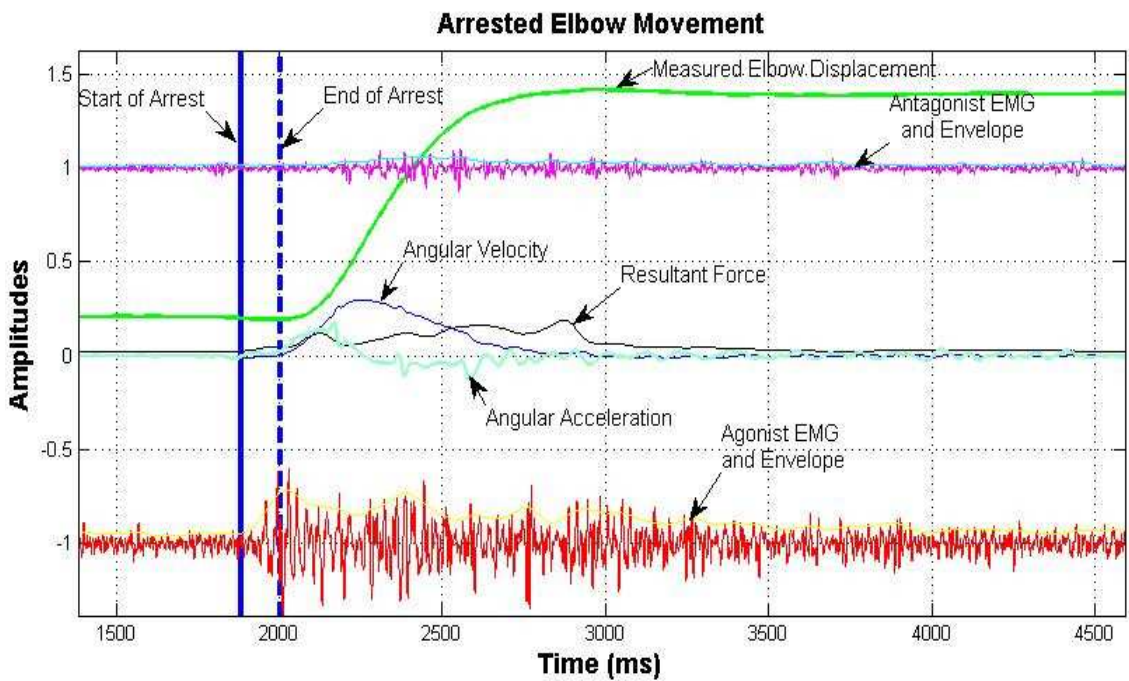


Figure 4.21 Arrested Movement of Elbow

In the arrested movements, perturbation in the test trials elicited substantial changes EMG pattern. The activity in the agonist muscle (BB) was prolonged and a high level of steady state, tonic activity was also maintained (see Figure 4.21). This activity was associated with the net static torque, which was close to maximal isometric torque (Feldman et al., 1995). The antagonist (TB) was suppressed during the dynamic and static phases of perturbed movement. The amplitude of the agonist burst was insignificantly affected by the perturbations, similar results were described by St-Onge and Adamovich (St-Onge et al., 1997).

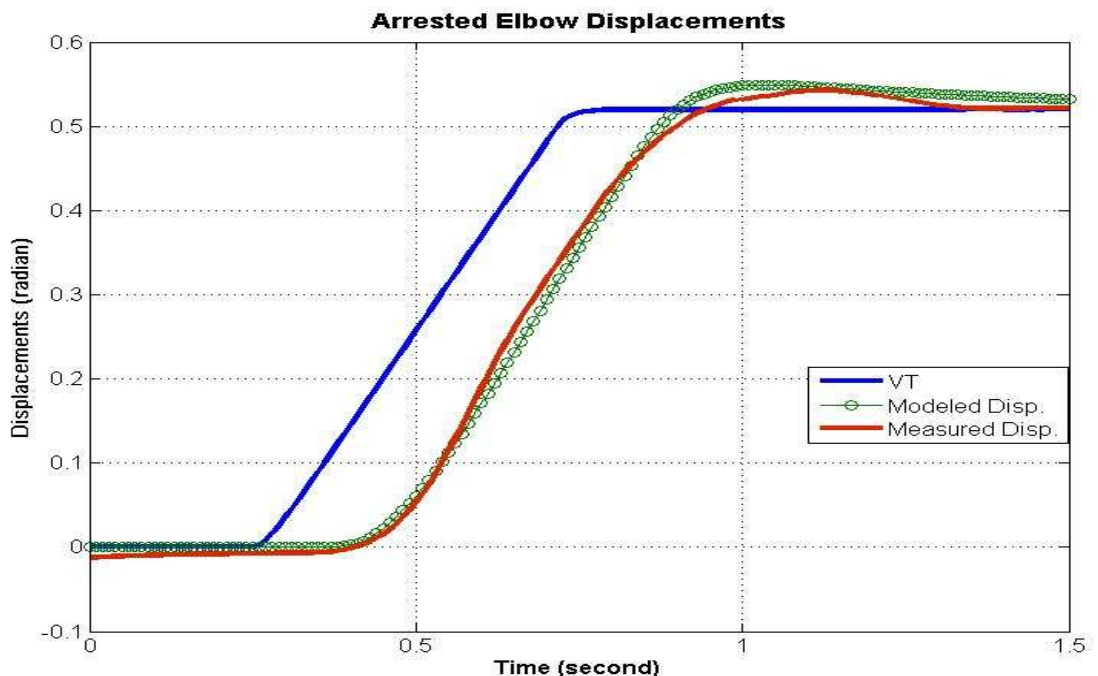


Figure 4.22 Arrested Elbow Displacement in the Simulink Model

Variance, previously optimized B and K for each subject for the HM only trial, as well as the previous VTs were used as in the perturbed trials. This VT and output of model are superimposed in the following Arrested trials in Figure 4.22. Compared with the control trials (virtual trajectory in black), the introduction of an arrested obstruction

delayed the onset of movement. After a 120 ms arrested period, the arresting force was removed (between the black and blue) and the arm arrived at a final position coinciding with that in virtual trajectory ($P>0.05$; Equifinality). Filled dots and solid blue show final positions of the model and control trials (measured position). Horizontal bar, (Y axis - Displacement marked as 0, 0.03, 0.95) show the initial, intermediate and final phases, respectively, at which measured steady state values of position and torque were used to plot the corresponding Equilibrium Points. Figure 4.22 shows elbow displacement curves obtained for the 0.52 radian movement with arrested task. Equifinality was observed ($P>0.05$) in each block of trials, as shown in Figure 4.17 and 4.21 for intermediate Equilibrium Point at Y axis 0.03 and 0.02 respectively. Comparing Figure 4.22 to 4.18 and 4.14 shows that arresting torques increase the time between the VT and arm trajectory, but unlike Figure 4.18, the actual trajectory parallels the VT as it does in Figure 4.14. And Figure 4.23 shows the actual and modeled moments.

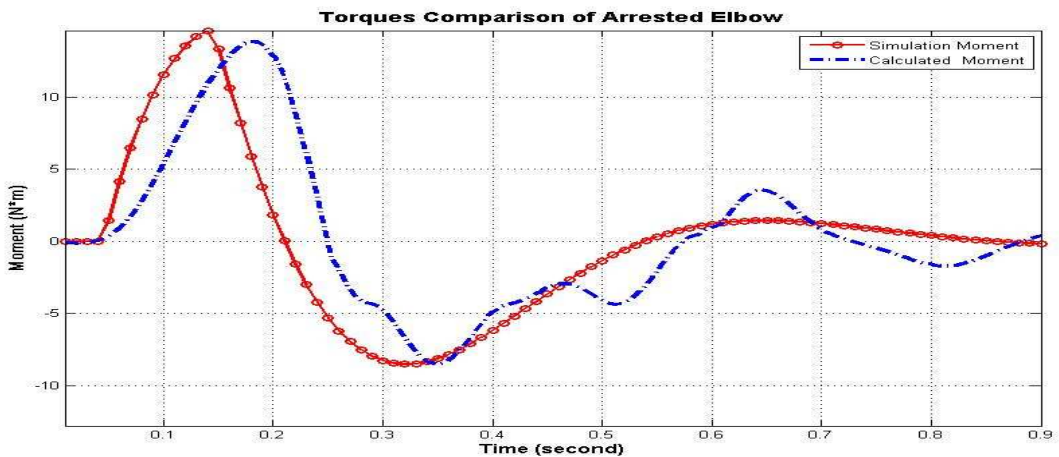


Figure 4.23 The Elbow Torques Plots (Experiment Vs Simulation)

But model moment appears smooth, with the experimental moment exhibited an unusual pattern in second half. This was found in the movement of all subjects only in the

arrested trials. This is mainly due to mechanical interference of HM, as it introduces a mechanical noise when the velocity changes near the peak value, it is random and related to the speed gear of HM. This noise introduces minor discontinuity in this actual trajectories which are accrued in the computation of velocity, see the Figure 4.24 for the zoomed observed noises from Figure 4.21.

Note blue jerks in arrested elbow movement, suddenly release of this arrest, the HM measured errors have been magnified in the elbow torques. A low pass filter has been applied in a reasonable low cutoff frequency, although a smoother curve has been achieved, the trend of torque curve has been distorted and some real movement information has been lost as well. Therefore, the study does not suggested to use the cutoff frequency under 10 Hz. Since these jerks were found in arrested movement only, the heavily dampened force could be the reason of these mechanical noise, as a result the study recommend either using a smaller arresting force or to embed the HM base to reduce noises.

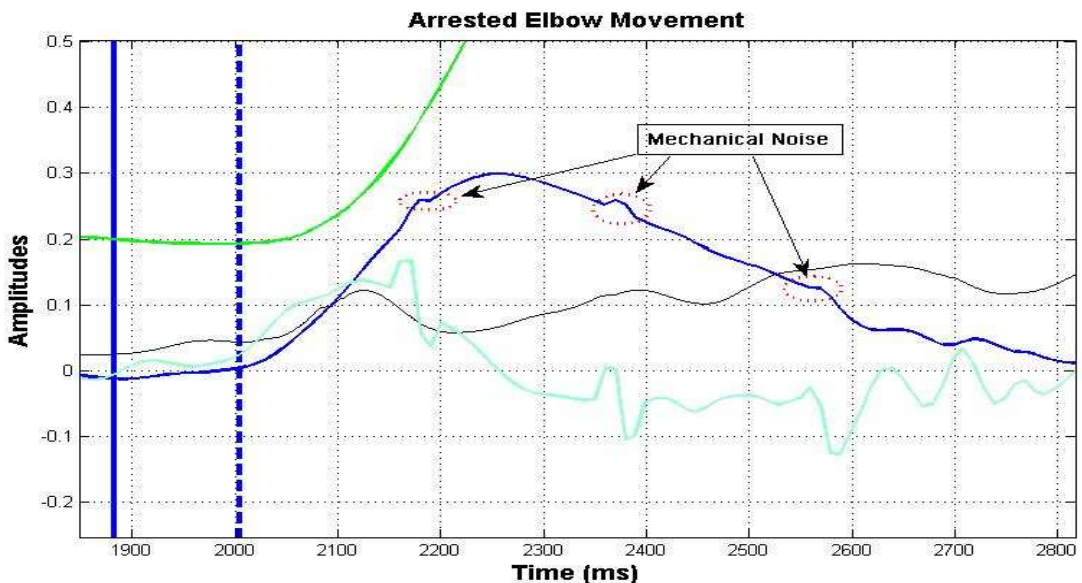


Figure 4.24 The Jerks in Arrested Elbow Movement

4.4 Optimization of Stiffness and Damping

Key to this research is the optimization of B and K for each subject based on their HM only experimental data. The results shown in each of sections confirm that those parameters. Along with an EMG determined VT can be used successfully to model the perturbed trials.

Table 4.2 shows an analysis of the optimization of multiple HM only trials by subject. The mean damping and stiffness coefficients are shown for each subject. The small averaged SSE variances indicate an excellent fit. And the small standard deviation shows that the optimization produces very consistent K and B with each subject's trials.

Table 4.2 A Least Squares Model Used to Optimize the Control Parameters Damping and Stiffness in the MATLAB Simulink

Subject	Sex	Moment of Inertia (kg·m ²)	Damping (Nm·s/radian)		Stiffness (Nm/radian)		Sum Squared Error of Optimization
			Mean	Std	Mean	Std	
S1*	M	0.426	---	---	---	---	---
S2	F	0.057	1.72	0.43	16.19	0.99	0.10
S3	M	0.284	3.31	0.14	9.74	0.61	0.02
S4	M	0.227	4.76	0.31	8.40	0.33	0.069
S5	F	0.153	2.31	0.19	12.07	0.85	0.084
S6	M	0.272	2.94	0.39	11.19	1.41	0.012
S7	M	0.300	4.2	0.12	14.76	0.95	0.031
S8	M	0.381	4.46	0.27	15.74	0.47	0.01
S9	M	0.254	4.11	0.34	19.15	1.07	0.025
S10	M	0.284	3.95	0.43	17.58	1.29	0.017

Note: Subject S1 does not have enough data to run statistic analysis significantly.

A new intrinsic damping parameter (0.1 Nm·s/m) has been used to substitute the previous one (0.35 Nm·s/m) for the elbow, the new damping parameter has based on the finding of experimental data by Darnell Simon (unpublished), which model and optimize the intrinsic damping from experimental arm data.

B and K varies shown in Table 4.2 roughly confirm to the expert critical damping relationship defined by $B = 2\sqrt{I * K}$. As this has been estimated for absolute damping, its use with reasonable absolute damping has not been established and is used one as a evidence.

In the study of potential impact of uncertainties in measurement, although the perturbation changed the kinematic behavior of the perturbed limb, the relation of the reported estimates of K and B to known muscle physiology and the impact of changes in mechanical properties on movement generation are linear. The K and B values in Table 4.2 were derived from optimization of the Simulink Models. If it is assumed that the torques needed to generate elbow motion are primarily determined by limb inertia, these values are ready to be estimated, and these values were used in perturbed and arrested movements. Cannon and Zahalak (Cannon and Zahalak, 1982) suggested that for an extensor moment of about 8 Nm, the stiffness was around 60 Nm/rad. This estimate was a much higher value than the best fit values in the optimized Simulink models in the present study, and was also higher than the mean value (10.545 Nm/rad) of K in the study. This difference can be attributed to a variety of physiological mechanisms, but constant static force-length slopes are nevertheless used effectively in the EPH elbow movement control models.

4.5 Sensitivity Analysis of Obstructed Elbow Movements

The same B, K, and VT were used to model the HM only, perturbed and arrested elbow movement. SSE of the model for all listed elbow movements have been provided.

4.5.1 Sensitivity Analysis with HM Only

The HM only data of Subject S3 has been used as in this test of HM only elbow movement modeling, measured elbow trajectory, modeled trajectory, modeled trajectories with $\pm 10\%$ variance of both damping and stiffness have been changed at same time and results shown in Figure 4.25.

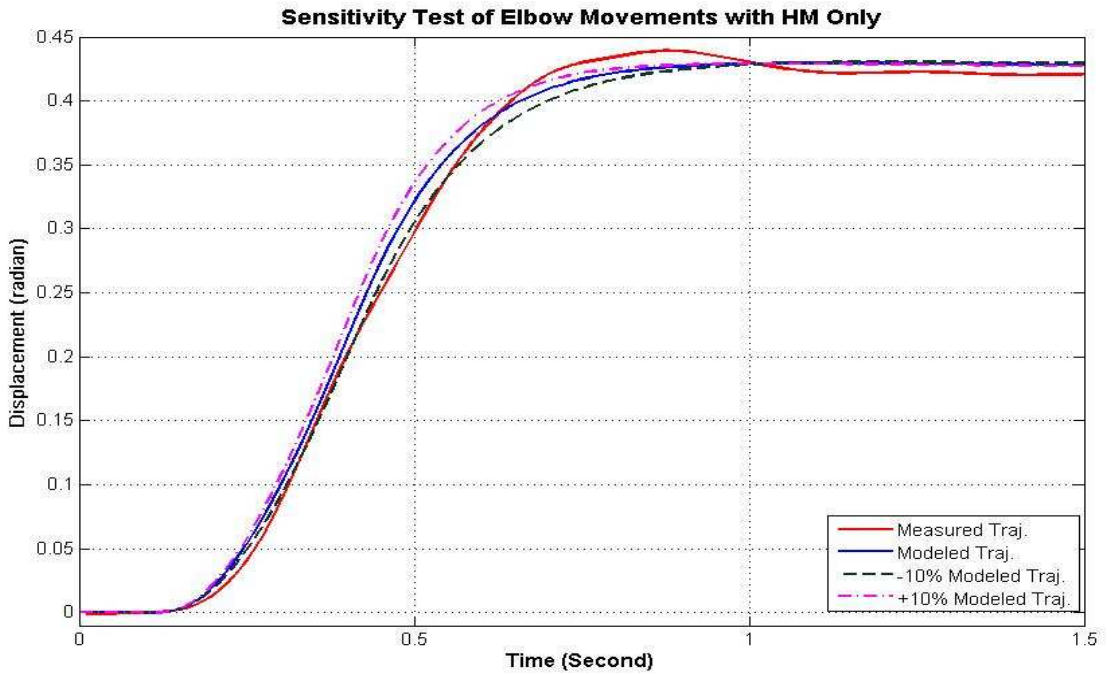


Figure 4.25 Sensitivity Test of Elbow Movements with HM Only

The results were shown in Figure 4.25, the modeled trajectory has a SSE value of 0.010 comparing with measured trajectory, the +10% modeled trajectory has a SSE of 0.017, the -10% modeled trajectory has a SSE of 0.019.

4.5.2 Sensitivity Analysis in Arrested Movement

The data of Subject S2 has been used in the analysis of arrested elbow movement modeling. Measured elbow trajectory, modeled trajectory, and modeled trajectories with $\pm 10\%$ variance of the damping and stiffness were shown in Figure 4.26.

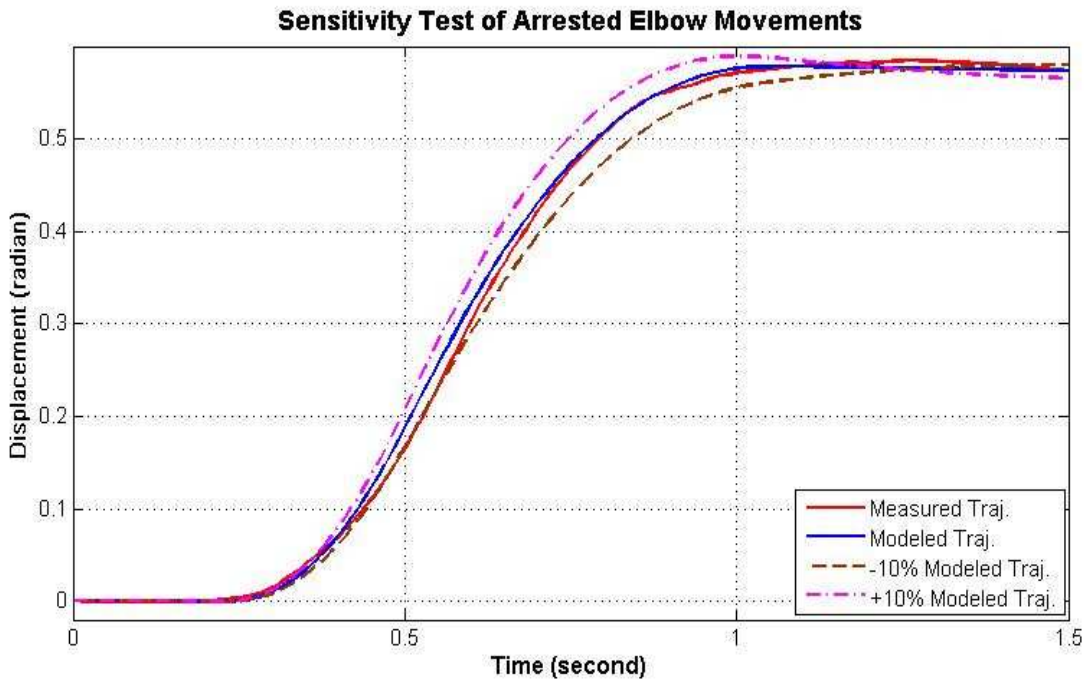


Figure 4.26 Sensitivity Test of Arrested Elbow Movement with $\pm 10\%$ Variance

The results showed that modeled trajectory has a SSE value of 0.014 comparing with measured trajectory, the +10% modeled trajectory has a SSE of 0.04, the -10% modeled trajectory has a SSE of 0.057.

4.5.3 Sensitivity Analysis in Perturbed Movement

Questions may rise whether the successful modeling of obstructed arm movement is based on a too small perturbation to influence the performance of the system. And if the damping and stiffness have been changed, will behavior of the become model unpredictable? Hence, the study performed two sensitivity tests of the model.

4.5.3.1 Sensitivity Test of Elbow Movement with a Larger Perturbation Force

In order to test performance of the model in larger force perturbations, this study increased the perturbation forces about 75% of the arrested force. The collected data and

analysis results were shown in Figure 4.27, the green curve is angular displacement (radian), blue curve is the angular velocity, blue lines are the indication of beginning and ending of the perturbation, black curve is the measured force (Newton) divided by 20 in order to display in the same figure.

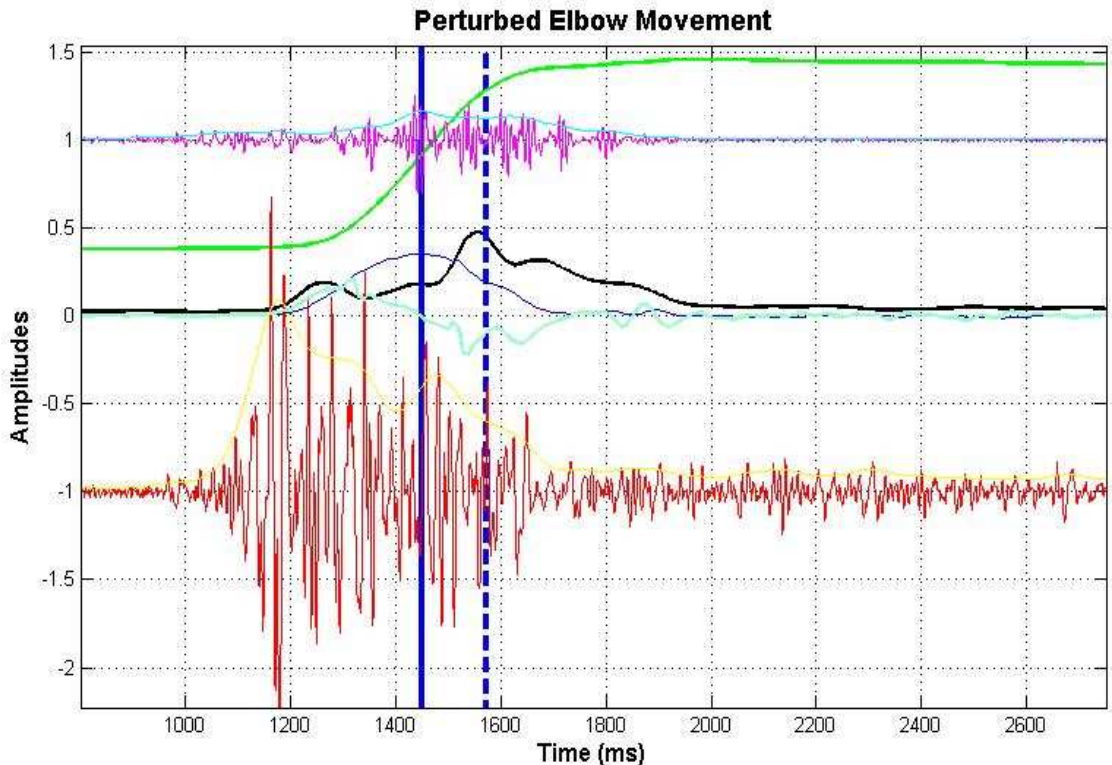


Figure 4.27 Sensitivity Test of Elbow Movement with a Larger Perturbation

The new data has been input into the modeled with optimized parameters obtained from unperturbed elbow movement optimization model, the result of the VT, measured perturbed elbow displacement and modeled elbow displace were shown in the Figure 4.28, the SSE of the modeled trajectory fitting to the measured trajectory is 0.047. It suggests the Simulink model of the study is robust enough to cover perturbed elbow movements regardless of the perturbed force equal or under the 75% of minimal arrested forces.

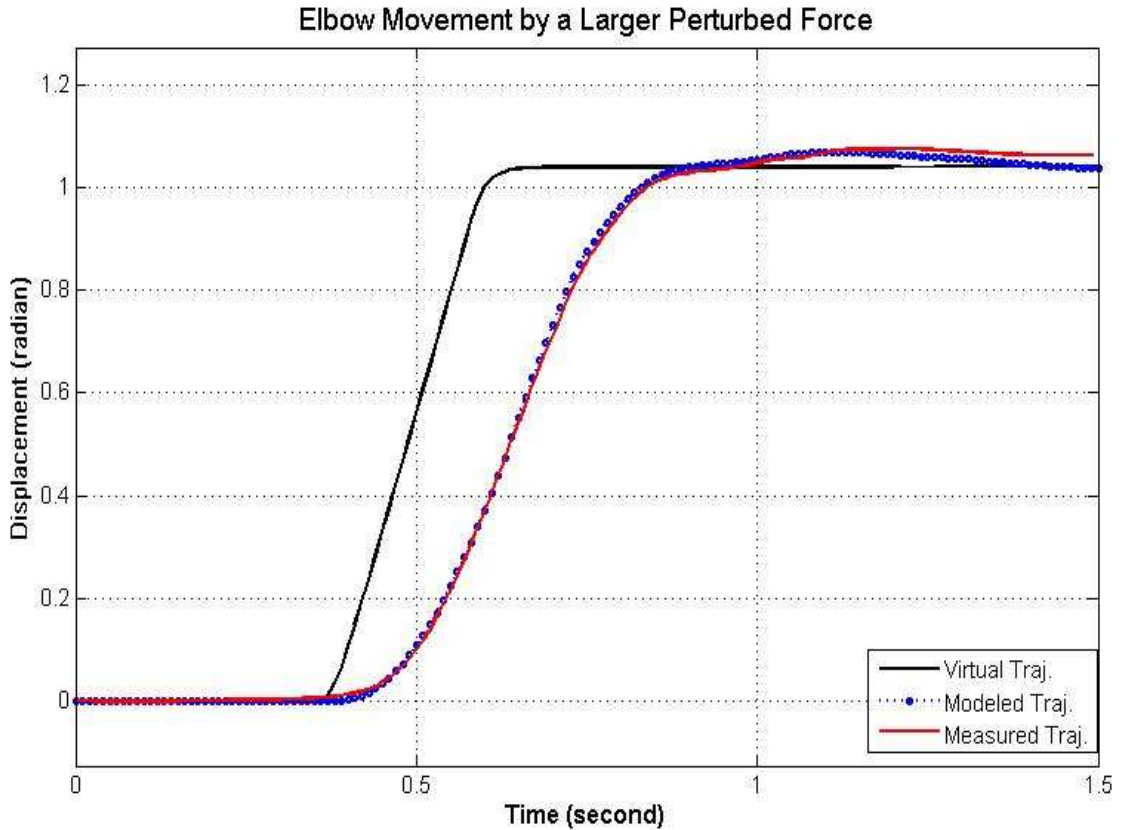


Figure 4.28 Sensitivity Result of Perturbed Elbow Movement in the Model

4.5.3.2 Sensitivity Test of Perturbed Elbow Movement

Same data has been used as section 4.5.3.1 for this sensitivity test. The damping and stiffness have been changed by $\pm 10\%$ at the same time. Measured elbow trajectory, modeled trajectory, and modeled trajectories with $\pm 10\%$ variance of the damping and stiffness have been shown in Figure 4.29.

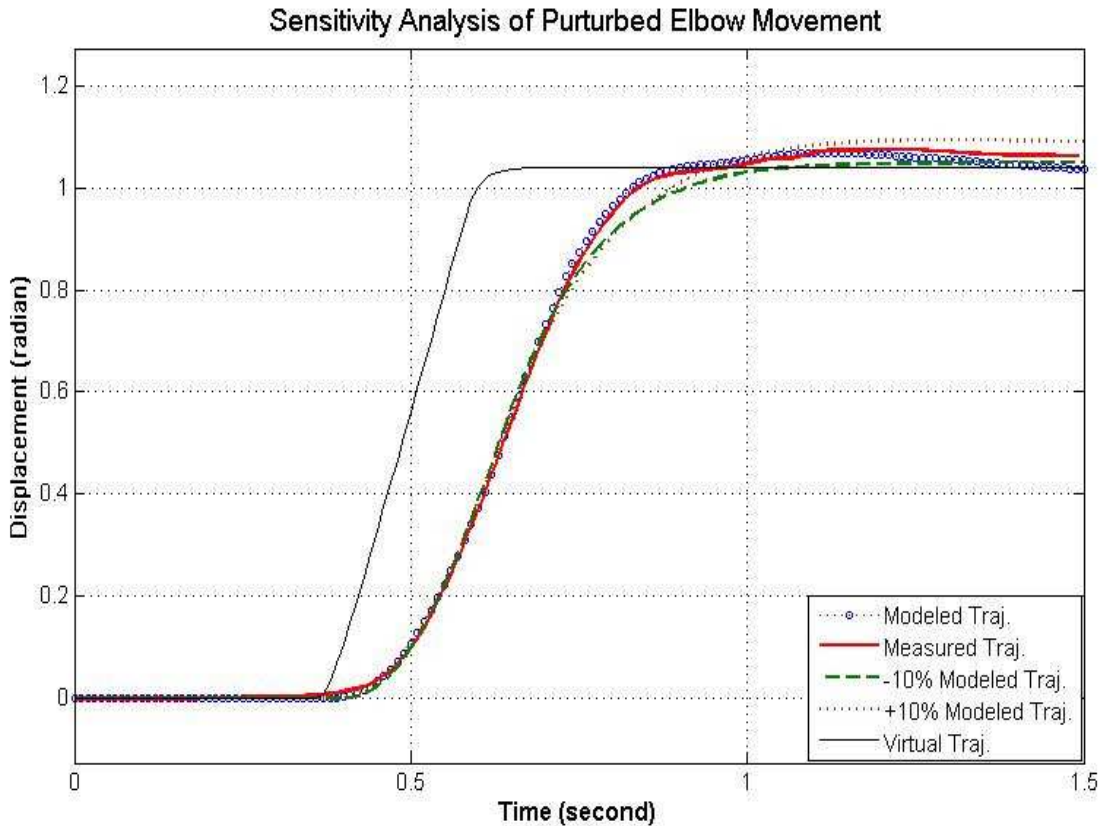


Figure 4.29 Sensitivity Test of Perturbed Elbow Movement in $\pm 10\%$ Variance

The results showed that modeled trajectory has a SSE value of 0.047 comparing with measured trajectory, the +10% modeled trajectory has a SSE of 0.131, the -10% modeled trajectory has a SSE of 0.09. These results of sensitivity tests in perturbed elbow movement demonstrated that the model is robust to cover only the larger perturbations, but also some variances of the model parameters.

Based on above results from HM, arrested and perturbed arm movement tests, all test results suggest that the success is depend upon on precisely optimized value of B and K rather than any lucky.

4.6 Mechanical Properties of Elbow during Obstructed Movements

Neville Hogan (Hogan, 1985) proposed a mathematical model in terms of impedance control of arm movement. Discussing this work, Dr. Hogan admits that it can not effectively model all aspects of the performance of the system. He said “*Controlling the complete dynamic behavior of the limb may be beyond the capacity of the central nervous system. If the disturbance is sufficiently abrupt, then, because of the inevitable transmission delays, continuous intervention based on neural feedback information will not be a feasible method of modulating these quantities.*”.

However, the model proposed in this study, accomplished most the work which Hogan believed was not feasible. The following points raised by this paper give a new insight for the future study of upper limb control.

4.6.1 The Duration of Shifts in the Equilibrium State

The elbow position is usually stabilized due to proprioceptive feedback and intrinsic, elastic and viscous muscle properties. Some researchers (Levin and Feldman, 1995) assumed that a movement from an initial to a final position cannot be produced unless the equilibrium state of the system is modified by independent, control variables, according to the physical definition of the concept of the equilibrium state of a dynamic system.

The results of modeling in the earlier study showed that monotonic, ramp shaped changes in this command ending before the peak velocity of movement, which can account for the measured kinematic and EMG patterns of fast elbow flexion movements made with self-paced movement. The assumption that fast movements were produced by brief shifts in the equilibrium state of the system was supported by the results of the simulation of effects of perturbation on kinematic and EMGs in the present study. The

study found a substantial decrease in the elbow joint velocity both in perturbed and arrested movements (2.183rad/s, 0.273 rad/s, respectively) with the perturbation duration of 120 ms. A plateau was found at the end of added perturbation lasting 30-40 ms, which was believed to be a transition from one equilibrium state to another due to the feedback. This transition behavior was a sign that the subject set an initial state of the neuromuscular system to counterbalance the perturbed force and was reluctant to change this state, even long after the releasing. In other words, responding to release, the subject kept some essential variables invariant (St-Onge et al., 1997). The nervous system continued to maintain the same joint angle before and after perturbation releasing.

A prolonged first agonist EMG burst was especially observed in the perturbed movements, and was maintained at a high level of tonic activity for as long as the perturbation was applied. Therefore, kinematic and EMGs of both perturbed and arrested were reproduced by using the same control patterns eliciting a monotonic shift in the equilibrium state of the system ending before or near the peak velocity of perturbed movement (see Figure 4.17 and Figure 4.21). The two figures show a substantial part of phasic EMG activity was generated after the end of shift. The EMG demonstration of the threshold position shift implies that neither mechanical variables, nor EMG patterns are programmed by the nervous system – these variables and patterns emerge following central resetting of the threshold position of the motor (St-Onge, Adamovich et al. 1997). In particular, TB EMG plots in two figures showed “tri-burst” EMG patterns plus found bell-shaped velocity profiles of arm movements, both of which can be considered as trivial consequences of threshold position resetting. And the same patterns of control were incorporated in both perturbed and arrested movement.

4.6.2 Relation of EMG and Cocontraction in Elbow Movement

Muscle cocontraction (or coactivation) is a primary means by which the nervous system stabilizes the position of the limb, and the evidence based on measures of joint stiffness suggest that in naturally occurring behaviors the control of coactivation and movement may be linked (Masataka Suzuki, Douglas M., 2001). Gribble (Gribble, 1998 b) has shown that in single-joint elbow movements increases in movement speed were accompanied by increase in stiffness. Similarly, in modeling studies, simulated commands for muscle coactivation must increase monotonically as a function of commands for movement velocity in order to increase speed and stiffness in parallel. His finding confirmed the methodology in the author's simulation model. More information about simulation model is discussed next in the Simulation section.

The pattern between the EMG activity and kinematic variables has been found to characterize muscle coactivation following perturbed elbow movement. In two cases, EMG magnitudes increased as a function of velocity at two perturbed movements. The phasic and tonic activation patterns suggested that the nervous system could use a relatively simple procedure to modify coactivation in which the signals that determine tonic EMG activity were scaled in relation to those that underlie the phasic signal. In addition, Masataka Suzuki (Suzuki et al., 2001) also found the EMGs' patterns of coactivation were found to mirror phasic activity within the first 30 ms of the initial agonist burst. The control of coactivation may be determined centrally prior to movement onset. The previous study found that the control signal was about 40 ms ahead of elbow movement onset.

4.6.3 Simulation Results

Figures 4.17 and 4.21 show two sets of ideal (virtual trajectory), measured and simulated movements during perturbed and arrested movement respectively. Not only have optimized damping and stiffness, but also neural translation delay plus perturbation plants (in Simulink) have been used and incorporated in the model. Measured movements performed for flexor elbow movement were simulated by varying the damping (B) and stiffness (K). The model accounted for the qualitative and quantitative features of measured kinematics. The perturbed movement was associated with the decrease of peak velocity achieved; and larger overshoot may be caused by under-damping. Meanwhile, arrested movement was associated with an increase of peak velocity, and final position showed almost no overshoot, which may be caused by over damping. However, more subjects are required to perform statistical analysis for more accurate results.

The model enabled us to perform perturbed tasks in simulation simply by changing the parameters of the perturbation plant in the model. The results in Figure 4.17 and 4.23 show shorter duration of movements, in which monotonic changes were also underlying shifts in the Equilibrium Point.

4.6.4 The Influence of Perturbation to Arm Movement

In Figure 4.17, a sudden release of perturbed force of arm muscles elicited a short-lasting silent period in the EMG activity of these muscles. The silent period was a result of shortening the length-sensitive receptors (muscle spindles): where shortening followed the release of perturbed force, and muscle spindles temporarily cease to facilitate α -motoneurons of the previously loaded muscles, thus interrupting the EMG activity.

The observations suggest that the first agonist burst may be relatively “immune” to variations in movement kinematics and reflex-mediated changes in EMG amplitudes. This could be the reason of the extension of EPH in describing changes in the first agonist burst with task parameters. Moreover, reflex-induced changes in antagonist EMG seemed to be important also during purposeful modifications of the motor command adapting to a change in the motor task. As a conclusion of perturbed movement, this present study suggests that subjects may maintain the same control patterns regardless of added perturbations associated with substantial changes in EMG activity and kinematics.

Thus, the basic idea of both perturbed and arrested movements control are suggested and the strategies are readily incorporated into the framework of the EPH that provides a better, more universal framework for simulation and analysis of elbow motor control.

4.7 Mechanical Properties of Arm during Unobstructed Involuntary Movement

The unobstructed involuntary arm movement provides evidence against existed dissociation between conscious vision for perception and unconscious vision for action. Recent studies have suggested that perceptual and motor decisions are based on a unique Equilibrium Point control, but distinct decisional planning during involuntary arm movement exists. Because sensory noise and feedback delay are potential sources of instability and variability for the real time control of movement. It is commonly assumed that predictions based on EPH allow the central nervous system (CNS) to anticipate the consequences of motor actions and protect the movements from uncertainty and instability. However, during motor learning and exposure to unknown dynamics, these

predictions can be inaccurate. Therefore, the hypothesis of whether a distinct strategy is necessary to preserve movement stability and accuracy, is tested in such situations in this study.

In the trials, participants performed speeded pointing movements towards a specified target as described in experiment setup for involuntary arm movement. The hypothesis was tested by asking subjects to hold a HM manipulandum in precision grip and to perform double-joint, continuous arm reaching during exposure to weightlessness (0 g), where the EPH models of the limb dynamics must be updated. Measurements of grip force adjustments from HM indicated that the internal predictions were altered during the early exposure to the 0 g condition. Indeed, the grip force/load force coupling reflected that the grip force was less finely tuned to the load-force variations at the beginning of the exposure to the novel gravitational condition. During this learning period, movements were slower with asymmetric velocity profiles and target undershooting. This effect was compared to theoretical results obtained in the context of optimal feedback control in unobstructed voluntary arm movement, where changing the movement objective can be directly tested by adjusting the EPH parameters.

However, the virtual trajectory in unobstructed involuntary movement can not be decided as the same as the assumption used in voluntary movement due to the different EMG activation patterns. The oscillation of force (using the absolute values in Figure 4.30) suggested the system was making dynamic adjustment rather than a stable condition, the aftermath EMG activity lasting near 2.5 seconds to reach the equilibrium state.

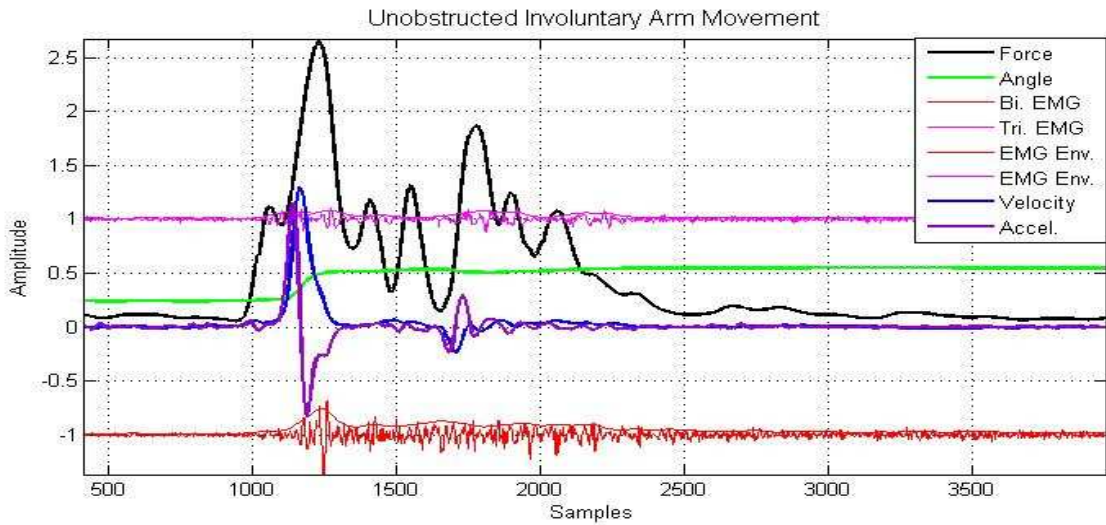


Figure 4.30 Unobstructed Involuntary Arm Movements

The observation in Figure 4.30 suggested that the effect on the movements may support and favor the hypothesis of a change in cost-function during the early exposure to a novel environment. The modified optimization criterion reduces the trial-to-trial variability despite that noise affects the internal prediction after analyzing multiple sets of data of the subject. Therefore, these observations support the idea that the CNS adjusts the movement objective to stabilize the movement when EPH models are uncertain.

CHAPTER 5

CONCLUSION AND DISCUSSION

5.1 Brief Summary and Discussion

The underlying concept of the EPH is that the CNS provides a virtual trajectory of joint motion, representing space and timing, with actual movement dynamics being produced by the interaction of limb inertia, limb load and speed/position feedback. The development of the EPH added complex virtual trajectories, non-linear damping, and time varying stiffness to support the EPH against criticism. While these features allow EPH models to adequately produce human joint velocities, they conflict with the EPH's premise of simple pre-planned monotonic control of movement trajectory. Therefore, planning more complicated parameters must require additional CNS capability that is on the order of the inverse dynamics. However, the study proposed methods based on the EPH which provides a simpler mechanism in the motor control without reasoning to complicated trajectories, stiffness, and damping.

The work of this investigation has proposed the addition of relative damping to the EPH model (Chen, 2008) to predict the single and two joint movement of the human arm. In addition to absolute damping, which is proportional to the joint velocity and is always dissipative in nature, relative damping produces a joint torque that is based upon the difference between the joint velocity and the velocity of the virtual trajectory. The term relative damping might better be called relative velocity gain, as it can be dissipative or additive. This addition to the model results in simulated trajectories that closely match experimental data, and suggests that this control model could be used in planning the multi-joint angular trajectories in fast and low velocity, without the need for time varying

or non-linear stiffness and damping, and with simple monotonic virtual trajectories. In the next study, this relative damping model has been further enhanced with an EMG-based determination of the virtual trajectory and with physiologically realistic neuromuscular delays. This model uses delays presented in the literature by other researchers in the preliminary study, and the study contributes to a resolution of the currently controversial argument in the motor planning as following:

- 1. The study demonstrated the potential for descending CNS signals to represent relatively simple, monotonic virtual trajectories of the time varying Equilibrium Point (virtual trajectory) to control human movement with known delays*
- 2. The expanded model uses realistic impedance values and produces expected joint trajectories and joint torques*
- 3. The model with relative damping suggests that reflex loops with constant coefficients can maintain the dynamic simplicity of the EPH, while being robust over the range of human joint velocities*

As the development of preliminary study, the study extended the relative damping concept and incorporated the influential factors of the mechanical behavior of the neural, muscular and skeletal system on the control and coordination of arm posture and movement.

A significant problem in motor control is how information about movement is used to modify control signals to achieve desired performance. The study favors

Feldman's EPH theory since the EPH drastically simplifies the requisite computations for multi-joint movements and mechanical interactions with complex dynamic objects in the context. Moreover, this instantaneous difference in his theory serves as a potential source of movement control related to limb dynamics and associated movement-dependent in extra load. The study used an EPH model to examine changes of controlling signals for arm movements in the context of adding load/perturbations in the format of forces and torques. The mechanical properties and reflex actions of muscles crossing the elbow joint were examined during a 1 radian voluntary elbow flexion movement. Brief unexpected torque/force pulses of identical magnitude and time duration were introduced at different stages of the movement in a random order. Single perturbations were injected in different trials in the movement onset during early, middle stages of the movement by a pre-programmed 3 DOF robotic arm (MOOG FCS HapticMaster). Changes in movement trajectory induced by a torque/ force perturbation, determined over the first 120 ms by a position/force prediction formulation, and then a modified and optimization K-B-I (stiffness-damping-inertia) model is fit to the responses. The optimized stiffness and damping coefficients estimated during voluntary movements were compared to values recorded during trials. The optimized stiffness and damping coefficients estimated during voluntary movements were compared to values among the subject, and the linearly related K-B-I was used in the Simulink to verify the EPH in perturbed movement conditions.

Therefore, the brief summary of obstructed involuntary arm movement can be concluded as following:

1. *Kinematic and Torque of both perturbed and arrested were reproduced by using the same control patterns eliciting a monotonic shift in the equilibrium state of the system ending before or near the peak velocity of perturbed movement*

2. *EMG magnitudes increased as a function of velocity at two perturbed movements. The phasic and tonic activation patterns suggested that the nervous system could use a relatively simple procedure to modify coactivation.*

3. *The models enable us to perform perturbed tasks in simulation by simply changing the parameters of the perturbation plant in the models*

4. *Both perturbed and arrested movement showed that a movement ended at the same Equilibrium Point, whether unperturbed or in the presence of a velocity dependent perturbation provided central commands remain unchanged*

5.2 Limitations of the Study

1. The study is a test of the EPH, which assumes the motor control was undergone with a monotonic descending command. Therefore, the study excluded other control schemes or higher level control by using simplest arm movement in the experiment, and any trials which found exclusive control mechanism have been abandon. However, the human movement control are the mixed or alternative control by multiple control schemes in real life, the multi-scheme motor control patters have not been addressed in this study.
2. In normal subjects, the study used mostly right hand dominant young adults as subjects. However, diversity of the subjects such as factors of age, gender, and left hand dominant have not been taken into the consideration.
3. Clinical subjects are essential in extension of the study. Subjects with different neural disorders should be divided into CP / spasticity group, stroke patients group and other disorder group to study the EPH control in different neural disorder conditions.

5.3 Conclusions

In unobstructed voluntary arm movement:

1. The EPH models use realistic impedance values and produces desired joint trajectories and joint torques in unperturbed voluntary arm movement.
2. The enhanced relative damping model allows the model to produce a trajectory that is reasonably fast and accurate in a variety of angular velocities, while being robust over the range of human joint velocities.
3. The model is able to incorporate the timing of a hypothetical EP trajectory that is taken from experimental EMG data and produce a realistic output that is close to the experimental data from which the EMG resulted

This present study suggests that subjects may maintain the same control patterns regardless of added perturbations associated with substantial changes in EMG activity and kinematics from the both experimental and simulation results.

1. Kinematic and EMGs of both perturbed and arrested were reproduced by using the same control patterns eliciting a monotonic shift in the equilibrium state of the system ending before or near the peak velocity of perturbed movement
2. The Simulink model results confirmed the assumptions in perturbed movement tasks by simply changing the model parameters.
3. Both perturbed and arrested movement showed that a movement ended at the same Equilibrium Point, whether unperturbed or in the presence of a velocity dependent perturbation provided central commands remain unchanged

5.4 Contributions

The study theoretically described the EPH origination and controversy, using experimental methods and cutting-edge scientific technique to test and verify the EPH as a mechanism of motor control under the variety conditions. The experimental results suggested the EPH is a valid theory in the human arm movement control not only in the unobstructed motions but also in the obstructed motions.

The parameters used in the mathematical model are in the reasonable range of human physiology. The real time feedback of the model, which is believed to be the cause of unstable system, were incorporated in the model, the results implied a strong robust of the model.

We believe that patients' abnormal movement patterns could be improved by the identification of the biomechanical factors that contribute to abnormal movement in the model and could be designed treatments accordingly.

5.5 Future Research

The obstructed voluntary arm movement has not been investigated in the multi-joint / segments control in terms of EPH. Further work in such situation could be done to support and widen the range of EPH applications in the motor control of obstructed arm movements.

A involuntary unobstructed arm movement in pulling arm by HM, is to be further investigated, as which mechanism is dominate in the passive arm movement is still unknown in terms of motor control. Therefore, a two joints multi-segments kinematics model and a more complicated neural control model are required to explore the control mechanism.

There are many factors (neural feedback, synaptic junctions, muscle elasticity, viscosity and so on) contributing to the overall properties of muscle, which dominate the K and B. However, these factors and their individual contribution are still unknown. It is essential to investigate these to support this study for neural and physiological foundations in the future.

Clinical data from subjects with CP, spasticity, stroke or other neural disorder subjects are necessary to verify both models and the assumptions with more incorporated parameters in the EPH model.

REFERENCES

- Adamovich SV, Levin MF, Feldman AG. (1997). Central modifications of reflex parameters may underlie the fastest arm movements. *J Neurophysiol.* Mar;77(3):1460-9.
- Adamovich S., Fluet G., Merians A.S., Mathai A., Qiu Q. (2009). Incorporating haptic effects into three-dimensional virtual environments to train the hemiparetic upper extremity. *IEEE Transactions on Neural Systems and Rehabilitation Engineering*, 17(5), 512-520.
- Allum JHH, Young LR (1976) The relaxed oscillation technique for the determination of the moment of inertia of limb segments. *J Biomech* 9:21-26.
- Asatryan,D.G., Feldman,A.G. (1965). Functional tuning of the nervous system with control of movements or maintenance of a steady posture. Mechanographic analysis of the work of the joint on execution of a postural task. *Biophysics*, 10 , 925-935.
- Ascension Technology Corporation Official Website (2010). *3D trakSTAR® Model for Short and Medium Range Applications*. Retrieved November 28, 2010, from <http://www.ascension-tech.com/medical/pdf/TrakStarSpecSheet.pdf>.
- Barto, A. G., Fagg, A. H., Sitkoff, N., Houk, J. C. (1999). A cerebella model of timing and prediction in the control of reaching. *Neural Computation*, 11, 565-594.
- Bernstein N. (1967). *The Co-ordination and Regulation of Movements*. Oxford,UK: Pergamon Press.
- Bennett, D. J., Hollerbach, J.M., Xu, Y., Hunter, I. W. (1992) Time-varying stiffness of human elbow joint during cyclic voluntary movement. *Experimental Brain Research*, 88, pp 433-442.
- Bigland B, Lippold OCJ. (1954). The relationship between force, velocity and integrated electrical activity in human muscle. *Journal of physiology, London*, 123: 214-224.
- Bizzi E, Accornero N, Chapple W, Hogan N. (1982). Arm trajectory formation in monkeys. *Exp Brain Res*. 46(1):139-43.
- Bizzi E, Accornero N, Chapple W, Hogan N. (1984). Posture control and trajectory formation during arm movement. *J Neurosci.* Nov;4(11):2738-44.
- Bizzi E. (1987). Motor control mechanisms. An overview. *Neurol Clin.* Nov;5(4):523-8.
- Brown SH, Cooke JD. (1986). Initial agonist burst is modified by perturbations preceding movement. *Brain Res* 377: 311-322.
- Cannon SC, Zahalak Gi. (1982). The mechanical behavior of active human skeletal muscle in small oscillations. *Journal of Biomechanics*, 15:111-121.
- Capaday C. (1995). The effects of baclofen on the stretch reflex parameters of the cat. *Exp Brain Research*, 104: 287-296.

- Chen K., Foulds RA, Adamovich SV, Qiu Q., Swift K. (2008). Modeling of relative damping in defining the equilibrium point trajectory for the human arm movement control. 2008 ASME International Mechanical Engineering Congress and Exposition, October 31- November6. Boston, Massachusetts USA. IMECE 2008 - 67879.
- Chen K, Foulds RA, Adamovich SV, Swift K. (2009). Experimental Study and Modeling of Equilibrium Point Trajectory Control in Single and Double Joint Arm Movement. ASME International Mechanical Engineering Congress and Exposition, November 13 - 19, 2009. Lake Buena Vista, Florida USA. IMECE2009-10251.
- Chen K, Swift K, Foulds RA. (2009). Toward a robust model of Equilibrium Point Trajectory control of human elbow trajectory. 35th Annual Northeast Bioengineering Conference, April 3-5, 2009. Harvard – MIT Division of Health Sciences & Technology Cambridge, MA, USA.
- Chen K, Foulds RA. (2010). The Mechanics of Upper Limb Posture and Movement Control. ASME International Mechanical Engineering Congress and Exposition, November 12 - 18, 2010. Vancouver, British Columbia Canada. IMECE2010-37201.
- Dizio P, Lackner JR (1995) Motor adaptation to Coriolis force perturbations of reaching movements: endpoint but not trajectory adaptation transfers to the nonexposed arm. *J Neurophysiol* 74:1787–1792.
- Dizio P, Lackner JR. (2001). Coriolis-Force Induced Trajectory and Endpoint Deviations in the Reaching Movements of Labyrinthine-Defective Subjects. *J Neurophysiology* 85:784-789.
- Feldman AG. (1966). Functional tuning of the nervous system with control of movement or maintenance of steady posture. II. Controllable parameters of the muscles. *Biophysics*, 11, 565-578.
- Feldman A.G., Orlovsky G.N.. (1972). The influence of different descending systems on the tonic stretch reflex in the cat. *Exp Neurology* 37: 481-494.
- Feldman AG. (1979). Central and reflex mechanisms of motor control. Nauka, Moscow (in Russian).
- Feldman, A. G.. (1986). Once more on the equilibrium-point hypothesis (lambda model) for motor control. *Journal of Motor Behavior*, 18, 17-54.
- Feldman AG, Adamovich SV, Levin MF. (1995). The relationship between control, kinematic and electromyographic variables in fast single-joint movements in humans. *Exp Brain Res* 103: 440-450.
- Feldman AG, Levin MF. (1995). The origin and use of positional frames of reference in motor control. *Behav Brain Sci* 18:723–806.
- Feldman AG. (1998) Ostry DJ, Levin MF, Gribble PL, Mitnitski AB. Recent tests of the equilibrium-point hypothesis (lambda model). *Motor Control*. July; 2(3):189-205.

- Feldman AG, Latash ML. (2005). Testing hypotheses and the advancement of science: recent attempts to falsify the equilibrium point hypothesis. *Experimental Brain Research*. 161, 91-103.
- Feldman A.G. (2008). Threshold position control signifies a common spatial frame of reference for motor action and kinesthesia. *Brain Research Bulletin*, 75 : 497-499.
- Feldman, A.G. (2009). Origin and advances of the Equilibrium-Point Hypothesis. *Advances in Experimental Medicine and Biology*, 629, 637-661.
- Flash T, Hogan N. (1985). The coordination of arm movements: an experimentally confirmed mathematical model. *J Neurosci*. Jul;5(7):1688-703.
- Flash T. (1987). The control of hand equilibrium trajectories in multi-joint arm movements. *Biological Cybernetics*, 57:257-274.
- Frans C.T. van der Helm, L.A. Rozendaal (1997). Musculoskeletal systems with intrinsic and proprioceptive feedback. In: Winters JM, Crago P (Eds). *Neural Control of Posture and Movement*. Springer Verlag, NY, 164-174.
- Ghafari, M., Feldman, A.G.. (2001). The Timing of control signals underlying fast point-to-point arm movement. *Exp Brain Research*, 137: 411-423.
- Gielen CCAM, van Bolhuis B. (1995). Reciprocal and coactivation commands are not sufficient to describe muscle activation patterns. *Behav Brain Sci* 18:754-755.
- Gomi H, Kawato M. (1996). Equilibrium-point hypothesis examined by measured arm stiffness during multi-joint movements. *Science*, 272: 117-120.
- Gomi H., Kawato M.. (1997). Human arm stiffness and Equilibrium Point trajectory during multi-joint movement. *Biological Cybernetics*, 76, 163-171.
- Gottlieb, G.L, Corcos, D.M. and Agarwal, G.C.. (1989). Strategies for the control of voluntary movements with one degree of freedom. *Behavioral and Brain Sciences* 12 , pp. 189-250.
- Gottlieb, G. L. (1994). The generation of the efferent command and the importance of joint compliance in fast elbow movements. *Experimental Brain Research*, 97, 545-550.
- Gottlieb G.L. (1998). Rejecting the equilibrium-point hypothesis. *Motor Control*. Jan;2(1):10-12.
- Grass Technologies (2010). *Model 15LT Bipolar Portable Physiodata Amplifier System*. Retrieved August, 2010, from <http://www.grasstechnologies.com/products/ampsystems/15lt.html>.
- Gribble PL, Ostry DJ, Sanguineti V, Laboissière R. (1998). Are complex control signals required for human arm movement? *J Neurophysiol*. Mar;79(3):1409-1424.
- Gribble P.L, Ostry D.J. (1998 b). Independent coactivation of shoulder and elbow muscles. *Exp Brain Res* 123, 355-360.
- Gribble, P. L., & Ostry, D. J. (2000). Compensation for loads during arm movements using equilibrium point control. *Experimental Brain Research*, 135, 474-482.

- Hinder MR, Milner TE (2003) The case for an internal dynamics model versus equilibrium point control in human movement. *J Physiol* 549:953–963.
- Hogan N. (1984). An organizing principle for a class of voluntary movements. *J Neurosci.* Nov;4(11):2745-2754.
- Hogan, N. (1985). The mechanics of multi-joint posture and movement control. *Biological Cybernetics*, 52, 315-331.
- H3D Open Source Haptics (2010). *MOOG FCS HapticMASTER System*. Retrieved July, 2010, from http://www.h3dapi.org/modules/mediawiki/index.php/MOOG_FCS_HapticMASTER.
- Lacquaniti, F., Moiola, C. (1989). The role of preparation in tuning anticipatory and reflex responses during catching. *Journal of Neuroscience*. 9 (1989):134-148.
- Latash, M. L., Gottlieb, G. L. (1991). Reconstruction of shifting elbow joint compliant characteristics during fast and slow movements. *Neuroscience*, 43, 697-712.
- Latash M.L. & Gottlieb G.L. (1991 b). An equilibrium-point model for fast single-joint movement. I. Emergence of strategy-dependent EMG patterns. *Journal of Motor Behavior* 23: 163-177.
- Latash M.L. (1993). *Control of human movement*. Champaign, IL: Human Kinetics.
- Lackner JR, Dizio P. (1994). Rapid adaptation to Coriolis force perturbations of arm trajectory. *J Neurophysiol.* Jul;72(1):299-313.
- Levin MF, Feldman AG. (1994). The role of stretch reflex threshold regulation in normal and impaired motor control. *Brain Res.* Sep 19;657(1-2):23-30.
- Levin M. F., Feldman A.G. (1995). The λ model for motor control: more than meets the eye. *Behavior Brain Science*, 18, 786-798.
- Marc H.E. de Lussanet, Jeroen B.J. Smeets, Eli Brenner. (2002). Relative damping improves linear mass-spring models of goal-directed movements. *Human Movement Science*, 21 : 85-100.
- McIntyre, J. , Bizzi, R. (1993). Servo hypotheses for the biological control of movement. *Journal of Motor Behavior*, 25, 193-202.
- Mussa-Ivaldi FA, Hogan N, Bizzi E (1985). Neural and geometric factors subserving arm posture. *Journal of Neuroscience*, 5, 2732-2743.
- Ostry, D.J., Feldman, A.G. (2003). A critical evaluation of the force control hypothesis in motor control. *Exp Brain Res*, 153, 275-288.
- Popescu FC, Rymer WZ. (2000) End points of planar reaching movements are disrupted by small force pulses: an evaluation of the hypothesis of equifinality. *J Neurophysiol* 84:2670–2679.
- Robertson, D.G., Caldwell, G.E., Hamill, J., Kamen, G., Whittlesey, S.N.. *Research Methods in Biomechanics*. Human Kinetics Press. 261-265.

- Sainburg, R.L., Latrinier, J.E., Latash, M.L., Bagesteiro, L.B.. (2003). Role of initial position information in reaching. *J. Neurophysiol.*, 89, 401-415.
- Slobodan Jaric, Latash, M.L.. (2000). The Equilibrium-Point Hypothesis is Still Doing Fine. *Human Movement Science*, Vol. 19 (6), December . pp 933-938.
- St-Onge N, Adamovich SV, Feldman AG (1997) Control processes underlying elbow flexion movements may be independent of kinematic and electromyographic patterns: experimental study and modelling. *Neuroscience* 79:295–316.
- Suzuki, M, Douglas S.M., Gribble, P.L. and Ostry J.D. (2001). Relationship between cocontraction, movement kinematics and phasic muscle activity in single-joint arm movement. *Exp Brain Res* 140 :171-181.
- VanderLinde, R.Q., et al.. (2002). The Hapticmaster, a New High-Performance Haptic Interface," *Proc. Eurohaptics, Edinburgh Univ.*, pp. 1-5.
- Windhorst, U. (1996). On the role of recurrent inhibitory feedback in motor control. *Progress in Neurobiology*, 49: 517-587.
- Winter, D.A. (2005). *Biomechanics and Motor Control of Human Movement*, John Wiley.
- Zahalak GI. (1986). A comparison of the mechanical behavior of the cat soleus muscle with a distribution-moment model. *Journal of Biomechanical Engineering*. 108 :131-140.